Bispecific Antibodies for the Treatment of Co-Circulating Flaviviruses and Antibody Derivatives for

Diagnostics in Checkpoint Immunotherapy

by

Adrian Esqueda

A Dissertation Presented in Partial Fulfillment
of the Requirements for the Degree
Doctor of Philosophy

Approved November 2019 by the
Graduate Supervisory Committee:

Qiang Chen, Chair
Charles Arntzen
Hugh Mason
Douglas Lake

ARIZONA STATE UNIVERSITY

December 2019

ABSTRACT

Flaviviruses (FVs) are among the most medically important arboviruses of the world with the Dengue virus (DENV) accounting for a large percentage of infections observed in tropical and subtropical regions of the world. Globalization, travel, and the expanding range of mosquito vectors, such as *Aedes aegypti*, have increased the potential of infection rates and illnesses associated with FVs.

The DENV and the Zika (ZIKV) FVs frequently co-circulate and generally cause mild self-liming febrile illnesses. However, a secondary infection with a heterologous DENV serotype may lead to life threatening dengue hemorrhagic fever (DHF) and dengue shock syndrome (DSS). DHF/DSS have been linked to antibody dependent enhancement of infection (ADE), a phenomenon that occurs when antibodies (Abs) formed against an initial infection with one serotype of DENV cross-reacts but does not neutralize a heterologous DENV serotype in a secondary infection. Furthermore, Abs raised against the ZIKV have been observed to cross-react with the DENV and vice versa, which can potentially cause ADE and lead to severe DENV disease. The ZIKV can be transmitted vertically and has been linked to devastating congenital defects such as microcephaly in newborns. FDA approved treatments do not exist for DENV and ZIKV illnesses. Thus, there is a need for safe and effective treatments for these co-circulating viruses. Here, a tetravalent bispecific antibody (bsAb) targeting the ZIKV and all four serotypes of the DENV was expressed in the *Nicotiana benthamiana (N. benthamiana)* plant. Functional assays of the DENV/ZIKV bsAb demonstrated binding, neutralization, and a significant reduction in ADE activity against both the DENV and the ZIKV.

A single chain variable fragment (scFv) and a diabody based on an antibody directed against the immune checkpoint inhibitor PD-L1, were also expressed in *N. benthamiana* leaves. The smaller sizes of the scFv and diabody confers them with the ability to penetrate deeper tissues making them beneficial in diagnostics, imaging, and possibly cancer therapy. The past few decades has seen long strives in recombinant protein production in plants with significant

improvements in production, safety, and efficacy. These characteristics make plants an attractive

platform for the production of recombinant proteins, biologics, and therapeutics.

DEDICATION

This body of work is dedicated to everyone who has supported my studies. I especially

dedicate this to my wife Jaquelyn Fernandez and daughter Melina Esqueda.

ACKNOWLEDGMENTS

TABLE OF CONTENTS

LIST OF TABLES

LIST OF FIGURES

x

LIST OF SYMBOLS/ NOMENCLATURE

AAs	Amino acids
ADE	Antibody-Dependent Enhancement of Infection
bsAb	Bispecific antibody
bsAbs	Bispecific antibodies
C	Capsid protein
CHKV	Chikungunya virus
DENV	Dengue virus
DF	Dengue fever
DHF	Dengue hemorrhagic fever
DSS	Dengue shock syndrome
E	Envelope protein
FV	Flavivirus
FVs	Flaviviruses
GI	Gastrointestinal
His	Histidine
Ig	Immunoglobulin
KiH	Knobs-into-Holes
M	Membrane protein
mAb	Monoclonal antibody
mAbs	Monoclonal antibodies
NKT	Natural killer T cells
NS1	Non-structural protein 1
NS2A	Non-structural protein 2A
NS2B	Non-structural protein 2B
NS3	Non-structural protein 3

NS4A	Non-structural protein 4A
NS4B	Non-structural protein 4B
NS5	Non-structural protein 5
prM	pre membrane protein
prM-E	pre membrane protein and E protein
RVPs	Reporter-virus particles
scFv	single chain variable fragment
T-DNA	Transferred DNA
Ti-Plasmid	Tumor-inducing-Plasmid
UTRs	Untranslated regions
VLPs	Virus-like particles
WNV	West Nile Virus
YFV	Yellow Fever Virus
ZIKV	Zika Virus

CHAPTER 1

INTRODUCTION

Flavivirus Transmission and Range

Flaviviruses (FVs) have been medically important human health burdens throughout history. Most FVs are arboviruses, transmitted by an insect vector such as a tick or mosquito. For example, one of the most infamous and archetype flavivirus (FV), the yellow fever virus (YFV), is transmitted by the *Aedes aegypti* (*A. aegypti*) mosquito (Figure 1A). The YFV is thought to have originated in Central and East Africa before spreading to West Africa and the Americas where it wreaked havoc during the colonial period of US history (The History of Vaccines, 2019) causing death and widespread fear.
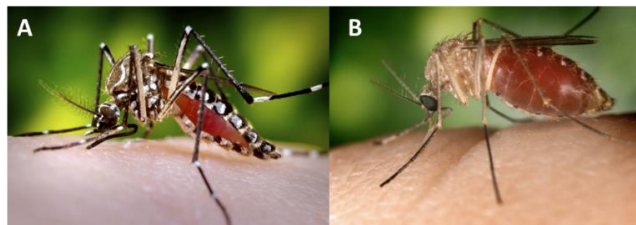
Figure 1. Common FV Mosquito Vectors. (A) The *A. aegypti* mosquito is found in areas where YF, Dengue, and Zika are endemic. *A. aegypti* is also the primary arthropod vector of Dengue and Zika viruses. (B) The mosquito *Culex pipiens* is the primary mosquito vector of the West Nile Virus. Image retrieved from. Image credit: (A) (Pasteur, 2006); (B) (flickr, 2012).

More recently, other FVs have caused great numbers of morbidity and mortality, such as the West Nile Virus (WNV), Dengue virus (DENV), and Zika virus (ZIKV). In 1999, the WNV was detected in New York city and within a few years it was also detected in Canada, Latin America, and the Caribbean Islands. The WNV was especially alarming since it was determined to be neuroinvasive and by 2004 it was estimated to have caused 7,096 cases of neuroinvasive disease in the US, mostly seen in elderly men (Edward et al., 2005). Unlike the DENV and ZIKV, the WNV is transmitted via the bite of the *Culex* genus mosquitoes such as *Culex pipiens* (Figure 1B).

The DENV has been especially detrimental to global health with estimates of 50-100 million infections per year and causing approximately 20,000 deaths per year (Cucunawangsih & Lugito, 2017). The DENV is endemic in 125 countries, ranging in regions of the Western Pacific, the Americas, and Southeast Asia. Interestingly, approximately 75% of global dengue disease is found in Southeast Asia and the Western Pacific (N. E. Murray, Quam, & Wilder-Smith, 2013).

ZIKV, the latest emergent FV, was first noticed to cause wide spread disease in the Yap Islands of Micronesia where an estimated three-quarters of the population island-wide were infected with the ZIKV in May of 2007 (Duffy et al., 2009). More recently in 2015, the ZIKV became a major cause for concern when microcephaly in newborns was linked to ZIKV infection of pregnant mothers in Latin America, particularly in north-eastern Brazil (Brady et al., 2019).

Taken together, and with a slight exception of WNV (due to a prevalence of WNV disease in the US, yet the virus was detectable in Latin America and the Caribbean), WNV, DENV, and ZIKV are medically important FVs that have been imposing a health burden on a significant percentage of the world's population. In addition, the *A. aegypti* mosquito, which is the primary vector for DENV and ZIKV, has been expanding its range not only based on climate change but also in response to changes in urbanization and socioeconomic factors (Kraemer et al., 2019). Furthermore, there's significant overlap in territories where the DENV and the ZIKV cause disease, making a co-infection with these two FVs a legitimate concern (Figure 2).
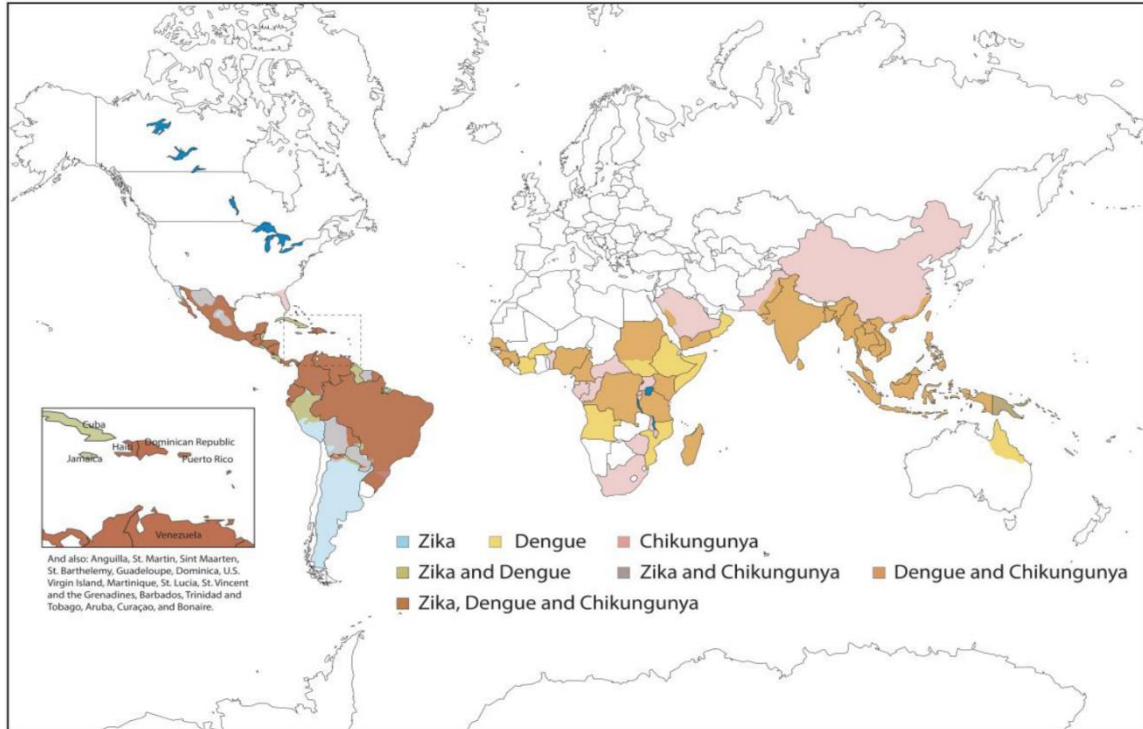
Figure 2. Approximate World Distribution of the ZIKV, DENV, and CHKV. The DENV circulates in most tropical and subtropical regions of the world. Interestingly, the closely related ZIKV and DENV FVs and the CHKV cocirculate in tropical and subtropical regions of the Americas whereas the DENV and CHKV cocirculate in Africa, India, and southeast Asia. Image credit: (Patterson, Sammon, & Garg, 2016)

Flavivirus Genome Organization

The family *Flaviviridae* has 4 genera which include *Pestivirus*, *Hepacivirus*, *Pegivirus*, and *Flavivirus* (Simmonds et al., 2017). FVs are enveloped viruses that are approximately 60 nm in diameter and contain an encapsidated RNA genome ranging from 9-11 kbp. The viral genome is translated into one large polypeptide that is processed by both host and viral proteases resulting in 3 structural proteins and 7 non-structural proteins (Figure 3). The 3 viral structural proteins are the capsid (C) protein, pre-membrane protein (prM), and the envelope protein (E). The non-structural proteins include NS1, NS2A, NS2B, NS3, NS4A, NS4B, and NS5. Whereas the structural proteins are involved in the formation of the structure of the virions, the non-structural proteins are involved in directing the replication of the viral genome and associated processes. Additionally, the 5' and 3' untranslated regions of the viral genome (UTRs) aide in the

replication of additional viral genomes and modulate host immune system evasion (Ng, Soto-

Acosta, Bradrick, Garcia-Blanco, & Ooi, 2017).
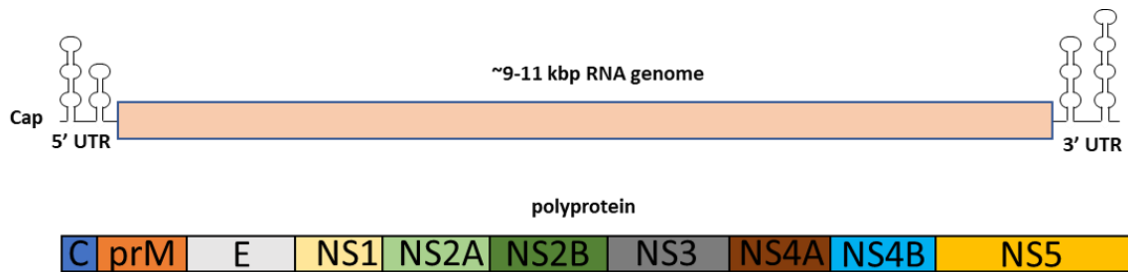
Figure 3. FV Genome. The FV genome consists of a 5' capped 9-11 kbp single stranded RNA molecule. Once the nucleocapsid is released into the cytoplasm, the capsid proteins dissociate from the genome and is directly translated by host ribosomes to produce a single large polyprotein. The polyprotein is then processed by host and viral proteases to produce the individual viral structural and nonstructural proteins.

Flavivirus Structure

The structure of FVs is comprised of the viral RNA encapsidated by the virally encoded C

protein whereby an icosahedral nucleocapsid is formed and wrapped by an ER derived

membrane containing virally encoded M and E proteins (Figure 4). Mature virions are

approximately 50 nm in diameter and have a smooth surface with trimers of dimers of the E

protein forming a herringbone like arrangement over the entire surface of the virions.

4
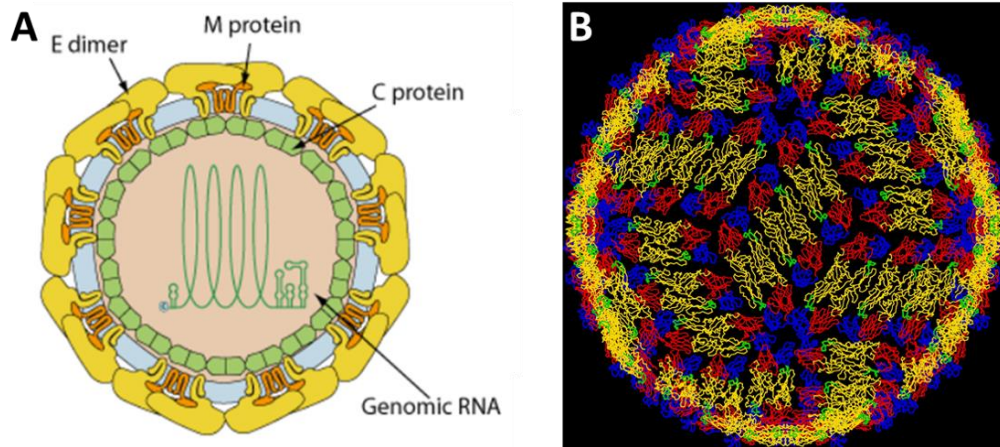
Figure 4. Structure of FVs. (A) The FV structure is composed of the 3 virally encoded proteins, the capsid (C), membrane (M), and envelope (E) proteins. The viral RNA is encapsidated by the C protein forming the icosahedral nucleocapsid. The nucleocapsid is wrapped by an ER derived membrane which contains virally encoded M and E transmembrane proteins. Virions are approximately 50 nm in diameter. (B) Crystal structure of the DENV where the E protein can be seen arranged as trimers of dimers forming a herringbone like arrangement. The E protein is color coded in red, yellow, and blue denoting domain I, II, and III, respectively. Image Credit: (A) Viral Zone 2016; (B) (Kuhn et al., 2002).

The FV virion surface is covered by 180 copies of the virally encoded E protein that are arranged in 90 homodimers of E (Mukhopadhyay, Kuhn, & Rossmann, 2005). These E protein dimers are further arranged in trimers of dimers that form the surface of the virion. The E protein is comprised of 3 domains. Domain 1 is denoted as the central structural domain and is flanked by domains 2 and 3 (Figure 5). Domain 2 contains the fusion peptide that facilitates the fusion of the viral envelope to the host's lysosome membrane and domain 2 is also responsible for the dimerization of the E protein. Domain 3 contains the putative receptor binding site, which varies among FV type.
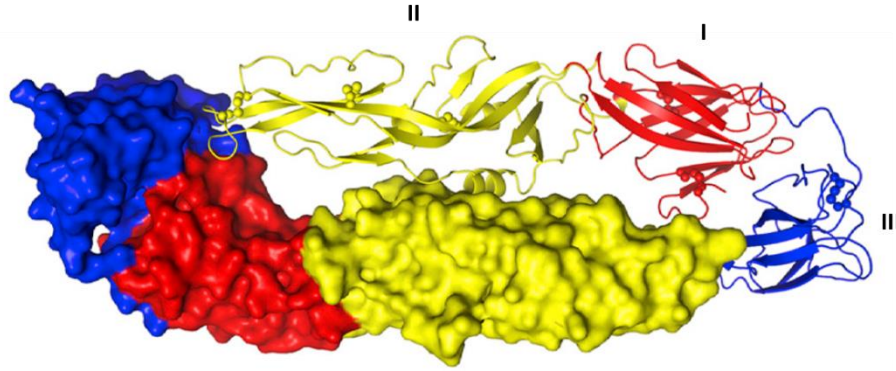
Figure 5. Structure of the FV E Protein. The FV E protein has 3 domains. Domain I (red) is a β-barrel like central structural domain. Domain II (yellow) contains the fusion peptide at its distal end and domain II is also responsible for the dimerization of the E protein. Domain III (blue) is immunoglobulin-like and is thought to contain the receptor binding site. Image credit: adapted from (Dai et al., 2016).

The E protein is a glycoprotein and is approximately 495 amino acids (AAs) long. Glycosylation sites on the E protein are largely found on domain 3 and the glycosylation sites vary among FV type (i.e. ZIKV, DENV). The site and extent of glycosylation is thought to modulate interactions with specific cellular receptors for binding specificity. The E protein is also the immunodominant viral protein, thus it is the main target of the host's humoral and cellular response.

The C protein forms a protective shell around the viral genome and is approximately 114 AAs long. However, after proteolytic cleavage by the viral NS2B-NS3 protease it is slightly shortened to 110 AA to become a mature homodimeric capsid protein (Oliveira, Mohana-Borges, de Alencastro, & Horta, 2017). Furthermore, the capsid protein has a stretch of AAs that is positively charged, aiding in the complexing with the negatively charged viral RNA to form the viral nucleocapsid. Because the C protein lies beneath the viral envelope and is effectively shielded from the environment, the C protein is usually not a target of the immune system.

The virally encoded pre-membrane (prM) protein is processed by a host protease to produce the M protein and is one of two proteins found on the viral membrane. During early steps of virion structure assembly, an E protein dimerizes with a prM protein to form a heterodimer. Subsequent steps of viral maturation expose the immature virion to increasing pH environments.

6

In the *trans*-Golgi network the host protease furin cleaves the pr-peptide from the pr-M protein to produce the M protein whereby homodimers of the E protein form and virions become mature (Smit, Moesker, Rodenhuis-Zybert, & Wilschut, 2011).

The 7 FV nonstructural proteins NS1, NS2A, NS2B, NS3, NS4A, NS4B, and NS5 are primarily involved in the replication of the viral genome. These nonstructural proteins include a virally encoded protease, helicase, and RNA dependent RNA polymerase (RdRp). Unique among the nonstructural proteins is NS1. NS1 is the only nonstructural protein that is secreted and elicits neutralizing antibodies and viral clearance (Y. C. Lai et al., 2017). NS1 is essential for infectious virion assembly and functions in early viral genome replication. NS1 also functions as a host immune system evasion agent. NS2A is required for RNA replication whereas NS3, NS4A, and NS2B form the viral protease (C. L. Murray, Jones, & Rice, 2008). NS3 is a helicase and a nucleoside triphosphatase (Li, Phoo, & Luo, 2014). NS5 is the essential viral RdRp responsible for viral genome replication (Brand, Bisaillon, & Geiss, 2017).

Flavivirus Virion Assembly

FV assembly is complex and some aspects of it remain elusive. Assembly of new virions can be described as biphasic, wherein the first phase is centered on the replication of the viral genome and translation of the polypeptide by host and viral proteases, whereas the second phase involves the interaction of viral proteins with host cellular proteins (Fowler et al., 2018). During the first phase and in the cytoplasm, there is evidence to suggest that vesicle packets derived from host membranous organelles, primarily from the ER, serve as scaffolding for the assembly of virions in their immature form (Apte-Sengupta, Sirohi, & Kuhn, 2014). It is in these modified membranes that translation and viral proteins are processed. In addition, the replication of the viral genome also occurs in these modified membranes.

Once viral RNA genome is replicated and complexed with viral capsid proteins, the resulting nucleocapsid buds into ER membranes that contain the virally encoded prM-E studded membrane proteins. These prM-E studded membranes envelope the nucleocapsid forming an

7

immature virion (Figure 6). A striking feature of the immature virions is their spiky appearance, which is due to the orientation of 60 trimers of prM-E heterodimers (Figure 7, left panel) (S. S. Hasan, Sevvana, Kuhn, & Rossmann, 2018). As the immature virion transits through the ER and to through various regions of the Golgi, the pH begins to decrease, thereby causing conformational changes in the immature virion where the E proteins change from spikes comprised of trimeric prM-E heterotrimers to dimers of E proteins that lie flat to form a herringbone-like pattern throughout the surface of the virion (T. C. Pierson & Diamond, 2012). As the immature virion continues to transit through the trans-Golgi network and exocytic pathway, the pH reaches approximately 5.7 at which point the cellular serine protease furin cleaves the pr-M protein to produce pr and M proteins. The M protein remains associated with the mature and infectious virion and the pr peptide is expelled to the environment as the mature virion is released (Figure 7, right panel; Figure 8).
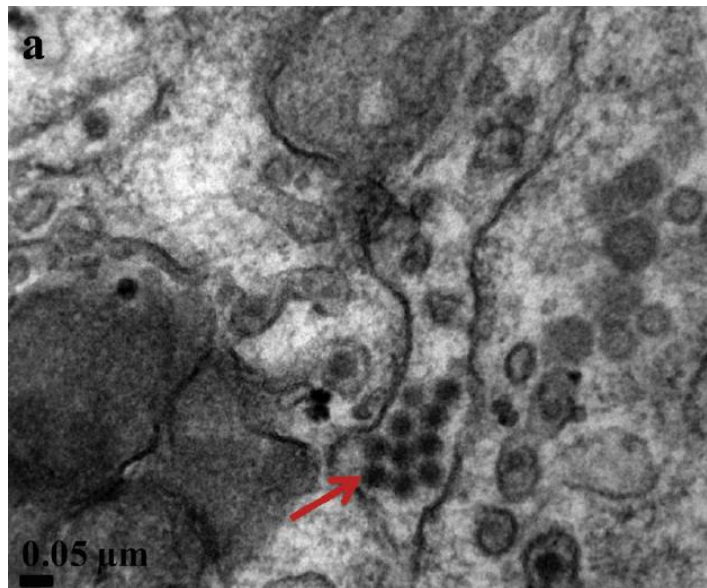
Figure 6. Immature DENV Virions in the ER. DENV virions assemble on the cytoplasmic side of the ER. After the formation of the nucleocapsid, enveloping of the nucleocapsid ensues by budding into the ER lumen and acquiring the prM-E containing envelope, thereby forming immature virions. The red arrow points at several DENV virions in their immature form. Image credit: (Chong, Chua, Tan, Tan, & Ng, 2014).
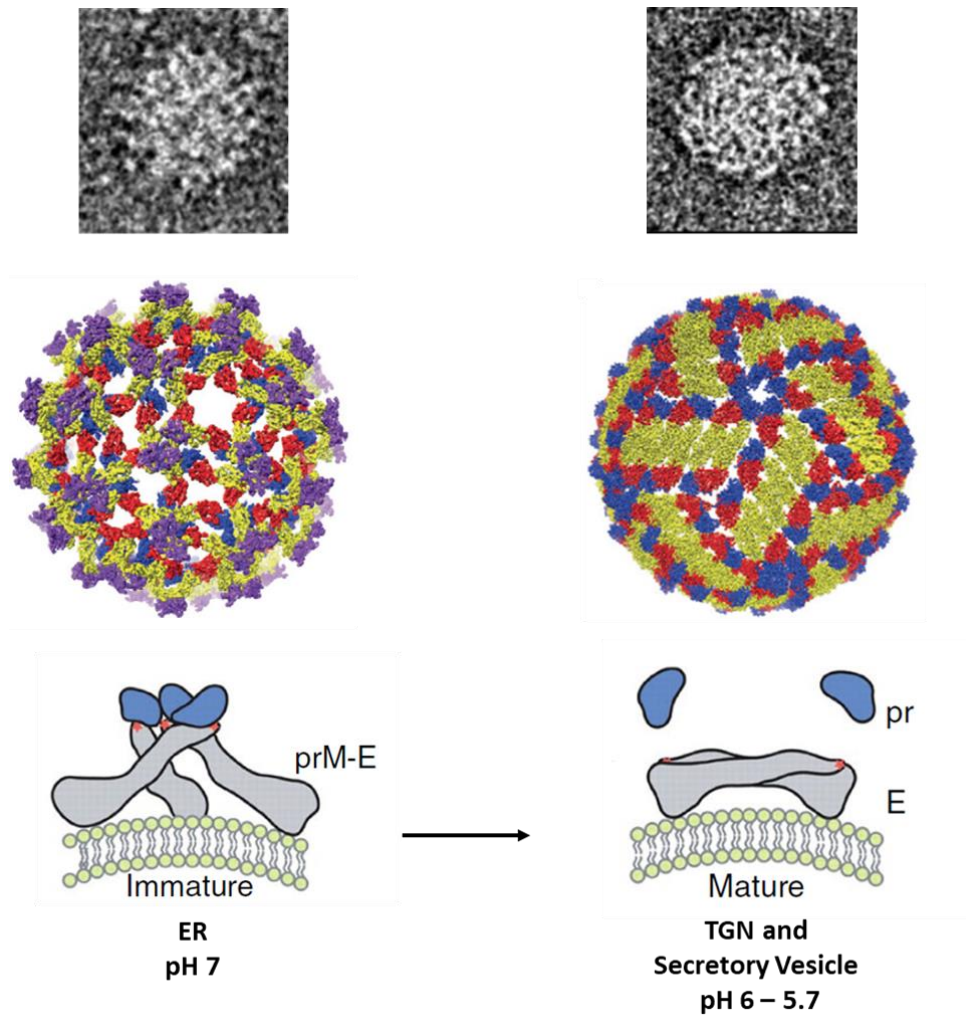
Figure 7. Conformational Change of prME Proteins During FV Maturation. Upon assembly and budding of new virions into the lumen of the ER, prM-E proteins are arranged in trimers that wrap the entire virion surface (left column, center and bottom row) forming a "spiky" appearance. Virion transit from the ER to the Golgi apparatus and Trans-Golgi Network (TGN) exposes the virion to increasing acidification (~ pH 6 - 5.7) causing the prME trimers to rearrange and form dimers of prM-E. In the distal regions of TGN and in secretory vesicles, the host enzyme Furin cleaves the prM-E protein to release the "pr" protein and produce mature/infectious virions with E and M proteins (right column, bottom row). E proteins dimerize and form trimers of dimers reminiscent of a herringbone arrangement (right column, center row). Cryo-EM images of the DENV in immature (left column, top row) and mature form (left column, right row). Image credits: Top row, (X. Zhang et al., 2013); Middle Row, (T. C. Pierson & Diamond, 2012); Bottom row: (S. S. Hasan et al., 2018).
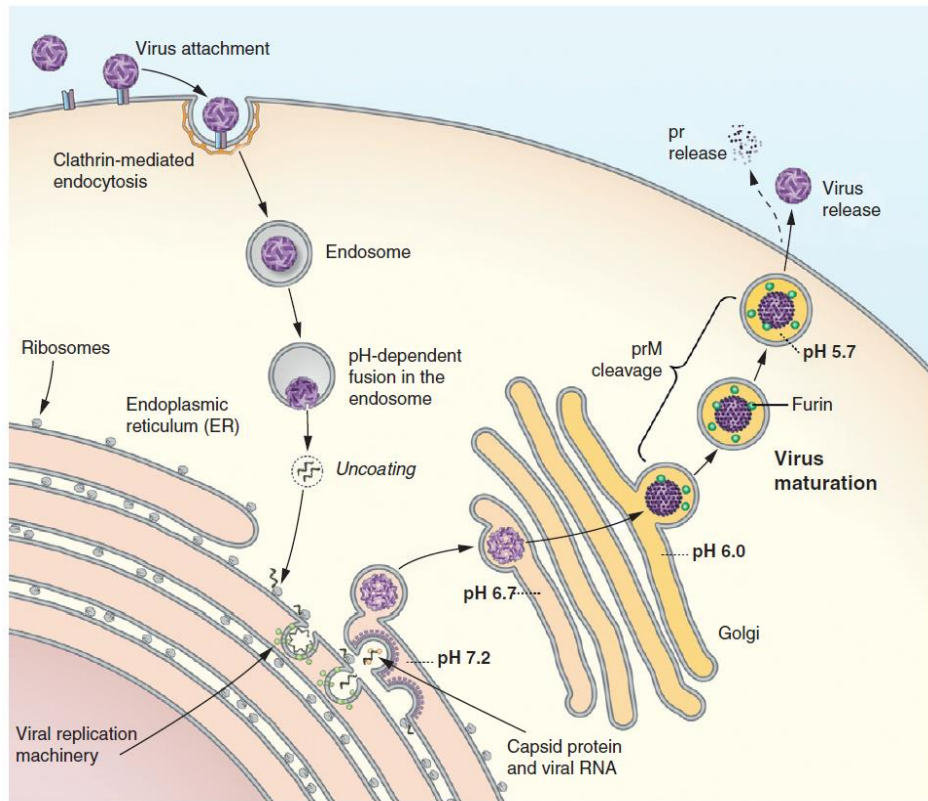
Figure 8. FV Assembly. FVs enter the cell via receptor mediated endocytosis. The receptors on target cells vary depending on the FV. The DENV binds to heparan sulfate residues triggering receptor mediated endocytosis. Acidification of the endosome causes a conformational change in the E protein exposing the fusion loop and subsequent release of the capsid. In the cytoplasm, the genome is released and used directly as mRNA for the translation of viral proteins and subsequent assembly of virions. The immature virions are trafficked through to exocytic pathway where viral and host proteases modify the virion surface proteins to produce a mature virion upon release of the virions. Image credit: (T. C. Pierson & Diamond, 2012)

DENV Transmission

Infections with the DENV are among the most common of arthropod born viruses in the world with the majority of infections occurring in the tropical and subtropical geographical regions of the world. An infection with the DENV is established when a DENV infected female *A. aegypti* mosquito takes a blood meal from a person. After 5-7 days viremia is high enough such that an

uninfected mosquito taking a blood meal from that patient will become infected. That mosquito is

then be capable of infecting other human hosts with the DENV (Figure 9).
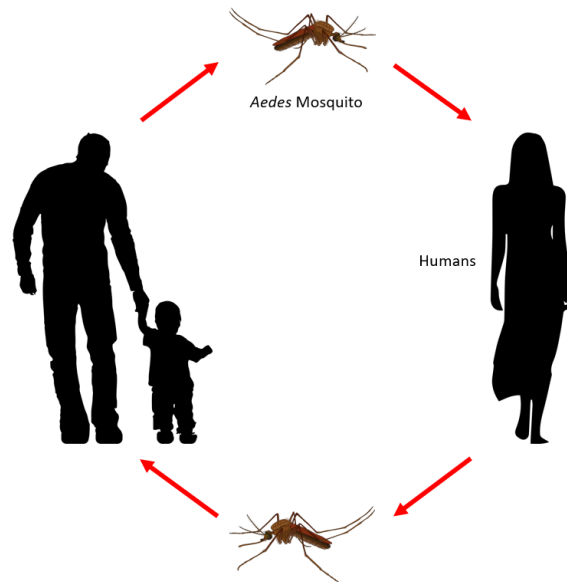
Figure 9. DENV Transmission in Humans. The DENV is primarily transmitted between humans and mosquitoes of the *Aedes* genus. Humans can infect mosquitoes with the DENV and vice versa. DENV infection in humans results in high levels of viremia that can result in the efficient infection of mosquitoes taking a blood meal.

Dengue Disease: Dengue Fever

Symptoms of an initial DENV infection are generally self-limiting and rarely extend past

symptoms such as nausea, vomiting, skin rash, high fever, and in some instances mild bleeding

(Figure 10).
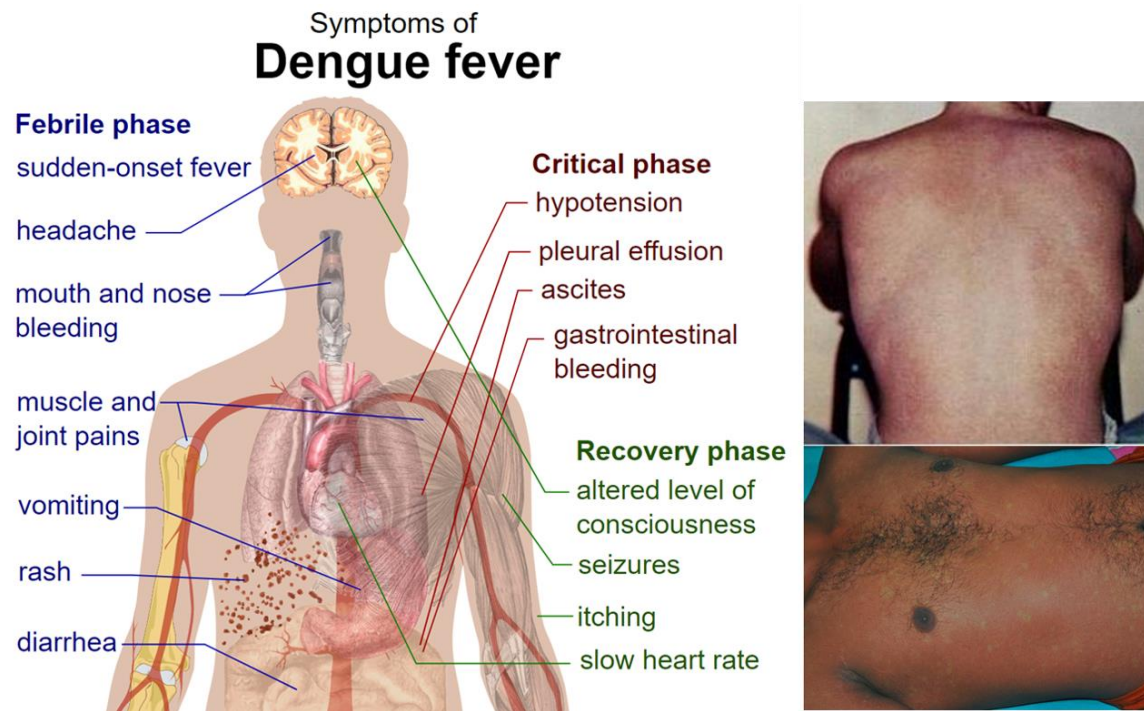
Figure 10. Symptoms of DF. A first-time infection with any serotype of the DENV causes mild and self-limiting disease. Patients generally make a full recovery without extensive medical intervention. Malaise, fever, and skin rashes are the most commonly reported symptoms.

Severe Dengue Disease: Dengue Hemorrhagic Fever and Dengue Shock Syndrome

Infections with the DENV can advance to more severe symptoms and can reach life threatening states. Infants, children, the elder, pregnant women, and those who have had previous dengue infections are at an increased risk of developing severe dengue disease, such as Dengue Shock Syndrome (DSS) and Dengue Hemorrhagic Fever (DHF). Infected individuals that progress to DHF will display symptoms such as a fever, a platelet count of $<100,000/mm^3$, petechiae, purpuric lesions, GI hemorrhage, epistaxis, and plasma leakage (Gubler, 1998). Worsening DHF symptoms lead to DSS. DSS is characterized by symptoms seen in DHF and additionally include a rapid weak pulse, blood pressure < 20 mm Hg, cold and clammy skin, and hypotension for the age of the patient (Rajapakse, 2011). Under these conditions that patient's life is in serious danger and requires intensive medical care with special attention to the careful management of fluids (S. Halstead, 2019).

Severe Dengue Disease Pathogenesis

The pathogenesis of dengue is multifaceted: the progression and severity of the disease is dependent on host immunological factors, host genetics, and viral factors. Upon initial infection with the DENV via a bite by a mosquito, the DENV present in the mosquito saliva are deposited along with other endogenous saliva components of the mosquito that modulate the immune response in the epidermis and dermis layers of the skin (Briant, Despres, Choumet, & Misse, 2014). The epidermis hosts various cell types with the vast majority of cells being keratinocytes, followed by melanocytes and Langerhans cells. Directly underneath the epidermis and within the reach of the mosquito's proboscis lays the dermis which contains blood vessels and hosts a variety of cells including a larger number of immune cells such as macrophages, dermal DC's, neutrophils, and natural killer T cells (NKTs). As a mosquito is in the process of taking a blood meal in search of a blood vessel it releases DENV virions via its saliva. It is widely believed that Langerhans cells in the epidermis are among the first cells to be infected with the DENV. Upon infection, Langerhans cells make their way to local draining lymph nodes where they inadvertently spread the virus to other mononuclear phagocytic cells. The vast majority of individuals infected with the DENV experience mild symptoms, such as nausea, vomiting, aches, joint and bone pain, but readily clear the virus within the course of a week. However, some patients advance to more serious symptoms as a result of the primary viremia. Primary viremia can progress to cause infection of splenic and liver macrophages and endothelial cells (ECs) lining the blood vessels of the pleural and abdominal cavities (Martina, Koraka, & Osterhaus, 2009). At this stage the patient may advance to dengue fever (DF) or DHF.

A variety of hypothesis have been suggested to explain the progression to DF and DHF. Among them are antibody-activation of complement, antibody-dependent enhancement of infection (ADE), T cell original antigenic sin (OAS), and exaggerated cytokine release. As the immune system mounts a response to the DENV infection, the humoral arm of the immune system produces antibodies against DENV structural and non-structural proteins. The E protein completely covers the DENV surface and is the immunodominant structural protein. NS1 is the

13

only secreted non-structural protein for which antibodies are also produced. NS1 binds to ECs of the lung and liver and has been shown to induce apoptosis via the caspase pathway, thereby contributing to plasma leakage seen in DHF (Malavige, Fernando, Fernando, & Seneviratne, 2004). The prolific release of NS1 by infected cells and IgG1 and IgG3 by the humoral arm of the immune system triggers a robust complement response. IgG1 and IgG3 are excellent complement fixers and it has been proposed that binding of antibodies to NS1 expressed on infected cells results in complement activation, leading to a consumption of complement and contributing to the pathogenesis of dengue. Furthermore, it has been shown that human antibodies against NS1 bind to ECs and platelets, thereby preventing an effective response against plasma leakage and exacerbating hemorrhagic events (Srikiatkhachorn, 2009).

The cellular immune response has also been suggested to play a role in dengue pathogenesis. Generally, a robust cellular immune response that includes CD4+ and CD8+ T cells is desired to clear infections involving intracellular parasites such as viruses. In immunocompetent individuals, few viruses pose (e.g. DENV and influenza) a challenge to the cellular immune response, however difficulties in clearing a virus is usually traced back to the antigenic similarity of some viruses. The DENV has four serologically distinct but related viruses. In OAS, T cells that were highly specific and effective for a primary infecting DENV serotype appear to be highly active and play a significant role in an immune response to a secondary heterologous DENV infection (Tian, Grifoni, Sette, & Weiskopf, 2019). This results in the expansion of preexisting cross-reactive T cells with low avidity to the new serotype, thereby delaying the control of the infection and possibly exacerbating peak viremia and the production of excessing cytokines, ultimately contributing to the pathogenesis of dengue (Yacoub & Farrar, 2014). The excessive production of cytokines is believed to increase vascular permeability leading to the damage of ECs.

The pathogenesis of DHF and DSS from a secondary and heterologous DENV infection has also been proposed to be the result of a "cytokine storm" where cytokines such as IL-6, IL-8, VEG-F, VCAM-1, TNF-α, and INFγ, increase vascular permeability of ECs, subsequently leading

14

to plasma leakage (Mangione et al., 2014). Immune cells such as monocytes, macrophages, and T cells release prolific quantities of cytokines that subsequently cause endothelial dysfunction leading to vascular permeability as seen in patients suffering from DHF (Malavige et al., 2012). Furthermore, there is some evidence suggesting that during DHF and DSS, cytokines characteristic of a Th2 dominant response are present, thereby leading to the exacerbation of DENV infections and an increase in vascular permeability as seen in DHF and DSS (Chaturvedi, Agarwal, Elbishbishi, & Mustafa, 2000).

Among the many hypothesis put forth to explain DENV infection pathogenesis leading up to DHF and DSS, ADE appears to be one of the most widely accepted mechanisms (S. B. Halstead, 2015). ADE occurs when antibodies produced from a primary infection with DENV enhance the infection of a secondary infection with a heterotypic serotype of DENV. DENV has four separate serotypes that are distinct enough such that antibodies produced against one serotype may not be neutralizing to other serotypes. Consequently, circulating antibodies may be non-neutralizing but are still able to bind to a heterotypic serotype of DENV and form a non-neutralized virus-antibody complex. Upon an encounter with an FcγR bearing cell, such as a macrophage or monocyte, the non-neutralized virus-antibody complex may gain entry into the FcγR bearing cell, thereby infecting the cell and increasing the viral load on the patient ultimately leading to severe forms of dengue disease such as DHF and DSS (Whitehead, Blaney, Durbin, & Murphy, 2007) (Figure 11).
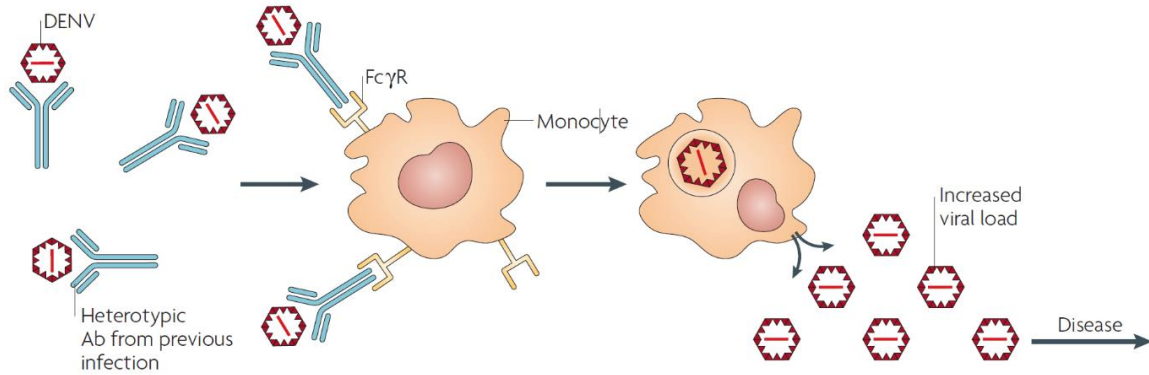
Figure 11. DENV Associated ADE. ADE occurs when subneutralizing antibodies produced from a previous infection with a heterotypic virus or suboptimal levels of neutralizing antibodies bind to a virus and facilitate the entry of antibody-virus complex into an FcγR bearing cell via FcγR and Fc-region of the antibody. This results in increased viral loads leading to severe dengue disease. Figure credit: (Whitehead et al., 2007).

ZIKV Infection and Disease

In 2015 a related FV to the DENV, the ZIKV emerged, as a major health concern in Northern Brazil where a significant increase in microcephaly in newborns was noticed (Brady et al., 2019). Symptoms of a ZIKV infection are generally like other FV infections, which include fever, rash, headaches, myalgia, and conjunctivitis to name a few (Figure 12A). As a member of the FV genus, the ZIKV shares all the structural and genome organization of the genus. Investigation into the cause of the microcephaly revealed that the ZIKV was the causative agent, placing the ZIKV in a unique position among FVs as a teratogen (Figure 12B).

Figure 12. ZIKV Infection Symptoms. (A) Similar to infections caused by the DENV and the YFV, an infection with the ZIKV can be characterized by mild symptoms such as fever, rash, and conjunctivitis, for example. The symptoms are self-limiting and usually subside between 7-14 days. A ZIKV infection is of great concern to expecting mothers since the virus can be transmitted to the fetus where it can have detrimental effects in the development of the central nervous system of the fetus, potentially resulting in lifelong debilitating consequences such as microcephaly. Image credit: A, Wikimedia; B, Center for Disease Control and Prevention.

Although the ZIKV is not unique among FVs in its ability to establish an infection in the nervous system, e.g. the WNV is a neurotropic FV that caused a major health concern in early 2000's in the Eastern United States, it is unique in that the ZIKV is able to cross the placenta in pregnant women and establish an infection in neuronal cells in the developing fetus that can lead to Congenital Zika Syndrome. Congenital Zika Syndrome is characterized by displaying severe microcephaly, decreased brain tissue content, and other impaired neurological developments of the fetus (Hickman & Pierson, 2016; Prevention, 2019). Of important note is also the possibility of sexually transmitting the ZIKV (Figure 13).
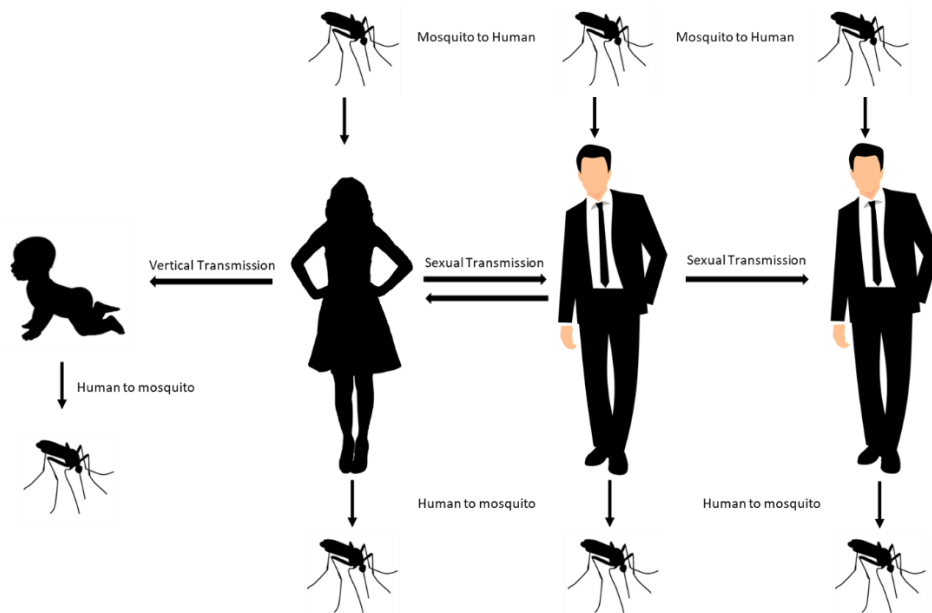
Figure 13. ZIKV Transmission. The ZIKV is unique among FVs in that it is transmissible vertically from mother to fetus and it is also a sexually transmissible virus. Vertical transmission of the virus in the first trimester of fetal development has been linked to Congenital Zika Syndrome, which includes microcephaly, a life-long debilitating condition.

An infection with the ZIKV is largely indistinguishable from other closely related FVs such as DENV. The most common symptoms of a ZIKV infection include fever, skin rash, joint pain, muscle pain, conjunctivitis, and headache (S. Hasan, Saeed, Panigrahi, & Choudhary, 2019). Investigation into ZIKV virology revealed that it had an increased cellular tropism, which includes placental, neural, testicular, and ocular tissue (Shaily & Upadhya, 2019). Although an infection with the ZIKV is largely self-limiting and poses no notable health risks in adults, serious ZIKV associated complications exist, such as the development of Guillain-Barré syndrome, in which the peripheral nervous system experiences inflammation resulting in acute flaccid paralysis (Leonhard et al., 2019).

Plant Produced Therapeutics

Steady progress in plant protein expression systems has been made since the first monoclonal antibody (mAb), an IgG1 against a phosphonate ester, was made in transgenic tobacco plants (Hiatt, Caffferkey, & Bowdish, 1989). Since then a variety of plants such as

carrots, alfalfa, lettuce, tomato, potato, including the seeds of some plants such as soybean have been used to express therapeutic proteins such as mAbs, enzymes, subunit vaccines, and virus-like particles (VLPs)(Chen, Santi, & Zhang, 2014). In May of 2012 the biologic "Elelyso," an enzyme produced in carrot cells used to treat type 1 Gaucher's disease, was the first plant made biologic approved by the US Food and Drug administration and later in August of 2014 an experimental drug named "ZMapp", which is comprised of a cocktail containing three mAbs targeting the Ebola virus (EBOV), produced in tobacco plants was compassionately used to treat two American health care workers during the Ebola epidemic of West Africa (Arntzen, 2015; Y. Zhang, Li, Jin, & Huang, 2014).

The type of plant used to express a biologic is largely dependent on the type of biologic to be expressed. The tobacco plant of Australian origin *Nicotiana benthamiana* (*N. benthamiana*) has a been the premier choice for expressing mAbs for a variety of reasons. For instance, *N. benthamiana* highly lends itself to a variety of transient expression systems and it is able to support high levels of protein production (Norkunas, Harding, Dale, & Dugdale, 2018; Sheludko, Sindarovska, Gerasymenko, Bannikova, & Kuchuk, 2007). Additionally, *N. benthamiana* is also a popular choice of host plant for a variety of studies because it can be readily transformed and it is susceptible to number of pathogens such as viruses, fungi, and bacteria (Goodin, Zaitlin, Naidu, & Lommel, 2008).

Agrobacterium tumefaciens and Plant Cell Transformation

Since its first reported use to transfer recombinant DNA into plants, the Gram-negative soil bacterium *Agrobacterium tumefaciens* (*A. tumefaciens*) has been extensively used to both stably and transiently transform a variety of plants (Grimsley N, 1986). *A. tumefaciens* is a natural pathogen of dicotyledonous plants where it causes crown gall disease. *A. tumefaciens* bacteria mediate the formation of the tumors observed in gall disease via the transformation of plant cells using Transfer-DNA (T-DNA) found in its Tumor inducing plasmid (Ti-plasmid) (Figure 13). In addition to bacterial factors that facilitate the transfer of the T-DNA, host plant cell proteins also

19

play a role in the transformation of the plant cell genome (T. Tzfira & Citovsky, 2002). In addition

to their natural hosts, under controlled experimental conditions, *A. tumefaciens* has successfully

transformed fungi, monocots, and human cells (Gelvin, 2003; T. L. Tzfira, B; Citovsky, V, 2018).

Thus, the mechanisms involved in the transformation of plants cells to produce a favorable

environment for the proliferation of *A. tumefaciens* have been successfully exploited to produce

several systems for stable and transient protein expression systems in plants.
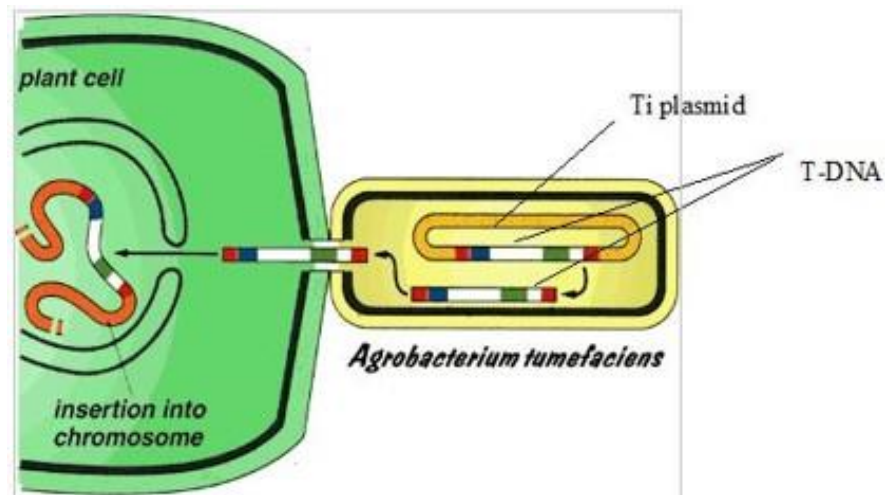
Figure 13. *A. tumefaciens* **Mediated Transformation of Plant Cells.** *A. tumefaciens* transfers
T-DNA from its Ti-plasmid to susceptible plant cells. The Ti-plasmid is shuttled from the bacterial
cell to the plant cell with the assistance of bacterial proteins. Once in the plant cell, plant proteins
also assist in the transformation process by facilitating the transfer of the T-DNA into the nucleus
for integration of the T-DNA to the plant cell genome. Image credit:
http://www.plantsci.cam.ac.uk/Haseloff/SITEGRAPHICS/Agrotrans.GIF

Transient Protein Expression in Plants

Plants express recombinant proteins via the delivery of transgenes of interest via two

overarching modes: direct and indirect delivery of the gene of interest (Rivera, Gómez-Lim,

Fernández, & Loske, 2012). Indirect methods generally involve the use of *A. tumefaciens* to

deliver a plasmid encoding the transgene whereas direct methods require the use of physical

delivery modes to deliver the gene of interest, such as biolistics (*e.g.* gene gun), electrophoresis,

and microinjection, for example (Darbani B, 2008). Plants can be stably or transiently

transformed. Stable transformation offers the advantage of producing plant lines that have

integrated into their genome the transgene(s) of interest allowing further generations to inherit the

transgenes (Hwang, Yu, & Lai, 2017). However, the production of stable transgenic plant lines

raises the concern of inadvertent exposure to unintended areas where the transgenes can spread

unchecked (Chen et al., 2013).

Transient transformation of plants provides an alternative method to stable transformation

and eliminates the potential of unintended widespread distribution of transgenes into the wild

since transient transformation does not require the integration of the gene of interest into the plant

genome (Chen et al., 2013). In recent years, transient transformation of plants to produce

recombinant proteins has been the choice method. Transient transformation also uses *A.

tumefaciens* to deliver the gene of interest and most transient expression system rely on the use

of genetic elements present in the Ti-plasmid to deliver the gene(s) of interest, notably the left

and right border nucleotide sequences that flank the T-DNA.

Transient Protein Expression: MagnICON System

One of the most widely used systems to transiently transform plants for protein

production is the MagnICON system (S. Marillonnet et al., 2004) (Figure 14). This system is

based on the deconstruction of plant viruses, such as the Tobacco Mosaic Virus (TMV), and is

composed of three modules (5' module, 3' module, and recombinase module) which together

form a replicon in the host cell nucleus that is capable of cell-to-cell movement, transcription,

translation, and replication. The three modules are co-delivered to plant cells via agroinfiltration,

in which separate preparations of *A. tumefaciens* contain either the 5' module, 3' module, or the

recombinase module. The 5' module generally contains a promoter for the RNA dependent RNA

polymerase, the movement protein, a selected promoter for the expression of the gene of interest

(GOI), and a recombinase sequence site for the recombinase. The 3' module contains the second

recombinase site, the GOI, and a terminator for the gene of interest. The recombinase module

contains PhiC31 integrase gene that codes for the recombinase that fuses the 5' and 3' modules

in the host cell nucleus that results in the formation of a replicon. This system has been shown to produce high levels of recombinant protein, up to 5 mg per g of fresh leaf weight (FLW)(Sylvestre Marillonnet et al., 2004).
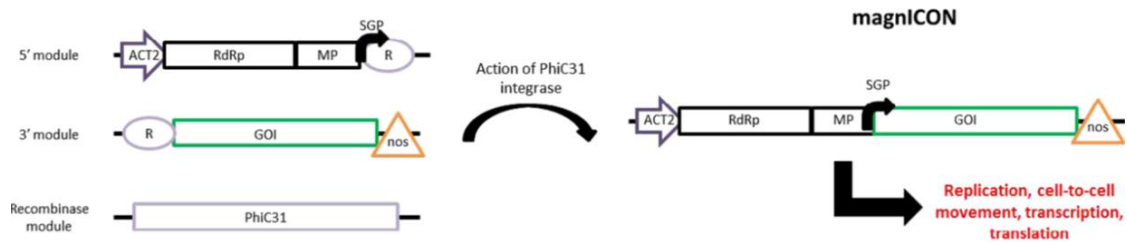
Figure 14. MagnICON Transient Transformation System. The MagnICON system is a deconstructed-viral vector system that separates genetic components of plant viruses into modules which are then co-delivered into plant leaves by agroinfiltration. Once the vectors are in the host cell nucleus, a recombinase in one of the MagnICON modules assembles the deconstructed viral vector to form a replicase that is capable of cell-to-cell movement. This system is noted to be one of the most prolific producers of recombinant proteins in plants. PhiC31: streptomyces phage 31 integrase, nos: nos terminator, GOI: Gene of interest, MP: movement protein, R: recombination site, SGP: TMV subgenomic promoter directing transcription of the gene of interest, ACT2: Arabidopsis actin 2 promoter, RdRp: TMV RNA-dependent RNA polymerase, TMV: tobacco mosaic virus. Figure credit: (Peyret & Lomonossoff, 2015)

Transient Protein Expression: Geminiviral System

Despite the robustness of the MagnICON system in producing recombinant proteins, the MagnICON system has some limitations. For example, at the moment it is not possible to produce a protein that is comprised of more than 2 subunits and the MagnICON requires the use of multiple modules that can increase the cost of production (Qiang Chen & Huafang Lai, 2015). The Geminiviral bean yellow dwarf virus (BeYDV) vector, derived from monopartite virus of the *Geminiviridae* family, allows for the production of multisubunit proteins due to its noncompeting nature that allows for the expression of multiple GOI in the same host cell (Chen, He, Phoolcharoen, & Mason, 2011). The BeYDV vector also relies on agroinfiltration for delivery of the vector to the host cell. The vector has greatly improved in its ability to express recombinant proteins since its initial introduction, however it has retained key elements through its generations. Among them, are the retention of the left and right borders of the T-DNA that indicate the segment of the construct to be transferred by *A. tumefaciens* replication initiator

22

protein (Rep A), long intergenic region LIR, short intergenic region (SIR), and the GOI (Qiang

Chen & Huafang Lai, 2015; Tsafrir S Mor, 2002)(Figure 15). Like the MagnICON system, the

BeYDV vector generates replicons, however, the BeYDV produces very high copy number of

replicons that are available for copious amounts of mRNA synthesis.
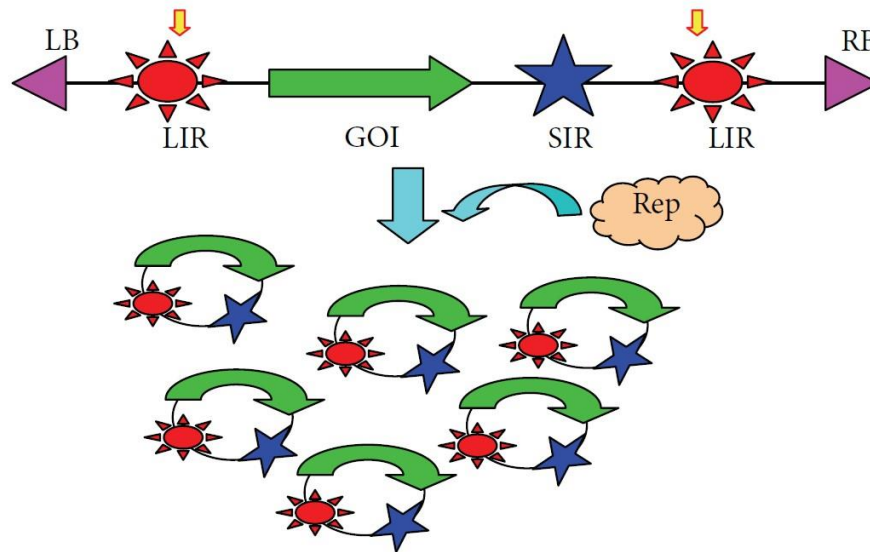
Figure 15. Replicon Formation via the BeYDV Vector. The BeYDV vector contains genetic
elements found in the BeYDV genome, which include LIRs (red suns), SIR (blue star), and Rep
protein (light brown cloud). Upon delivery to the host cell nucleus, the BeYDV vector nicks the
LIRs via the expression and function of the Rep protein. The released ssDNA is then circularized
and a complimentary strand is made to produce dsDNA. The dsDNA is then used to produce
copious amounts of mRNA for recombinant protein production. Image credit: (Qiang Chen &
Huafang Lai, 2015).

N-linked Glycosylation in Plants and Animals

A core principle of biology is the tight association of structure and function. The structure

of proteins is dictated by its primary (amino acid sequence), secondary (hydrogen boding among

side chains, disulfide bonds), tertiary (resulting molecule shape), and quaternary (additional

protein molecules to form multimeric protein) structures. In addition, some proteins also rely on

post-translational modifications (PTM) for proper folding, function, and regulation. Examples of

PTM include phosphorylation, acetylation, methylation, ubiquitination, and glycosylation. PTM can

be done on a protein's N or C termini or on amino acids between the termini. *N*-linked and O-

linked glycosylation are important PTM as they assist in the proper folding, function, solubility, and stability of the protein.

       N-linked glycosylation is observed in all domains of life, and as such, plants are fully equipped to perform this type of PTM (Aebi, 2013). However, there are some important differences between plant and mammalian *N*-linked glycosylation, the most important in terms of plant produced biologics for therapeutic use, is the attachment of carbohydrates found only in plants. This poses a potential problem since foreign carbohydrates can be immunogenic and potentially cause adverse effects. The initial steps in *N*-linked glycosylation are conserved in animals and plants, however, two plant specific carbohydrates that are not present in animals, β1,2-xylose and α1,3-fucose, are added in plant *N*-linked glycosylated proteins, which can be potentially immunogenic for human use (R. Strasser, Altmann, Mach, Glössl, & Steinkellner, 2004). Advances in plant glyco-engineering have led to the generation of plants that are capable of producing human-like *N*-linked glycans that forgo potential immunogenic consequences by producing glycans that lack β1,2-xylose and α1,3-fucose and produce the GnGn glycan structure (Schahs et al., 2007; R. Strasser et al., 2008)(Figure 16). The GnGn glycan structure is non-immunogenic and, when present in immunoglobulins (Ig), has benefits that will be discussed in the following chapter.
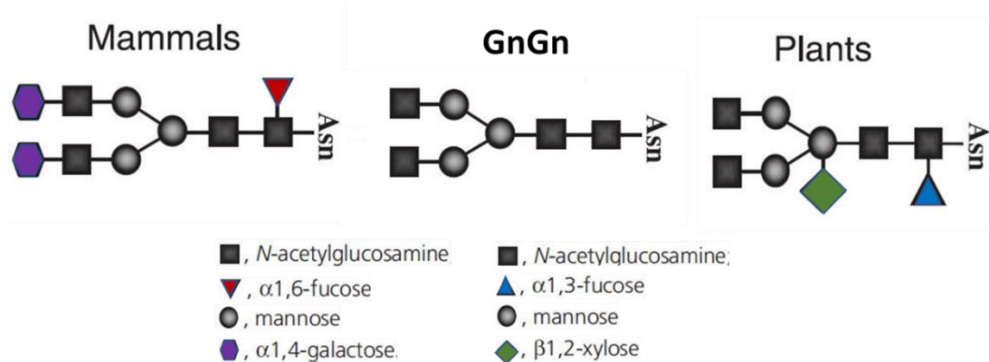
Figure 16. *N*-linked Glycosylation in Mammals and Plants. The initial steps in *N*-linked glycosylation is conserved among plants and animals. However, plants add the carbohydrates β1,2-xylose and α1,3-fucose, which are not present in mammals and may cause adverse effects if therapeutic proteins containing those carbohydrates are administered in medical use. Advances in plant glycoengineering have led to transgenic plants that are capable of producing *N*-linked glycan structures (e.g. GnGn) that are mammalian-like. Image adapted from: (Schahs et al., 2007).

The ability to glyco-engineer plants has allowed for the tailor-making of therapeutic recombinant proteins with defined *N*-glycans that no longer pose concerns for use in medical treatments and diagnostics. Furthermore, the speed and reduced cost at which plants are capable of producing therapeutic proteins makes plant-based platforms attractive in producing urgently needed biologics in both developed and developing countries.

Bispecific Antibodies

The concept of bispecificity on a single antibody molecule was described in 1960, over half a century ago (Nisonoff, Wissler, & Lipman, 1960). Since then, two bsAbs have been approved and are on the market as anti-cancer therapeutics with the first bsAb made available in 2009 (Catumaxomab) and the second in 2014 (Blinatumomab) (Kontermann & Brinkmann, 2015). Interestingly, one of the first envisioned applications for bsAbs was an anti-cancer where one arm targeted T cell specific molecules (e.g. CD3) and the other arm targeted an antigen on a cancerous cell (Perez, Hoffman, Shaw, Bluestone, & Segal, 1985; Staerz, Kanagawa, & Bevan, 1985).

A large number of bsAb designs and strategies to assemble them have been described since then. However, technical difficulties in assembly of the bsAbs have hampered progress in their evaluation both in laboratory and clinical settings. During the assembly of bsAbs in the same producer cell, no preferential pairing of a specific light chain with a specific heavy chain has been observed, thus multiple strategies to guide the pairing of two cognate heavy and light chains of each arm of the bsAb have been devised (Kontermann & Brinkmann, 2015). One of the first strategies described to achieve heterodimerization of heavy chains to form a bsAb was the use of the "Knobs-into-Holes" (KiH) strategy (Ridgway, Presta, & Carter, 1996). In the KiH strategy, mutations are introduced in the CH_3 domain of the heavy chain in which bulky amino acid side chains are substituted to produce a "knob" and less-bulky amino acids are also substituted into the CH_3 domain of the partner heavy chain to form a "hole," thereby driving the

25

heterodimerization of these heavy chains. A similar approach involving the substitution of

oppositely charged amino acids on contact regions of the CH_3 domains of the heavy chains to

drive heterodimerization has also been described (Figure 17) (van Gils & Sanders, 2017).
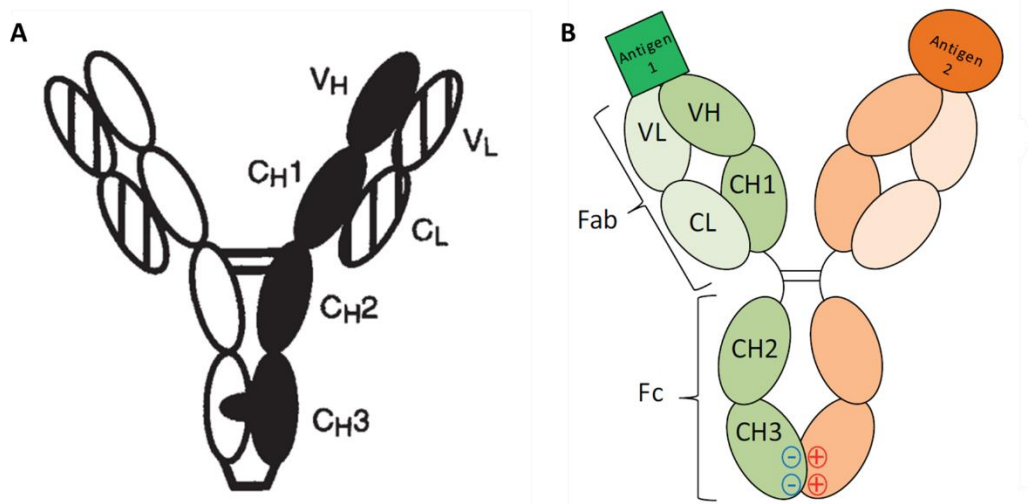
Figure 17. Heterodimerization of Heavy Chains in bsAb Assembly via Knobs-into-Holes and Electrostatic Interactions. (A) Heterodimerization of heavy chains for bsAb assembly can be driven via the mutation of specific amino acids in the CH_3 domain with bulkier side chains on one heavy chain and the substitution of amino acids with less bulkier side chains on the opposite heavy chain. (B) Heterodimerization of heavy chains can also be driven by electrostatic interactions via the substitution of oppositely charged amino acids on heavy chains. Image modified from: (A) (Ridgway et al., 1996), (B) (van Gils & Sanders, 2017).

Designs of bsAbs fall into two main categories, bsAbs that contain an Fc region and

bsAbs that do not contain an Fc region (Kontermann & Brinkmann, 2015). Designs that contain

an Fc region generally offer the effector functions that, for example, a bsAb based on an IgG1

has, such as binding to C1q for complement activation, ADCC, antibody dependent cellular

phagocytosis (ADCP), neonatal receptor (FcRn) binding, and binding to a variety of FcRs on

immune cells. On the contrary, bsAbs that only contain antigen binding regions do not offer more

than their binding to two different antigens and generally have shorter half-lives. However, these

Fc-less designs are typically smaller in size and can better serve some purposes over their Fc

bearing counterparts, such as improved tissue penetration.

The application of bsAbs covers areas in which medical needs have not been met or can

be beneficial on their own or complementary to existing treatments. As mentioned above, bsAbs

have been on the market for the treatment of certain cancers whereby one arm of the bsAb binds to an immune cell, generally a T cell (e.g. binds to CD3), and the other arm binds to an antigen on a cancerous cell (e.g. binds to CD29 on B cells), thereby bringing the cells together and facilitating the killing of the cancerous cell by the T cell (Trabolsi, Arumov, & Schatz, 2019).

Furthermore, in cases where neuroinvasion of an infectious pathogen has occurred, e.g. neurotropic WNV or rabies virus infection, the administration of a single or cocktail of mAbs will not suffice to neutralize the virus due to the inability of the mAb to cross the blood-brain barrier (BBB) and access the brain parenchyma to neutralize the pathogens. In these instances, a bsAb with one arm targeted against a receptor (e.g. the transferrin receptor) that will trigger transcytosis and facilitate its transport across the BBB is needed. Once in the brain parenchyma, the other arm of the bsAb can now access and neutralize the pathogen and clear the neurotropic infection.

Similarly, bsAbs with an arm that affords them access to a compartment where they are subsequently exposed to a target epitope has also been described. Like in the above example, the use of separate parental mAbs would not yield the desired result, owing to a lack of accessibility to the target. An example of this "Trojan horse" approach was described where a highly effective bsAb against Ebola targeted the surface glycoprotein (GP) of the virus with one variable region of the bsAb and the second variable region of the bsAb targeted the receptor Niemann-Pick C1 (NPC1) found in the late endosome. Once the bsAb bound to NPC1, the EBOV was unable to escape the endosome thereby terminating the infection (Wec et al., 2016). The administration of the parental mAbs as a cocktail would not terminate an EBOV infection since the anti-NPC1 mAb would not have access to the late endosome on its own (where the NPC1 receptor is exposed) and the anti-GP mAb would not bind to the NPC1 receptor.

The application of bsAb is broad and offers an alternative to the challenging development of highly needed effective vaccines. The simultaneous targeting of two antigens on the same molecule offers advantages that cannot be achieved by the administration of a cocktail

of parental mAbs. Furthermore, in the case of highly related co-circulating viruses, such as DENV and ZIKV, the use of a bsAb can help by neutralizing both viruses and circumvent ADE.

Summary

Among arboviruses, FVs pose the greatest threat to human health. Recently, an FDA approved vaccine for Dengue (Dengvaxia) was approved, however, it has limitations on potential recipients of the vaccine. The ZIKV lacks an FDA approved vaccine and treatment. Furthermore, these two FVs co-circulate and may cause co-infections. Reports have also indicated cross-reactivity of mAbs produced against one virus to the other, thereby potentially triggering ADE in both of these viruses. Plant biotechnology has advanced to a state where therapeutic recombinant proteins can be produced at speeds, quantities, and with safety and efficacy profiles that match and outperform traditional protein production platforms. The application of bsAbs is wide, ranging from infectious diseases and cancer. The use of bsAbs is necessary when the binding of two different epitopes or antigens by one molecule is required.

Dissertation Overview

The goal of the research presented in this dissertation was to 1) design and produce new bispecific antibodies for potential therapeutic use against co-circulating FVs like the DENV and ZIKV, 2) demonstrate the safety and efficacy of the bsAb, 3) produce a plant-made bsAb that can neutralize and prevent ADE. Plants offer many advantages over traditional systems of therapeutic mAb production, among them the use of glycoengineered plants. Glycoengineering in plants has led to the ability to not only produce human like *N*-linked glycans, but also tailor make *N*-linked glycans with specific carbohydrates to modulate an immune response. We also aimed to produce antibody derivatives in plants such as diabodies and single chain variable fragments (scFvs). Diabodies are small bivalent molecule based on the variable regions of mAbs and due to their small size, are able to better aid in diagnostics, imaging, and potential therapeutic use in cancer therapy.

CHAPTER 2

PLANT-PRODUCED ANTI-DENGUE VIRUS MONOCLONAL ANTIBODIES EXHIBIT REDUCED

ANTIBODY-DEPENDENT ENHANCEMENT OF INFECTION ACTIVITY

Introduction

The *A aegypti* mosquito is the primary vector of the DENV, both of which are endemic in

tropical countries of Africa, Southeast Asia, and the Americas (N. E. Murray et al., 2013). The

DENV belongs to the *Flaviviridae* family, which includes medically important viruses such as the

YFV, WNV, Japanese Encephalitis Virus (JEV), and the recently re-emerged ZIKV. The genome

of these viruses consists of positive sense single stranded RNA with a single open reading frame

that is directly translated by the host cell to produce a single large polypeptide that is

subsequently cleaved by viral and host cell proteases into 3 structural and 7 non-structural

proteins. The 3 structural proteins include the C protein, premembrane/Membrane (prM/M)

protein, and E protein. The seven non-structural proteins include NS1, NS2, NS2A, NS3, NS4A,

NS4B, and NS5. The E protein is the most immunodominant viral structural protein and is the

main target of the humoral response (Beltramello et al., 2010). The structure of the DENV E

protein is exemplary of the genus, containing a three domains EDI-EDIII, in which EDI is the

central β-barrel domain, ED2 is elongated and contains at its tip the conserved FV fusion loop,

and EDIII at the C-terminus of the protein is immunoglobulin-like and is the putative receptor

binding domain (Kuhn et al., 2002; Mukhopadhyay et al., 2005).

The DENV has four serotypes (DENV1-4) and applies a severe health concern and

burden in tropical and subtropical countries with 3 billion people at risk of infection (N. E. Murray

et al., 2013). An initial infection with any of the DENV serotypes is usually self-limiting with

patients experiencing mild fevers, rash, and general discomfort. However, a subsequent infection

with a heterologous serotype can lead to severe and life threatening forms of DENV caused

illness such as DHF and DSS (S. B. Halstead, 2007; Rothman, 2004). There has been an

increase of incidence of DHF/DS in regions where the DENV generally caused DF (Murphy &

Whitehead, 2011; Rico-Hesse et al., 1997). This shift has been attributed to an increase in international travel and globalization, which may have allowed for the inadvertent range expansion its mosquito vector and introduction of all four serotypes into new regions (Kyle & Harris, 2008; Wilder-Smith & Gubler, 2008). In light of the increased expansion of the DENV to regions outside of its normal range, treatment for the diseases caused by the virus are largely supportive. Recently, Dengvaxia, a DENV vaccine, was FDA approved. However, Dengvaxia comes with limitations whereby candidates for the vaccine must be first screened for prior DENV infection (Thomas & Yoon, 2019). Seronegative results of the screening eliminate candidacy for Dengvaxia vaccine use, leaving out a major portion of susceptible individuals. Thus, a therapy is urgently needed to treat potential DENV infected patients.

There has been an increase in passive immunotherapy treatments in the form of monoclonal antibody (mAb) use for a variety of diseases ranging from viral diseases to cancers. This form of therapy is an attractive option due to the efficacy and specificity that are inherent in mAbs. Additionally, the production capabilities of these therapeutics in various platforms makes mAbs attractive (Chen & Lai, 2014). Difficulties in offering a DENV therapeutic mAb for clinical use have been encountered, mainly due to the induction of the phenomenon known as ADE. ADE occurs when non-neutralizing mAbs produced against an initial infection with a particular DENV serotype bind to but do not neutralize subsequent heterologous DENV serotypes in secondary infections (Morens, 1994). This leads to an increased infection of $Fc\gamma R$ bearing cells, such as monocytes and macrophages. Consequently, an increased viral load and progression to severe forms of DENV disease such as DHF and DSS ensues. In this instance, an effective mAb would have the ability to neutralize all DENV serotypes and forgo ADE. Furthermore, effector functions conferred by the Fc regions of the mAb, such as ADCC and CDC would be preferable and advantageous to the therapy.

The main platform of therapeutic mAb production has been mammalian cell culture, in particular the use of Chinese Hamster Ovary cells (CHO), however, plants have recently become an attractive option for mAb production due to their ability to produce safe, efficient, and scalable

quantities of mAbs (Chen & Davis, 2016). The most important and widely used plant for this application has been the tobacco plant *N. benthamiana*, as it has been extensively used to produce biologics such as enzymes, vaccines, and mAbs (Tuse, , Tu, & McDonald, 2014). As an example of the application of *N. benthamiana* made mAbs, during the Ebola outbreak of 2014 in Western Africa, three health care workers infected with the EBOV were treated with ZMapp. ZMapp is a cocktail of 3 anti-EBOV mAbs produced in *N. benthamiana* plants (Arntzen, 2015). Additionally, an anti-WNV mAb (E16) produced in *N. benthamiana* protected mice from a lethal infection with WNV despite administering the mAb 4 days post-infection (J. He et al., 2014; H. Lai et al., 2010; H. Lai et al., 2014).

IgG mAbs are *N*-linked glycosylated at Asn297, a residue that lies in the CH2 domain of the gamma chain. The *N*-linked glycan in that position consists of the "GnGn" type glycan, which contains three mannose and two N-acetylglucosaminyl carbohydrate residues. This *N*-linked glycan structure is present irrespective of the type of cell producing it (e.g. plant or animal cell). However, the GnGn structure is further modified differently in animal and plants cells, wherein plants the $GnGnXF_3$ glycoform is dominant and is composed of the addition of β1,2-xylose and α1,3-fucose (F_3), whereas the animal cell will produce β1,4-galactose (A) and α1,6-fucose (F_6) among many other modifications (Chen, 2016). The plant specific carbohydrates β1,2-xylose and α1,3-fucose have caused concern for fear of an adverse immune response if present in glycoproteins to be used in human clinical use.

Thus, the glycoengineering of plants, specifically *N. benthamiana*, was pursued to knock down or knock out enzymes responsible for adding plant-specific glycans in *N*-linked glycosylation and simultaneously introduce genes that would introduce human carbohydrates to *N*-linked glycosylation to produce human like glycoproteins (Chen, 2016; Richard Strasser, Altmann, & Steinkellner, 2014). In an attempt to achieve such glycosylation profiles, Strasse et al. produced a mutant ΔXTFT *N. benthamiana* plant by employing RNA interference (RNAi) to silence the β1,2-xylosyltransferase and α1,3-fucosyltransferase genes responsible for adding β1,2-xylose and α1,3-fucose, respectively, and produce the GnGn type glycan as the principle

31

glycan (R. Strasser et al., 2008). Their attempts were successful and mAbs produced by the

ΔXTFT *N. benthamiana* plant not only produced the GnGn *N*-linked glycan, but it also produced a

homogenous mixture of it. This was an immensely impactful result since the high level of

homogeneity seen in *N*-linked glycans produced in plants is virtually absent in other systems,

such as mammalian cell cultures (Loos & Steinkellner, 2014; R. Strasser et al., 2008).

Furthermore, the identity of carbohydrates present in *N*-linked glycans is a major determinant in

the affinity to which an IgG binds to different FcγRs present in humans. Thus, plant

glycoengineering has now allowed us to bias if not direct an IgG to bind to specific FcγRs and

promote effector functions such as ADCC and CDC or avoid adverse effects such as ADE.

In the present study, the previously described chimeric E60 mAb was produced in both

WT and int the ΔXTFT *N. benthamiana* plant using a transient expression system. Furthermore,

the ability of each mAb to forgo ADE was evaluated. The E60 mAb binds to the fusion loop found

on domain 2 of the DENV E protein and is able to neutralize all four serotypes of the DENV (T. C.

Pierson et al., 2007). The plant derived E60 mAbs displayed GnGnXF3 or GnGn type *N*-linked

glycans to a remarkably high degree and, like the mammalian cell produced E60, they were able

to potently neutralize both DENV-2 and DENV-4 serotypes in a plaque reduction neutralization

test (PRNT). Furthermore, the *N*-linked glycans on both WT and ΔXTFT *N. benthamiana*

produced E60 (pE60) conferred them with the ability to elicit effector functions such as ADCC,

CDC, and binding of C1q. C1q is an important component of the complement system in both the

classical and alternative pathways of complement activation.

The present study demonstrates the superiority of both WT and ΔXTFT *N. benthamiana*

made E60 mAbs when compared to mammalian cell made E60 (mE60). The data presented here

showed that the pE60 mAbs have the ability to significantly reduce ADE and retain abilities to

promote effector functions such as ADCC, CDC, and C1q binding. An aglycosylated E60 (aE60)

mAb variant may have the ability to significantly reduce ADE, however, the aE60 may not

promote ADCC, CDC, C1q binding abilities, and have a severely impacted half-life. All results

considered, the pE60 mAb may be the best option for potential passive immunotherapy in urgent situations of DENV disease.

Materials and Methods

Construction of E60 expression vectors.

The human IgG coding sequences for CH and LC were fused to the coding sequences of synthesized VH and VL of E60 (GenBank accession nos KC254889.1 and KC254888.1), respectively. The E60 CH and LC coding sequences where then cloned into pICH21595 and pICH11599 MagnICON plant expression vectors using the EcoRI and BamHI restriction enzymes. The resulting plant expression vectors were then transformed into *A. tumefaciens* GV3101 for delivery to plant cells as previously described (Junyun He, Lai, Brock, & Chen, 2012; H. Lai et al., 2010). The CHO-K1 cells were lipofectamine transfected with the pcDNA3.1 (Thermo Fisher Scientific) expression vector after cloning the E60 LC and HC sequences using BamHI and NotI restriction enzymes. 1 ug each of HC and LC containing expression vectors were mixed with 100 uL of Opti-MEM media (Thermo Fisher Scientific) and 12 uL of lipofectamine and incubated at RT for 45 min. Thereafter, the complexes were diluted with 300 uL of Opti-MEM and 200 uL of the diluted composed was added to 200 uL of F12 media and mixed. The mixture was then overlaid onto 3.5 X 10^5 CHO-K1 cells that were at approximately 90% confluence in a 12-well plate and incubated for 5 hours in 5% CO_2. Then, 10% final concentration of serum was added to each well and incubated for an additional 48 hours. Thereafter, 96-well plates containing F12 media with 250 ug/mL of zeocin and 300 ug/mL of hygromycin, were used to add 5-10 cells   to select for successfully transfected cells. After 21 days, positive single-cell colonies were transferred to 48 well plates and allowed to reach near full confluency and then transferred to larger volume well-plates.

Transient Expression of pE60 mAb variants in WT and ΔXTFT *N. benthamiana* leaves.

A ratio of 4:1 HC and LC, respectively, was used to enhance he assembly of the pE60 using the MagnICON system with associated modules to agroinfiltrate both WT and ΔXTFT *N. benthamiana* leaves as previously described (Chen & Lai, 2015; Chen et al., 2013).

Extraction and purification of pE60 variants from plant leaves.

To assess the expression levels of pE60, the agroinfiltrated leaves were harvested at 5, 6, 7, 8, and 9 DPI. Agroinfiltrated leaves were harvested at 8 DPI for other protein analyses purposes. Briefly, the leaves were homogenized in extraction buffer containing 50 mM Tris/HCl at pH 7.5 and 150 mM NaCl. The sample was then centrifuged at 15K G for 30 min at 4 C to clarify the sample. The pE60 containing samples were then further clarified by a two-step purification process that included $(NH_4)_2SO_4$ precipitation followed by protein A affinity chromatography, as previously described (H. Lai et al., 2010; H. Lai, He, Engle, Diamond, & Chen, 2012).

Purification of mE60 from CHO cell culture.

Supernatant from the E60 transfected CHO-K1 cells was clarified by centrifuging at 15K G for 30 min at 4 C. mE60 in the clarified media was directly loaded onto a protein A affinity chromatography column for purification as described by (H. Lai et al., 2012).

Enzyme-linked Immunosorbent Assay (ELISA)

To assess the binding of pE60 to the DENV-2 E protein, ELISA was performed as previously described (Junyun He et al., 2012). Briefly, DENV-2 E protein was coated on 96-well plates and subsequently treated with plant or cell culture E60 variants. An HRP conjugated anti-gamma mAb was used to detect the E60 mAbs. A generic human IgG was used as a negative control and the mammalian cell made E60 was used as a positive control and the plates were developed with tetramethylbenzidine substrate (KPL). The experiments were done in triplicates and 3 separate times. The K_d was determined by non-linear regression analysis using a one site

binding model via the GraphPad Prism software. K_d values were compared between pE60 and

mE60 mAbs and P values were determined by unpaired t-test. P value of <0.005 indicated

statistically significant differences.

Antibody-dependent enhance of infection (ADE) assay.

ADE for mAbs was assessed by using K562 cells bearing FcγR2a receptors (ATCC CCL-

2243). Briefly, eight 3-fold serial dilutions of E60 mAb variants or a negative control human IgG

were incubated with DENV-2 (ATCC VR-1584) for 1 hour at 37 C. The virus-mAb complex was

then mixed with K562 cells at a MOI of 1. The cells were then incubated for 48 hours, thereafter

the cells were washed with PBS, fixed with 4% paraformaldehyde (Sigma) and permeabilized

with 0.1% saponin (Sigma). The cells were then stained with 4G2 (ATCC HB112) that was

conjugated with Alexa 488 (Invitrogen), washed and then analyzed with a Navios flow cytometer

(Beckman Coulter) to determine the percentage of infected cells (4G2-positive).

SDS-PAGE, Western blot, and inducible yeast display assay.

Electrophoresis analysis was performed under non-reducing and reducing (5% v/v, β-

mercaptoethanol) conditions on 10% or 4-20% gradient SDS-PAGE. The resulting gels were

stained with Coomassie blue or the mAbs were transferred to a PVDF membrane for Western

blot analysis. E60 mAbs were detected using human-kappa LC or human-gamma HC (Southern

Biotech) HRP-conjugated mAbs (H. Lai et al., 2014). DENV-2 E DI-II was expressed on an

inducible yeast surface display assay. Following induction, the yeast were stained with mAb

variants and analyzed with a Becton Dickinson FACSCalibur flow cytometer as previously

described (H. Lai et al., 2010).

DENV-2 and DENV-4 Focus Reduction Neutralization Test (FRNT).

mAb variants were 0.5-fold serially diluted in serum free medium (SFM) (Opti-MEM, Life

Technologies) whereas DENV-2 and DENV-4 (TUP-2174, kindly provided by Dr. John F.

Anderson) were diluted in SFM to reach 100 p.f.u. per well. After dilutions, DENV-2 and DENV-4 were added to eh diluted mAbs and incubated for 1 hour at RT then the dilutions were added to 90-95% confluent Vero cells (ATCC CCL-81, 1 X106 cells/mL in SFM and incubated for an additional hour at 37 C. The medium was then removed and fresh medium containing OptiMEM-glutamax, 2% FBS, and 1% methylcellulose was added and incubated in 5% CO2 at 37 C for 4 days. The overlay medium was then removed, cells washed twice with PBS and treated with 4% paraformaldehyde (PFA). Thereafter, the cells were washed and blocked with 2% normal goat serum (Life Technologies) with 0.4% Triton-X100 (Sigma) for 1 hour at RT. The cells were then probed with the 4G2 mAb (ATCC D1-4G2-4-15 HB-112) at a 1:100 dilution overnight at 4 C. The cells were then washed again with PBS and detected with polyclonal goat anti-moue-HRP secondary IgG (KPL) at a 1:1000 dilution for 2 hours at RT. The plates were developed with TrueBlue peroxidase substrate (KPL) and counted as focus forming units using (f.f.u.) an Axiostar Plus light microscope (Zeiss). Percentage neutralization was calculated using the following equation: [(number of DENV f.f.u. per well w/o mAb) - (# of DENV f.f.u./well of diluted mAb)/(# of DENV f.f.u./well w/o mAb) X 100]. The EC50 of each mAb was determined using the GraphPad Prism software.

_N_-linked glycan analysis.

_N_-linked glycosylation profiles were determined by liquid chromatography electrospray-ionization mass spectrometry (LC-ESI-MS) as described previously (Stadlmann, Pabst, Kolarich, Kunert, & Altmann, 2008).

Results

Expression and assembly of E60 mAb in _N. benthamiana_

After cloning of E60 HC and LC into MagnICON expression vectors and subsequent transformation into _A. tumefaciens_ strains, _N. benthamiana_ WT and ΔXTFT variants were agroinfiltrated (Chen et al., 2013; Giritch et al., 2006). HC and LC genes of E60 were also cloned

into the pcDNA3.1 vector for Chinese hamster ovary (CHO) cell production of mammalian E60 (mE60). Western blot analysis was performed to evaluate the expression of pE60 in ΔXTFT *N. benthamiana*. Results indicated the presence of the light chain (anti-kappa detection) at the expected 25 kDa position under reducing conditions (Figure 18a, lane 3) and at approximately 150 kDa under non-reducing conditions was observed (Figure 18a, lane 6). For comparison, the WNV E16 LC was also detected using an anti-kappa approach in both reducing (Figure 18a, lane 1) and under non-reducing conditions (Figure 18a, lane 4). Unfiltered leaves yielded no signal when probing for the LC under reducing conditions (Figure 18a, lane 2) and non-reducing conditions (Figure 18a, lane 5). Detection of the LC in non-reducing condition at the expected position of approximately 150 kDa indicated proper assembly of the mAb via the forming of HC and LC dimers. WB analysis of WT *N. benthamiana* yielded similar results. Evaluation of the expression of the HC via Western blot analysis was also done, where the heavy chain of the pE60 was detected using an anti-gamma-HRP conjugated mAb revealed a signal band at the approximate 50 kDa position (Figure 18b. lane 3). As a control, the WNV heavy chain was also detected at 50 kDa (Figure 18b, lane 1). Uninfiltrated leaves yielded no signal for a HC (Figure 18b, lane 2). Western blot analysis of the HC and LC of mE60 yielded similar results with the HC and LC appearing in their expected banding regions of 50 and 25 kDa under reducing conditions, respectively.
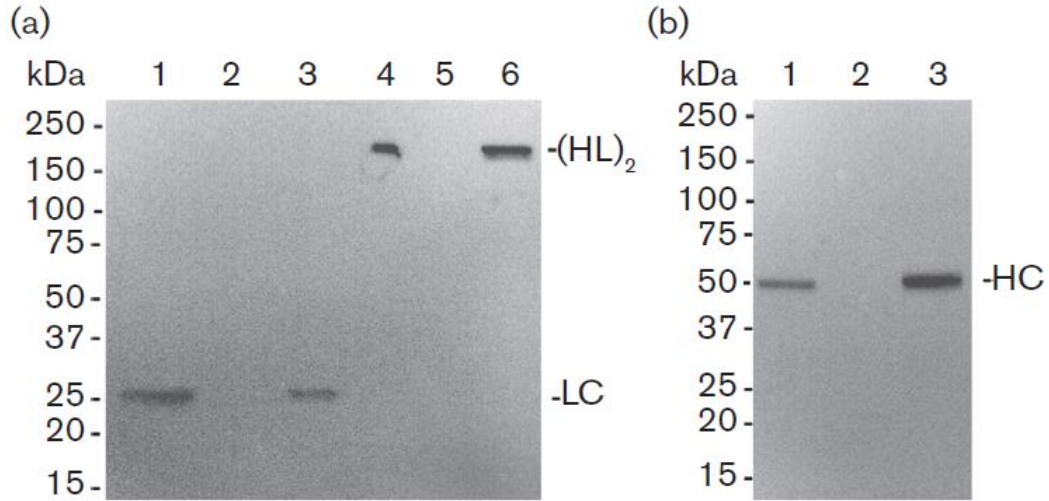
Figure 18. Western Blot Analysis of pE60. (a) The light chain of pE60 was observed at the approximate 25 kDa position under reducing conditions (lane 3). Under non-reducing conditions, the LC was detected at approximately 150 kDa, indicating full assembly of the pE60. As a comparison, the LC of the WNV E16 mAb was detected at approximately 25 kDa in reducing conditions (lane 1) and at approximately 150 kDa in a fully assembled E16 mAb under non-reducing conditions (lane 4). Lanes 2 and 5 detect no LC in uninfiltrated leaves. (b) The heavy chain of the pE60 was detected at approximately 50 kDa under reducing conditions (lane 3) and no signal of a HC was detected in uninfiltrated leaves (lane 2). As a comparison, the HC of the WNV E16 was also detected at approximately 50 kDa under reducing conditions (lane 1).

The expression level of pE60 was also evaluated, which revealed maximum expression on day 8 and reduced expression thereafter. (Figure 19).
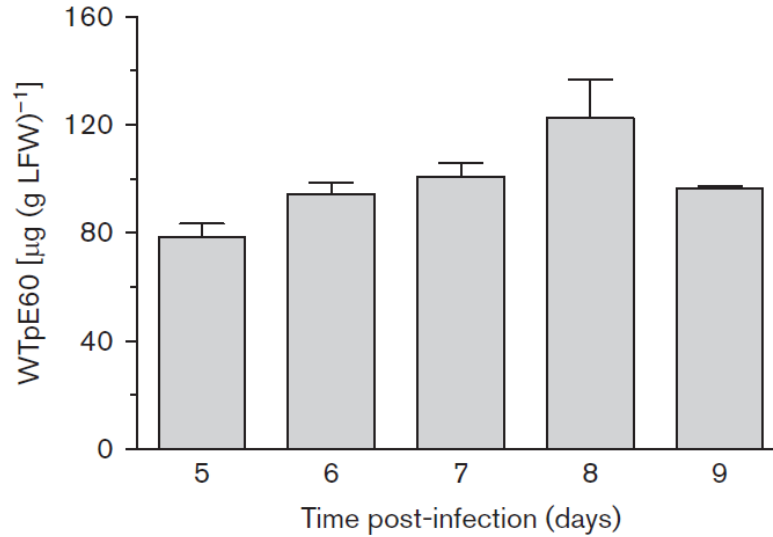
Figure 19. Expression Levels of pE60 from *N. benthamiana* Leaves 5-9 DPI. The expression level of pE60 5-9 DPI was assessed via ELISA. The maximum expression level of pE60 was day 8 at approximately 120 (ug/g LFW) and expression level decreased thereafter. LFW = leaf fresh weight.

Purification of pE60 from leaves of *N. benthamiana*

The purification of WT and ∆XTFT *N. benthamiana* produced E60 was achieved via a two-step process. $(NH_4)_2SO_4$ precipitation was used first followed by protein A affinity chromatography (H. Lai et al., 2010; H. Lai et al., 2012). A purity of >90% was achieved for both WT and ∆XTFT *N. benthamiana* produced E60 and CHO cell produced mE60 (Figure 20.)
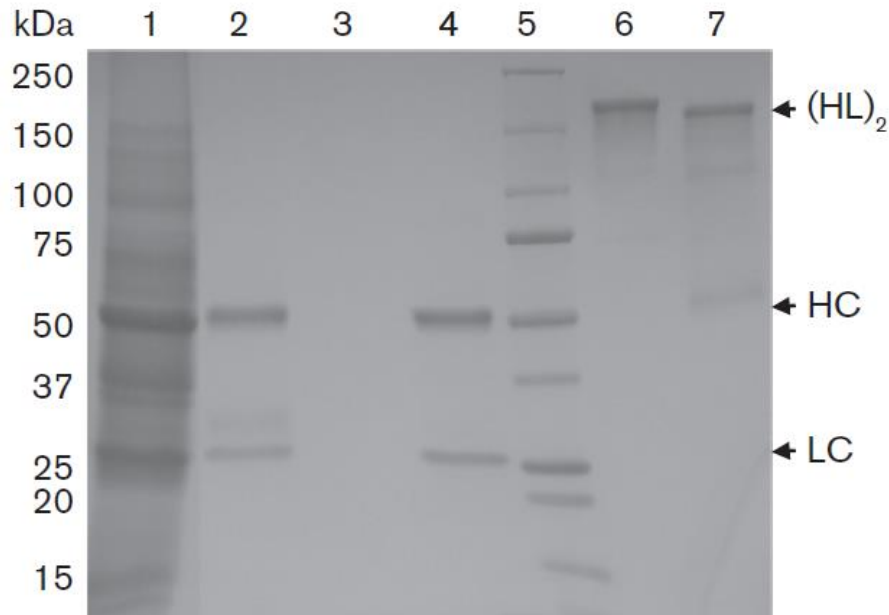
Figure 20. Purity Assessment of pE60 via Coomassie Stained SDS-PAGE Analysis. The two-step purification process yielded >90% purity of the pE60. ΔXTFT *N. benthamiana* produced E60 under reducing conditions yielded two bands, HC at approximately 50 kDa and LC at approximately 25 kDa (lane 2). Under non-reducing conditions, a fully assembled pE60 mAb was observed at the approximate 150 kDa position (lane 6). Lanes 4 and 7 show banding patterns of the plant made WNV E16 under reducing conditions (lane 4) and non-reducing conditions (lane 7). Lane 1 contains total soluble protein extract from the leaves.

_N_-linked glycosylation profiles of pE60

      N-linked glycosylation at Ans297 of the Fc region is important in both pharmacokinetics and effector functions of mAbs. The glycosylation profile of both WT and ΔXTFT *N. benthamiana* produced E60, mE60, and pE16 were assessed via liquid chromatography electrospray-ionization mass spectrometry (LC-ESI-MS) (Table 1). The results indicate an astonishing near homogenous mixture of the GnGn type glycan lacking the potentially immunogenic β1,2-xylose and α1,3-fucose residues. The WT *N. benthamiana* produced E60 showed a slight mixture of glycans, with the major glycan present GnGnXF3 at 70% followed GnX and GnGn at 10% each. The mammalian cell made E60 displayed 50% $AGnF_6$ and 40% AAF_6 type glycans. These results reveal the unmatched ability of the ΔXTFT *N. benthamiana* to produce near homogenous GnGn type glycans.

Major *N*-glycan species	WTpE60 (%)	ΔXFTpE60 (%)	mE60 (%)	ΔXFTpE16 (%)
GnGnXF$_3$	70			
GnX	10			
GnGn	10	95		95
AGnF$_6$			50	
AAF$_6$			40	

Table1. Glycosylation Profile of WT and ΔXTFT *N. benthamiana* Produced E60. The glycosylation profiles of WT and ΔXTFT *N. benthamiana* produced E60 were analyzed by LC-ESI-MS. The results indicate that pant produced E60 and the anti-WNV E16 mAb were 95% glycosylated with the same glycans, GnGn for ΔXTFT *N. benthamiana* produced E60 and E16. WT *N. benthamiana* produced E60 revealed 70% GnGnXF$_3$ type glycans and 10% of GnX and GnGn respectively. These results are significant in that *N*-linked glycans can now be produced with near homogeneity in glycoengineered plants. This provides the ability to determine the roles specific glycan or carbohydrates play in biological interactions. In contrast to *N. benthamiana* produced E60, mammalian cell produced E60 contained AGnF$_6$ and AAF$_6$ glycans at 50 and 40%, respectively.

Binding specificity and kinetics of pE60 to antigen

The WT and ΔXTFT *N. benthamiana* produced E60 were also assessed for their binding kinetics and binding affinities via ELISA. DENV-2 E DI-II was immobilized and tested against pE60 and mE60 mAbs (Figure 21). The results indicated k_D values of 13.6, 12.7, and 12.7 for WT E60, ΔXTFT E60, and mE60 respectively. These results show similar affinities among the E60 mAbs, indicating the proper folding and structure of pE60 mAbs as compared mE60.
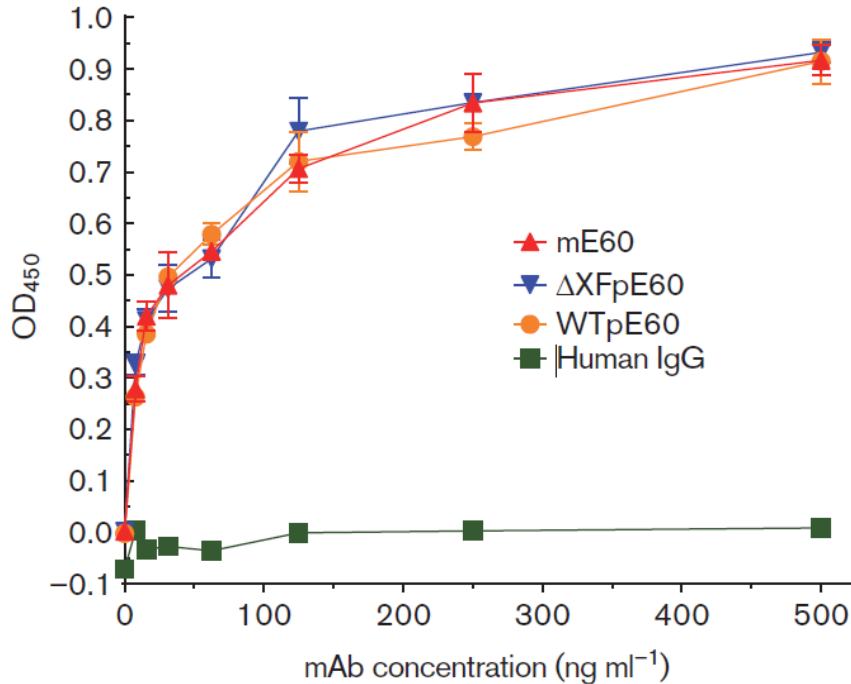
Figure 21. Binding Affinities of pE60 and mE60 to DENV-2 EDI-II via ELISA. ELISA analysis of pE60 and mE60 binding affinities were quite similar, with kD values of 13.6, 12.7, and 12.7 for WT E60, ΔXTFT E60, and mE60 respectively. A generic human IgG did not show any significant binding to DENV-2 E DI-II. These results indicate proper folding and structure of the pE60 variants and comparable binding affinities to mE60.

The specificity of WT and ΔXTFT *N. benthamiana* produced E60 was also assessed by an induced yeast display assay where yeast displayed DENV-2 EDI-II on their surface. The results showed that WT and ΔXTFT *N. benthamiana* produced E60 bound to the yeast displayed DENV-2 EDI-II, as shown by the observance of a new fluorescent peak, similar to that of the mammalian cell produced E60 (Figure 22). Uninduced yeast and a negative control mAb (pGP1) did not show a second fluorescent peak.
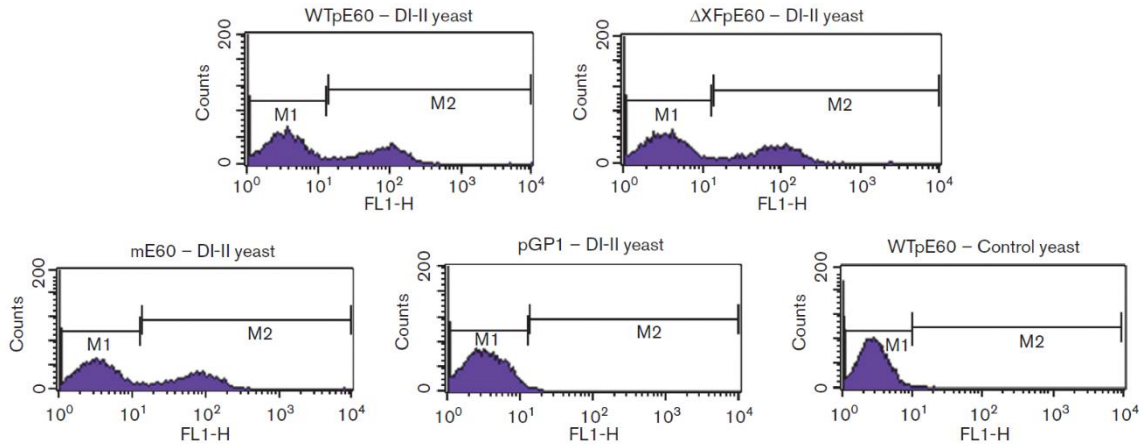
Figure 22. WT and ΔXTFT *N. benthamiana* Produced E60 Bind to DENV-2 E DI-II Displayed on the Surface of Yeast. The WT and ΔXTFT *N. benthamiana* produced E60 showed binding specificity to DENV-2 E DI-II displayed on the surface of yeast by the observation of a second peak of fluorescence, which was also observed when the mammalian cell made E60 was used in the same assay. In contrast, a negative control IgG (pGP1) and uninduced yeast did not show a second peak of fluorescence. The results shown here indicate that the pE60 mAb variants are expressed and correctly assembled in plants and are able to bind to its target.

Neutralization of DENV-2 and DENV-4 by mE60 and pE60

The neutralization abilities of the WT and ΔXTFT *N. benthamiana* produced E60 mAb against DENV-2 and DENV-4 was assessed via a focus reduction neutralization test (FRNT). The results revealed neutralization of the DENV-2 and DENV-4 viruses by both pE60 mAbs. In neutralizing DENV-2, the ΔXTFT produced E60 had the lowest EC_{50} of 230.7 ng/mL, followed by the mE60 with an EC_{50} of 362.1 ng/mL, and finally the WT pE60 with a 433.5 ng/nL EC_{50}. The DENV-4 neutralization data revealed a slightly different trend with the lowest EC_{50} displayed by the WT pE60 at 377.8 ng/mL, followed by ΔXTFT pE60 at an EC_{50} of 658.5 ng/mL, and the mE60 had an EC_{50} of 678.9 ng/mL.

mAb	DENV-2 EC_{50} (ng ml^{-1})$\pm$SEM	P value	DENV-4 EC_{50} (ng ml^{-1})$\pm$SEM	P value
mE60	362.10 ± 179.60		675.87 ± 200.34	
WTpE60	433.51 ± 82.29	0.75	377.82 ± 95.92	0.31
ΔXFpE60	230.77 ± 71.60	0.57	658.57 ± 14.03	0.94

Table 2. DENV-2 and DENV-4 Focus Reduction Neutralization Test with mE60 and pE60 mAbs. The FRNT test revealed mixed trends in mAb EC_{50} against DENV-2 and DENV-4. The ΔXTFT pE60 had the lowest EC_{50} at 230.7 ng/mL in the DENV-2 FRNT whereas the WT pE60 showed the lowest EC_{50} at 377.8 ng/mL in the DENV-4 FRNT.

Antibody-dependent enhancement of infection (ADE) characteristics of pE60 variants.

ADE has been suggested to be the main causative mechanism for pathogenesis in severe dengue disease leading to DHF and DSS. The binding of sub-neutralizing mAbs to DENV virions and subsequent receptor mediated endocytosis via binding of FcγRs on myeloid cells such as monocytes and macrophages leads to an increased replication of virions and subsequent increase in viral load leading to severe disease states. The identity of the glycan on of the Fc region of IgGs can influence its binding affinity to the various FcγRs. An ADE assay was performed using K562 cells bearing FγR2a, a receptor that has been implicated in binding to virus-mAb complexes and facilitating the entry of non-neutralized virions into the cell. The GnGn core glycan found on pE60 variants was assessed and compared to the mammalian cell mE60 for its ability to promote ADE. The results indicate ADE promotion when the mE60 mAb is complexed with DENV-2 (Figure 23). Conversely, no ADE was observed when the plant variants of E60 were complexed with DENV-2, which was also observed in the negative control generic human mAb.

The pE60 mAb variants and the mE60 mAb variants share identical DNA coding sequences and only differ in the cell which they are produced. Thus, the only difference is the identity of the *N*-linked glycans in their Fc region. Thus, it is believed that the glycan backbone on

the Fc region is responsible for the apparent lack of binding to the cellular FcγR2a receptors on

the K562 cells

The data demonstrate that pE60 mAb variants were able to virtually prevent ADE, unlike

the mammalian made mE60 mAb, suggesting a better mAb therapeutic against severe dengue

disease can be obtained in plants.
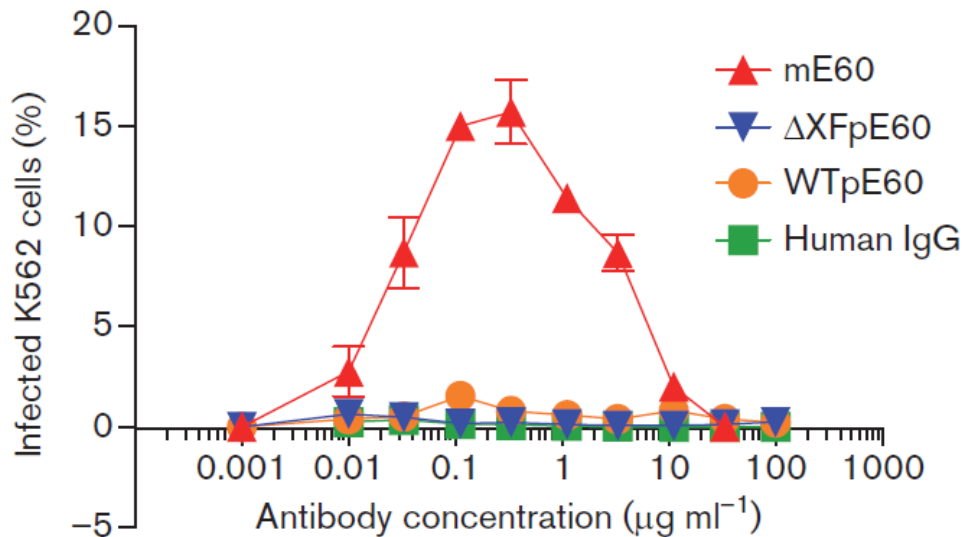
Figure 23. WT and ΔXTFT *N. benthamiana* Produced E60 mAb Virtually Prevent ADE. An
ADE assay was performed to assess the capabilities of pE60 mAbs variants in preventing ADE *in
vitro*. K562 bearing FcγR2a receptors were treated with DENV-2-pE60 mAb or DENV-2-mE60
complexes and assessed for ADE activity. The data show ADE occurring when mE60 mAb was
used, whereas no ADE was observed when any of the pE60 mAb variants were used. Thus, the
pE60 mAb variants may present a better option for treating DENV infections in urgent situations.

Discussion

The mainstay for therapeutic mAb production has been the CHO cell with many

examples of FDA approved therapies on the market. However, plants offer an alternative to

therapeutic recombinant protein production. The plant recombinant protein production platform

offers several advantages over mammalian-cell based platforms including shorter development

time and cost, while simultaneously producing recombinant proteins such as mAbs with

comparable yield, quality, and in some cases, improved safety and efficacy (Bendandi et al.,

2010; Chen, 2011; Q. Chen & H. Lai, 2015; Giritch et al., 2006; Zeitlin et al., 2011). Furthermore, the use of glycoengineered plants allows for the production of mAbs with tailor-made N-glycans that will allow for the enhancement of desired effector functions such as ADCC and CDC.

In this study, two plant produced E60 mAbs (WT or ΔXTFT *N. benthamiana* produced) were assessed for their ability to neutralize the DENV-2 and DENV-4 viruses and, importantly, assessed their ability to forgo ADE, which is a major concern in mAb therapeutics against DENV serotypes. The immunological humoral response plays an important role in combating viral infections and closely related FVs pose a particular challenge. The surface of FVs is covered with E proteins that become the immune systems primary target. As a result, antibodies produced against the E protein for one FVs has the potential to cross-react with a closely related FV, thereby creating the possibility of ADE (Dejnirattisai et al., 2015). However, exceptions have been found where cross-reacting mAbs directed against the highly conserved fusion loop in DII of the E protein are neutralizing in many FVs (Deng et al., 2011).

The E60 mAb was originally found as a result of research on the E protein of the WNV, however, subsequent investigation found the mAb to be neutralizing against all four serotypes of the DENV (Balsitis et al., 2010; T. Oliphant et al., 2006). The E60 targets an epitope on the E protein's DII highly conserved fusion-loop, conferring it the potential to be a therapeutic for all DENV serotypes. Unfortunately, studies have shown mE60 to display ADE activity both *in vitro* and *in vivo*, discounting it as a serious candidate for clinical use, as ADE can lead to severe dengue illness such as DHF and DSS (Balsitis et al., 2010).

The identity of *N*-linked glycans on the Fc region of mAbs is important in effector functions, FcγR type binding, pharmacokinetics, and stability (Houde, Peng, Berkowitz, & Engen, 2010). Despite attempts at producing mAbs with homogenous glycoforms in mammalian cell culture, including attempts with mutations in the *N*-linked glycosylation pathway, has not been possible (Jefferis, 2005). Plants have a smaller glycobiome than mammals and the developments in plant glycoengineering has allowed for the production of human-like glycan profiles in homogenous form. Furthermore, the use of WT plants for therapeutic recombinant protein

production was for the most part viewed in a negative light due to the possibility of adverse immunological reactions to plant specific glycans. However, studies have indicated that those assumptions may not have been completely sound and plant produced therapeutics with plant specific *N*-linked glycans may not cause alarming adverse effects (Shaaltiel & Tekoah, 2016). Furthermore, the advancements in glycoengineering, and the resulting homogenous mixture, will allow us to assess the particular contributions a specific carbohydrate makes in a system, such FcγR and C1q binding, in addition to the elimination of plant specific carbohydrates (Chen, 2016; Loos & Steinkellner, 2014).

The design of safe and efficacious recombinant proteins, such as mAbs, is now possible due to plant glycoengineering, where we can now produce *N*-linked proteins with defined glycans to bias towards desired effector functions, such as CDC and ADCC. In a striking example of a biased effector function towards ADCC, the 13F1 anti-EBOV mAb produced in ΔXTFT *N. benthamiana* plants was able to show greater ADCC activity over its mammalian-cell produced counterpart, where an enhanced potency against the EBOV was observed (Zeitlin et al., 2011). The m3F16 mAb was determined to have 3-5 glycoforms whereas the p3F16 mAb was determined to have the GnGn type glycan, lacing the fucose carbohydrate thereby increasing its affinity to the FcγR3 receptor for enhanced ADCC activity (Zeitlin et al., 2011).

The DENV is the most important arbovirus affecting much of the tropical countries of the world for which there is very little treatment and a limited use vaccine. The WT and ΔXTFT *N. benthamiana* produced E60 mAb demonstrated their retained abilities to bind to their target, neutralized DENV-2 and DENV-4, and virtually display no ADE activity. Furthermore, *N*-linked glycan analysis revealed a near homogenous human-like core GnGn structure in the E60 mAb produced in ΔXTFT *N. benthamiana*, thereby eliminating any concern of potential adverse immune reactions for potential clinical use in urgent settings. This salient feature was made possible by the advances of glycoengineering in plants which now allows us to tailor make recombinant proteins, like mAbs, with specific *N*-linked glycans to modulate effector functions.

CHAPTER 3

PLANT-PRODUCED BISPECIFIC ANTIBODIES FOR THE TREATMENT OF CO-CIRCULATING

FLAVIVIRUSES

Introduction

FVs are perhaps the most important arthropod born viruses. They endanger the health of

millions of people each year and, due to the illnesses they cause, also apply a considerable

burden on the economic wellbeing of tropical countries in the form of health care costs and loss of

productivity. Furthermore, children tend to be the most susceptible to certain FV infections and

suffer the most severe forms of the diseases, such as DHF and DSS. The danger of a ZIKV

infection is especially of alarming concern in pregnant women since ZIKV infected women can

potentially transmit the ZIKV to their developing fetuses where the virus can cause spontaneous

abortions or lifelong debilitating and development complications (e.g. microcephaly).

Recently, the FDA approved Dengvaxia, a tetravalent vaccine that offers protection

against all four serotypes of DENV. Dengvaxia is a live attenuated chimeric virus vaccine that

uses the YFV 17D vaccine strain to express the pre-membrane (prM) and E proteins of all 4

serotypes of the DENV (Thomas & Yoon, 2019). Although a DENV vaccine was urgently needed,

Dengvaxia came with some limitations that must be strictly observed to avoid the induction of

severe DENV disease such as DHF and DSS via ADE. It has been observed, in particular in

children, that vaccination with Dengvaxia without prior infection to any of the 4 DENV serotypes

may lead to severe forms of dengue disease after vaccination and subsequent infection with any

of the 4 DENV serotypes (Rosa, Cunha, & Medronho, 2019). In these circumstances, it is

believed that the pathogenesis of DENV is driven by ADE. Antibodies elicited by the Dengvaxia

vaccine may be weakly binding and non-neutralizing to any of the 4 DENV serotypes, thereby

promoting receptor mediated endocytosis of the virus-mAb complex via FcγR2a bearing cells and

resulting in increased viremia and severe dengue disease.

Vaccine design against DENV has been hampered by host immune responses that produce non-neutralizing mAbs. This is problematic, in particular with DENVs for which there are 4 serotypes in the same genotype but are distinct enough to escape the immune response elicited by the other serotypes. The DENV E protein, which covers the entire surface of the virions, is immunodominant and shares considerable sequence homology within the four serotypes. The sequence of the fusion loop, which is located on domain 2 of the E protein, is conserved among all 4 serotypes and tends to elicit non-neutralizing mAbs (Rodenhuis-Zybert et al., 2011). Furthermore, the E protein fusion loop of the ZIKV also shares 100% sequence homology with the DENV fusion loop, implying the possibility of cross-reacting mAbs against the DENV potentially leading to ADE (Gunawardana & Shaw, 2018).

The DENV and the ZIKV co-circulate in certain regions of the world. Additionally, the Chikungunya virus (CHKV), an arthropod borne alphavirus, also co-circulates with the DENV and the ZIKV in certain regions of the world (Figure 1) (Patterson et al., 2016). The CHKV, like the DENV and the ZIKV, is also transmitted by the *A. aegypti* mosquito. Initial symptoms caused by an infection with any of these viruses are remarkably similar (Beltrán-Silva, Chacón-Hernández, Moreno-Palacios, & Pereyra-Molina, 2018). All of these viruses typically cause mild and self-limiting febrile illnesses. However, severe forms of CHKV infection causes arthritis like symptoms that are long lasting, ranging from months to years (Couderc & Lecuit, 2015). Like the ZIKV and the DENV, CHKV treatment is limited to supportive care and careful observation of the hydration status of the patient.

Plants have become an attractive option for the production of therapeutic recombinant proteins because they offer significant advantages over traditional systems, such as rapid production of recombinant proteins, improved safety profile of recombinant proteins, and plants offer the ability to immensely increase the scale of production of the therapeutic recombinant proteins (Yao, Weng, Dickey, & Wang, 2015). Furthermore, advances in plant glycoengineering have led to the ability of plants to produce recombinant glycoproteins with mammalian-like *N*-linked glycans (Castilho & Steinkellner, 2012). This advancement has been highly impactful since

it was previously thought that plant specific carbohydrate residues on glycans, such as β1,2-xylose and α1,3-fucose, may lead to adverse immune responses, thereby excluding plant-made biologics for clinical use. Glycoengineering has largely alleviated that concern with the development of glycoengineered plants that can produce *N*-linked glycans on proteins with human-like carbohydrates, thereby forgoing potential immunogenic responses and now viable for clinical and therapeutic use.

The endomembrane system is conserved among animals and plants, thereby conferring plants with the necessary organelles and enzymes to perform posttranslational modifications. Additionally, animals and plants share an initial *N*-linked glycosylation pathway that forms a core "GnGn" central structure (Figure 24)(Chen, 2016). It has been observed that, unlike mammalian cell-based mAb production systems, mAbs produced in plants tend to produce homogenous *N*-linked glycosylated profiles in Fc regions of mAbs. The GnGn central structure is further modified with different carbohydrates differently in animals and plants. Human IgG1 molecules contain a conserved *N*-linked glycosylation site in the Fc region, specifically at amino acid residue Asn297 of the heavy chain in domain 2. This site is important for both binding to some FcγRs and for immunoglobulin elicited effector functions such as C1q binding, ADCC and CDC. The glycosylation profile of the Fc region of an IgG can greatly influence its effector functions and circulatory half-life.
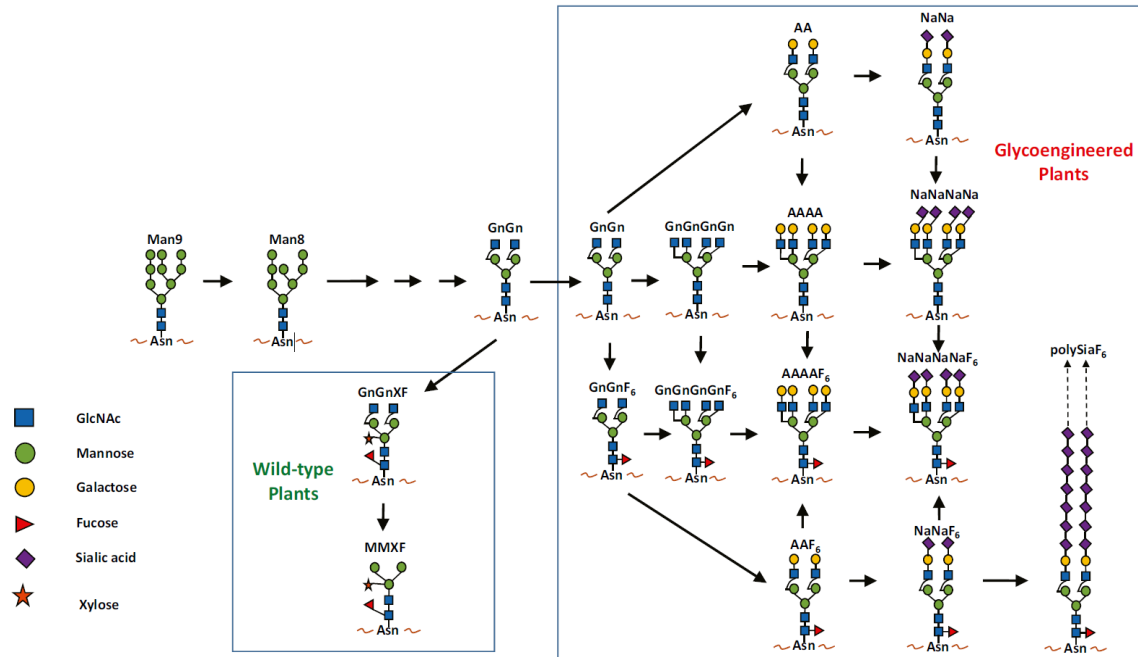
Figure 24. Advancements in *N*-linked Glycoengineered Plants. The initial steps in the *N*-linked glycosylation pathway is conserved amongst plants and animals leading up to the "GnGn" core structure. Glycosylation pathways diverge thereafter, where in WT plants the major *N*-linked glycan observed is of the GnGnXF type. A myriad of glycosylation profiles is observed in animal *N*-linked glycoproteins. Advances in glycoengineering has led to the conferring of plants with the ability to *N*-link glycosylate proteins with mammalian-like glycans in a homogenous fashion. These advancements have made plant made glycoproteins an attractive option for recombinant glycoprotein production and therapeutic use. Image Credit: (Chen, 2016)

Co-circulating FVs cause a global public health concern and place a burden on the majority of countries found in the tropics. With the possibility of the expansion of the ranges of the mosquitoes that vector these viruses, an increase in DENV and ZIKV associated illness can be expected beyond the tropics (Ebi & Nealon, 2016). An FDA approved vaccine for dengue disease exists, albeit its use is limited, and no FDA approved vaccine for the ZIKV or the CHKV exists. Thus, there is still a need for safe and effective vaccines and therapeutics for those globally spread viruses. Here I describe the design, construction, expression, and testing of a plant-made bsAb for the treatment of the co-circulating FVs and the CHKV virus. Plant-made therapeutics can be potentially accessible to all regions of the world with reduced investment of capital when compared to traditional cell culture-based systems. Furthermore, glyco-engineered plants produce homogenous and mammalian-like glycans that are safe and effective. Here I show that

the Z54scFv-CH$_{1-3}$ + E60scFv-CL bsAb designed against the co-circulating DENV-2 and the ZIKV viruses is able to neutralize both these viruses and virtually eliminate ADE *in vitro*.

Materials and Methods

Construction of bsAbs

bsAbs were constructed by first converting all parental mAbs to scFvs and fusing them to either the CH$_{1-3}$ regions of a human IgG or the light chain (CL) of the kappa type (Figure 25 and 26). PCR was used to introduce the EcoR1 site on the 5' end of the VH sequence and Nhe1 was introduced at the 3' VL region for all scFvs constructed. The 18 amino acid peptide linker between the variable regions of the heavy and light chains to construct the scFv was coded by GGTTCAACTTCAGGAGGAGGATCAGGTGGTGGTTCAGGAGGTGGA GGATCTTCT and was partly incorporated into the 3' end of the VH and 5' end of the VL region primers of each of the constructs. scFvs to be fused with the CH$_{1-3}$ region of a humanized IgG1 contained EcoR1 and Nhe1 sites. Overlapping PCR was then done to form the final scFv. scFvs were then cloned into a plasmid containing EcoR1 and Nhe1 sites and the coding sequences of CH$_{1-3}$ or coding sequences of the CL. The cloned scFvs fused to either the CH$_{1-3}$ or CL were then cloned into MagnICON vectors for fusion protein expression in *N. benthamiana*. The MagnICON vectors were individually transformed into *A. tumefaciens* GV3101 by electroporation.

Expression, extraction, and purification of bsAbs in N. benthamiana

A. tumefaciens GV3101 strains containing scFv fusion clones were grown and agroinfiltrated into WT or GnGn transgenic *N. benthamiana* tobacco plants as previously described (J. He et al., 2014). The infiltrated leaves were harvested 5-7 days post infiltration, depending on the construct and condition of leaves. Harvesting included removing the stem and midrib vein with a razor blade leaving only the leaves to be homogenized. The leaves were then homogenized in homogenization buffer using the following ratio: homogenization buffer = 1.5 mL/g X (xg of leaf fresh weight). The homogenization buffer was comprised of PBS pH 5.2, 1 mM

EDTA, 2 mM PMSF, and 10 mg/mL of NaAsc, kept on ice. Following homogenization, the sample was clarified by centrifugation at 14.8 kG for 30 minutes at 4 C, twice. The pH of the sample was then readjusted to pH 5.2 and left overnight at 4 C to remove Rubisco. The sample was then centrifuged one more time at 14.8K G for 30 minutes at 4 C to remove the rubisco. The pH was then adjusted to 7.4 and centrifuged two more times at 14.8K G for 30 minutes and 4 C. The sample was then passed through a 0.22 uM Fast Flow Low Protein Binding filter (EMD Millipore Corporation, Billerica, MA) and loaded onto a MabSelect protein A column (GE Healthcare). The column was then washed with 20 volumes of PBS and eluted with 50 mM sodium citrate pH 2.5 and immediately neutralized with 1 M TRIS-base to reach a final pH of 7.4. The purity of the bsAbs was assessed by Coomassie stained SDS-PAGE gels.

SDS-PAGE and Western blot

The purified bsAbs were loaded onto 4% to 12% SDS-PAGE under reducing conditions using β-mercaptoethanol at 5% v/v. The gels were then stained with Coomassie blue for 1 hour on a rocker and then de-stained with de-staining buffer containing 70% water, 20% methanol, and 10% acetic acid, thrice for 30 min on a rocker. When used for Western blots, the bsAbs were transferred to PVDF membranes and detected using HRP-conjugated antibodies against human gamma chain or human-kappa light chain.

Flow cytometry with yeast surface display

Yeast displaying WNV DIII and DENV-2 DI-II (separate yeasts) on their surface were generated, stained with mAb variants, and analyzed with a Becton Dickinson FACSCalibur flow cytometer as described by (J. He et al., 2014; Theodore Oliphant et al., 2005).

N-linked glycan analysis

N-linked glycan analysis was achieved by LC-ESI-MS as described by (Stadlmann et al., 2008).

Antibody-dependent Enhancement of Infection Assay (ADE)

ADE for some of the bsAbs was assessed by an ADE assay previously described by (Dent et al., 2016). K562 cells, which are $Fc\gamma R2a^+$, were used. Eight 3-fold serial dilutions of a bsAb or generic human IgG as a negative control were incubated with the DENV-2 or the ZIKV for 1 hour at 37 C and then mixed with K562 at a MOI of 1. Forty-eight hours thereafter, the cells were washed with PBS and fixed with 7% paraformaldehyde and permeabilized 0.1% saponin. The cells were then stained with the mAb 4G2 that was conjugated with Alexa 488 (Invitrogen), washed and then analyzed with a Navios flow cytometer (Beckman Coulter) to determine the percentage of infected cells.

DENV-2, ZIKV, and WNV RVP Neutralization Assay

Anti-DENV-2 and anti-ZIKV bsAbs were serially diluted in serum free Opti-MEM medium (Life Technologies). The DENV-2 and the ZIKV were diluted to a working concentration of 100 plaque forming units (PFU) per well. The bsAb dilutions were then added to the wells containing the ZIKV or the DENV-2 and incubated for 1 hour at 37 C. Thereafter, the bsAb-virus complex was added to 90-95% confluent Vero cells on plates and incubated for 1 hour at 37 C. The medium was then removed and overlaid with 5% FBS and 1 % agar DMEM media and incubated at 37 C, and 5% CO_2 for 5 days (DENV-2) or 3 days (ZIKV). The DENV-2 infected cells were then stained with neutral red, placed back in the incubator and recorded the visible plaques 16 hours thereafter. The ZIKV infected cells were then fixed with 4% paraformaldehyde and incubated overnight at room temperature. Thereafter, the plates were stained with crystal violet and plaques were counted. Percent neutralization was determined by the following formula: [((100 PFU) - (# of PFU per well of diluted bsAb))/(100 PFU)X100]. The EC_{50} of each bsAb was calculated using

Graph Pad Prism. The WNV RVP neutralization assay was performed as described by (Theodore C. Pierson et al., 2006). The neutralization of WNV RVP was performed using bsAbs containing an anti-WNV component.

Results

Construction of scFv from parental mAbs and fusion to CH$_{1-3}$ or CL

Parental mAbs were first converted to scFv. This approach was taken to reduce the number of potential combinations bsAbs when attempting to assemble a bsAb in an environment where two distinct heavy chains and two distinct light chains exist (Figure 25). There is no observed preferential pairing of a heavy chain and a light chain, thus in the presence of multiple heavy or light chains in the same cell can result in the formation of multiple bsAbs. Thus, the conversion of the parental mAbs to scFv and then fusion to CH$_{1-3}$ of an IgG1 molecule was chosen to reduce the number of HCs and LCs expressed in the same cell, thereby increasing the possibility of assembling the target bsAb (Figure 26).
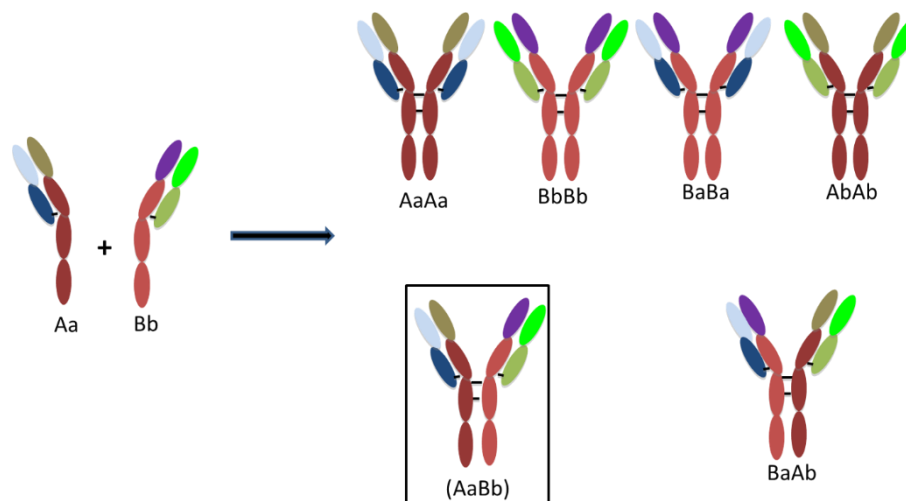
Figure 25. Possible bsAb Combinations when Expressing Two Different HCs and LCs in the Same Cell. When two different HCs and two different LCs are expressed in the same cell with the aim of assembling a specific bsAb, a few combinations of HCs and LCs form due to the lack of preferential pairing between HCs and LCs. Two possible resulting molecules are the re-assembly of the parental mAbs and four combinations of bsAbs are possible, of which only one is the desired bsAb (boxed in black). With this method, there is a one in six chance of assembling the target bsAb.

Construction of bsAbs began with the E60 mAb, which is an IgG1 mAb that neutralizes all four serotypes of the DENV by binding to the fusion loop located in D2 of the E protein. PCR was performed to clone the VH and VL regions of the E60 mAb while including sequences in the primers to introduce an 18 AA peptide linker between the VH of VL to form the scFv. Overlapping PCR cloned the VH and VL of E60 into the final scFv, forming an expected band size of approximately 800 bp (Figure 27). The resulting E60scFv was then cloned into a vector containing human IgG1 CH$_{1-3}$ and subsequently cloned into a MagnICON *A. tumefaciens* expression vector.
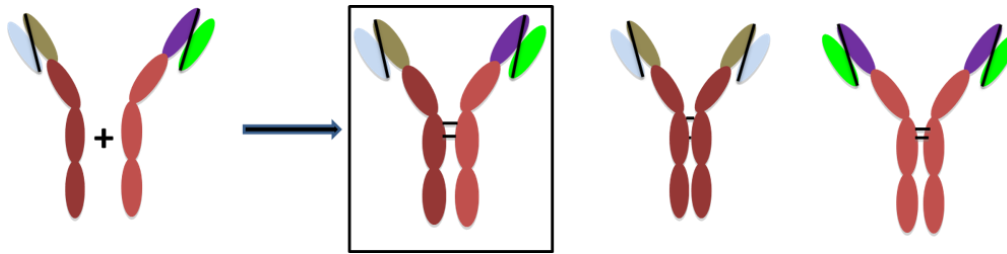
Figure 26. Possibility of Assembly of Target bsAb is Significantly Increased When scFv-CH$_{1-3}$ Molecules are Used. The conversion of parental mAbs to scFv fused to CH$_{1-3}$ increases the possibility of assembling the target bsAb in the same cell. A one in three chance is possible with this method whereas a one in six chance is possible if two different HCs and LCs are expressed in the same cell.
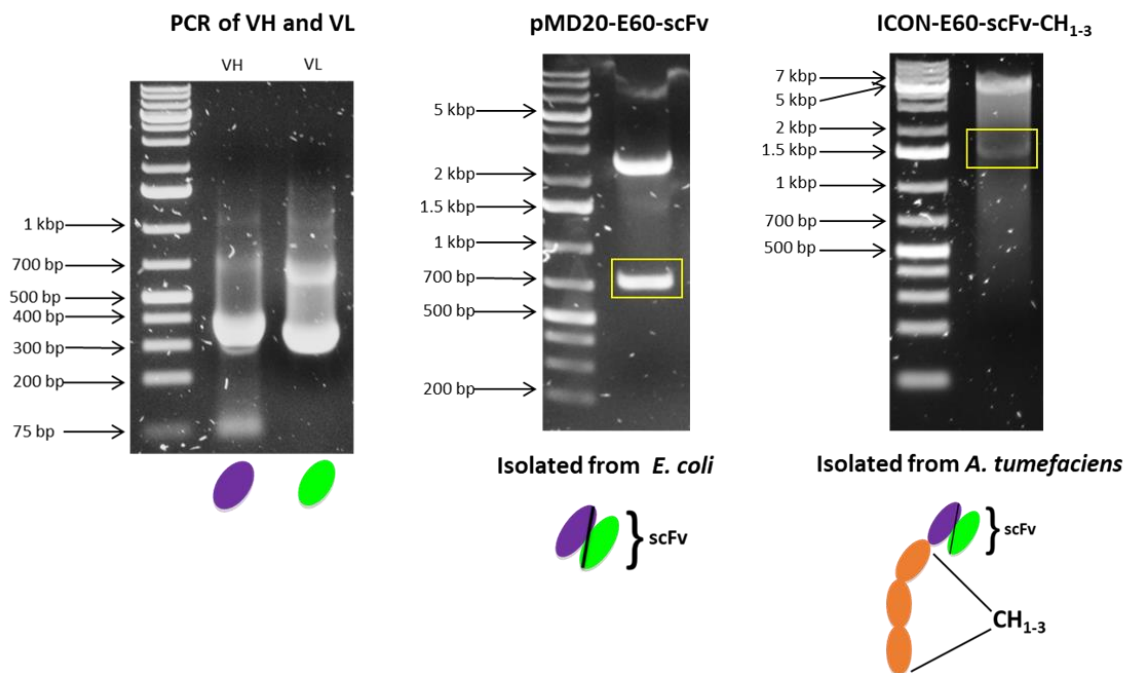
Figure 27. Cloning and Conversion of the E60 mAb to an E60scFv-CH$_{1-3}$. The variable regions of the E60 mAb, an anti-DENV serotypes 1-4 neutralizing mAb, were cloned and converted to an scFv with an 18 AA peptide linker. The scFv was subsequently fused with the CH$_{1-3}$ regions of an IgG1 to form the E60scFv-CH$_{1-3}$. A MagnICON protein expression vector was the final destination of the cloned scFv-CH$_{1-3}$, which was then transformed into *A. tumefaciens strain* GV3101.

N. Benthamiana plants were agroinfiltrated with GV3101 *A. tumefaciens* harboring the

expression vector for the E60scFv-CH$_{1-3}$ and the rest of the modules of the MagnICON system.

The MagnICON system was syringe infiltrated with a final OD$_{600}$ of 0.6. The plants were then

moved to a growth chamber and left there for a 7-day incubation period. On the 7th day the leaves

were harvested and subjected to a series of clarification steps. The sample was then passed

through a protein A chromatography column for isolation of the E60scFv-CH$_{1-3}$ (Figure 28)
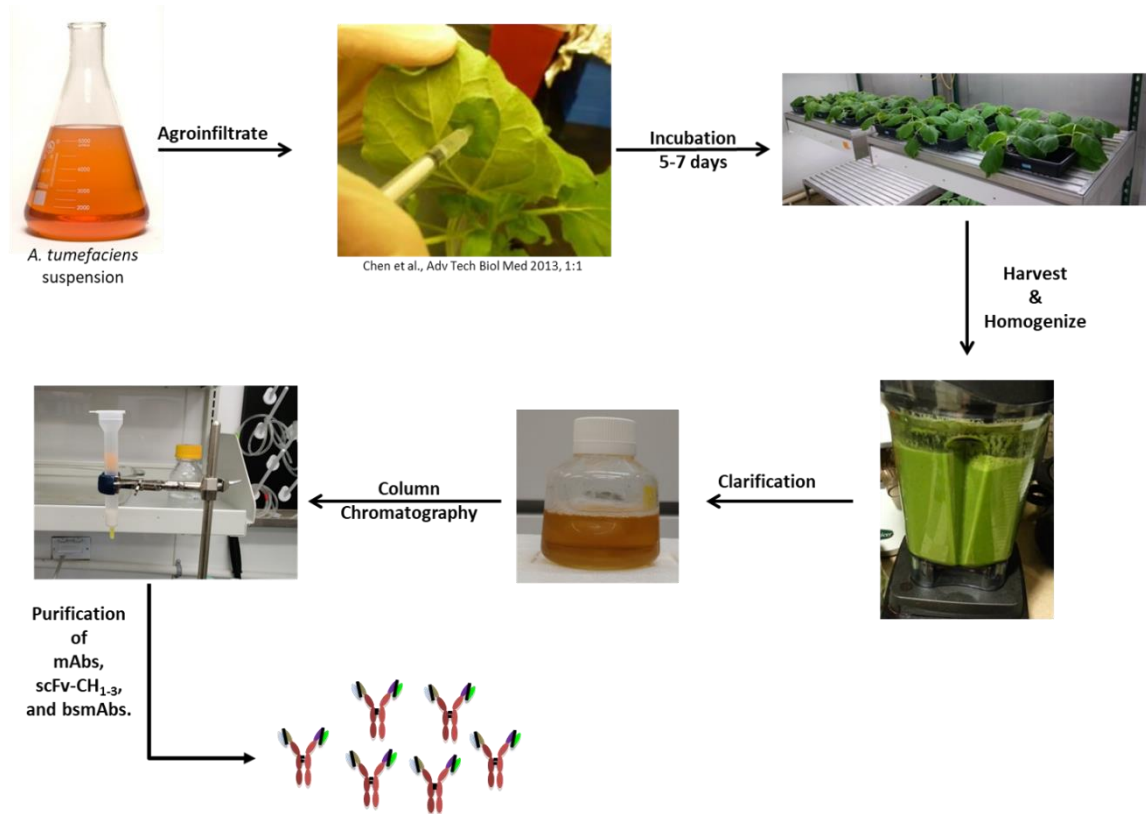
Figure 28. Agroinfiltration and Purification of mAb Derivatives. Suspensions *of A. tumefaciens* cultures, each harboring a particular MagnICON module for recombinant protein expression, was prepared and diluted to an appropriate OD$_{600}$ for agroinfiltration into plant leaves. After agroinfiltration the plants were incubated for 5-7 days, at which point they harvested and homogenized followed by a series of clarifications steps. The resulting sample was then filtered and loaded on to a column containing protein A to capture and separate mAbs from the sample.

An aliquot of the sample was taken and mixed with SDS-PAGE sample loading buffer

under reducing conditions. Coomassie stained SDS-PAGE analysis revealed a prominent band

between the 75 kDa mark and the 50 kDa mark, but closer to the 75 kDa mark. The E60scFV-

CH$_{1-3}$ was expected to have a MW of 67 kDa, which was in accordance with the band observed

on the gel. To verify the identity of the E60scFv-CH$_{1-3}$ a Western blot was done using and HRP-

conjugated anti human IgG1 mAb, which revealed a band at the approximate 67 kDa expected

position (Figure 29).
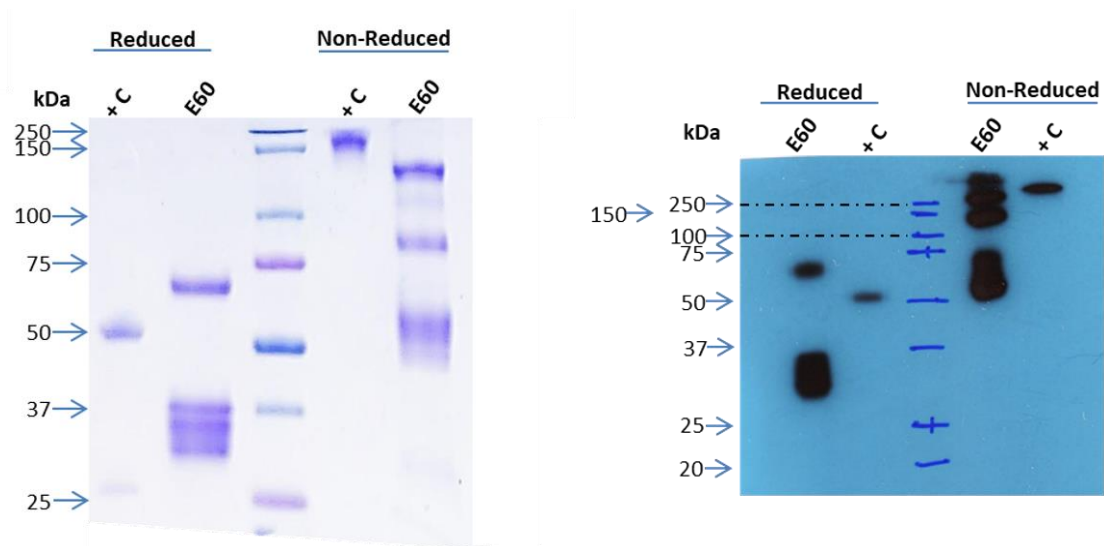
Figure 29. E60scFv-CH$_{1-3}$ Coomassie Stained SDS-PAGE and Western Blot. Under reducing conditions, SDS-PAGE analysis showed banding of the E60scFv-CH$_{1-3}$ below the 75 kDa MW mark. The estimated MW of the E60scFv-CH$_{1-3}$ construct was 67 kDa, which correlated with SDS-PAGE data. Under non-reducing conditions, the E60scFv-CH$_{1-3}$ construct was estimated to have a MW of 134 kDa. Non-reducing SDS-PAGE analysis showed banding of the E60scFv-CH$_{1-3}$ construct just below the 150 kDa mark, which correlated with our predictions. WB analysis corroborated with SDS-PAGE analysis and verified the identity of our construct. Additionally, a series of banding patterns were observed below the 37 kDa mark in both SDS-PAGE and WB analysis, alerting of possible degradation products of the E60scFv-CH$_{1-3}$ construct.

In addition to the expected bands on both SDS-PAGE and Western blots, a series of

bands were observed just underneath the 37 kDa mark. More specifically, a triplet of bands can

be discerned. Those bands were also present in the Western blot and believed to be degradation

products of the heavy chain since they were detected in the Western blot using an anti-gamma

HRP conjugated mAb. In an attempt to eliminate if not reduce the degradation of the heavy chain,

we reexamined mAb assembly and came to the conclusion that the lack of the presence of the

constant region of light chain (CL) might be driving the degradation of the heavy chain. It has

been reported that the immunoglobulin binding protein, or BiP, plays an important role in

immunoglobulin assembly. A study conducted by Lee et al. revealed that BiP remains associated

with the CH$_1$ domain of the heavy chain and remains associated to it until the CL displaces it

(Lee, 1999) (Figure 30). Once the CL displaces BiP from the CH_1 domain of the heavy chain, the proper folding of the heavy chain occurs. We hypothesize that in our design of the E60scFV-CH_{1-3}, which is lacking the CL, the BiP is bound to E60scFv-CH_{1-3} and is being retained and accumulated in the ER. Since there is no CL to displace BiP, accumulated E60scFv-CH_{1-3} might trigger and ER stress response thereby causing the degradation of proteins, including our E60scFv-CH_{1-3}.
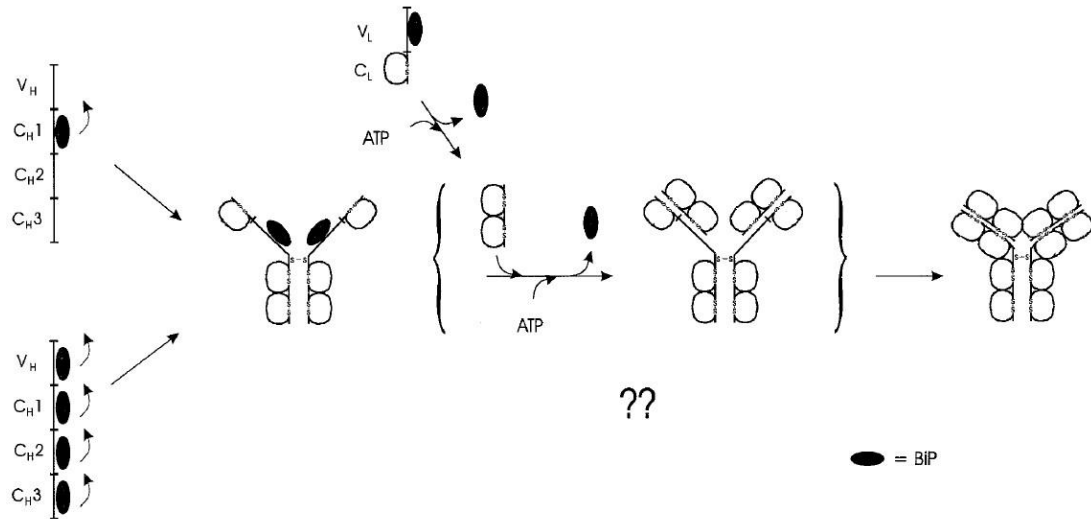
Figure 30. The CL Displaces BiP from the CH_1 Domain of the HC. A study conducted by Lee *et al.* found evidence to suggest that CL displaces the BiP protein bound to the CH_1 domain of the HC, thereby allowing for the proper folding of the HC and assembly of the immunoglobulin. Our E60scFv-CH_{1-3} lacks the CL and thus may be trigger an unfolded protein response in the ER thereby causing the degradation of our E60scFv-CH_{1-3}. Image credit: (Lee, 1999).

To test this hypothesis, *N. benthamiana* plants were co-infiltrated with E60scFv-CH_{1-3} and the CL using the MagnICON system. With this experiment, we expected to reduce or eliminate the degradation of our E60scFv-CH_{1-3} design. The same previous E60scFv-CH_{1-3} procedure was used to harvest and purify this co-infiltration of E60scFv-CH_{1-3} + CL experiment. Coomassie stained SDS-PAGE analysis revealed remarkably reduced degradation bands (Figure 31). This data suggests that it is likely that our E60scFv-CH_{1-3} was being degraded in the ER per our hypothesis. Furthermore, our data supports and reinforces cell biology principles in

immunoglobulin assembly, whereby the CL and BiP play an important role in immunoglobulin

heavy chain proper folding and overall immunoglobulin assembly.
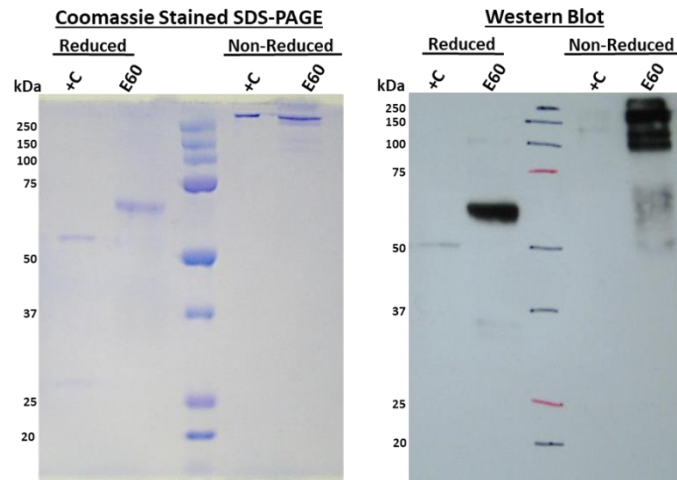
Figure 31. Coomassie Stained SDS-PAGE and Western Blot of E60scFv-CH$_{1-3}$ + CL. SDS-PAGE analysis of the co-expression the E60scFv-CH$_{1-3}$ + CL constructs showed a significant reduction in the degradation products seen just below the 37 kDa mark in previous E60scFv-CH$_{1-3}$ expression experiments. This suggests that the co-expression of the CL may aid in the assembly of the E60scFv-CH$_{1-3}$ construct, specifically by aiding in the proper folding of the CH$_{1-3}$ regions, consequently reducing degradation products. Western blot analysis supported SDS-PAGE analysis findings, notably a significant reduction in degradation products.

Glycosylation profile of E60scFv-CH$_{1-3}$

Based on SDS-PAGE and Western blot analysis, it appeared that our E60scFv-CH$_{1-3}$ was

being expressed and assembled. We next sought to determine the glycan composition of the

E60scFv-CH$_{1-3}$. To that end we sent E60scFv-CH$_{1-3}$ samples produced from WT and Δ*XTFT N.*

benthamiana plants to be analyzed by LC-ESI-MS (Figure 32). The parental mAb, E60, produced

in CHO cells and both WT and ΔXTXF plants were also sent for glycan analysis for comparison

and reference to our E60scFv-CH$_{1-3.}$

Glycan analysis of the parental E60 mAb produced in WT *N. benthamiana* plants

revealed a glycosylation profile in which the GnGnXF glycan type completely dominated. A similar

result was observed for the E60 mAb glycan profile produced in the ΔXTXF plant, where only

GnGn glycan profiles were detected. In contrasts, the glycan profile of the E60 mAb produced in

61

CHO cells revealed approximately a dozen types of glycan profiles. Analysis of the glycan profiles revealed that the plant produced mAb was near homogenous in composition whereas the CHO cell produced mAb was heterogeneous. These results are significant in that they offer evidence for the superiority of glycoengineered plants in producing specific glycan profiles on target proteins, thereby providing us with the ability to tailor make glycoproteins to target or steer towards a particular outcome based on the specific glycan profile.
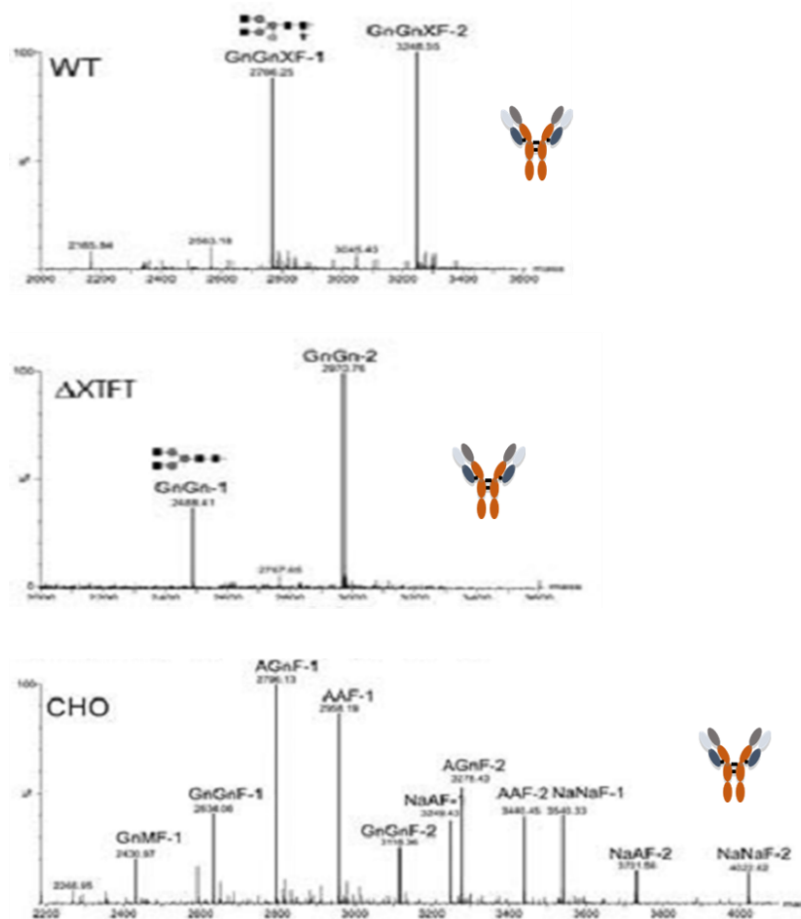
Figure 32. Glycan Analysis of the Parental E60 mAb Produced WT and ∆XTXF *N. benthamiana* Plants and in CHO Cells. Glycan analysis of the E60 mAb produced in WT *N. benthamiana* plants showed a dominance of GnGnXF, that is the GnGn glycan with xylose and fucose, whereas the ∆XTXF *N. benthamiana* produced E60 mAb showed a dominance of GnGn glycans to virtual homogeneity. Conversely, glycan analysis of the CHO cell produced E60 mAb showed nearly a dozen glycans. This data demonstrates the ability of both WT and ∆XTXF *N. benthamiana* plants to produce glycans to near homogeneity when compared to CHO cells.

Glycan analysis of the E60scFv-CH$_{1-3}$ produced by WT plants revealed a mixture of aglycosylated, Man8, Man7, XTFT, Man9, and GnGnXF glycan profiles (Figure 33). The aforementioned glycan profiles were the most prominent, however, other glycans were detected but at a much lower frequency. Glycan analysis of the E60scFv-CH$_{1-3}$ produced in the ΔXTFT plant revealed a prominence of aglycosylated E60scFv-CH$_{1-3}$ and GnGn, Man8, Man9, and Man7 glycan profiles.
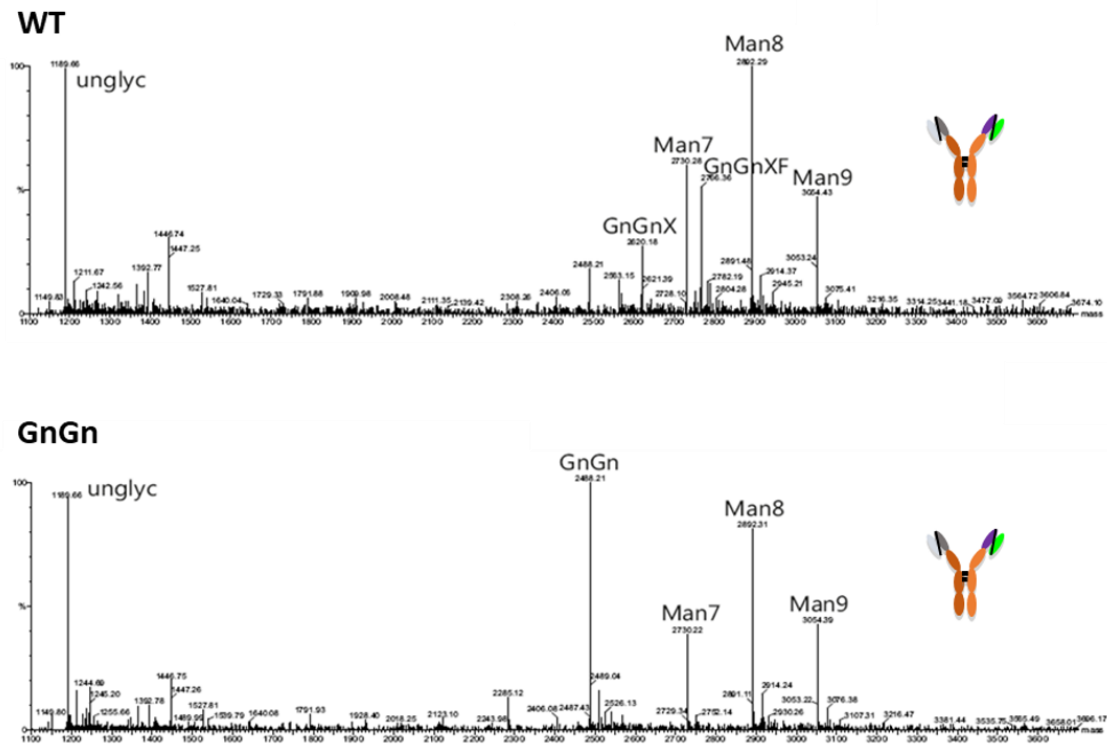
Figure 33. Glycan Analysis of E60scFv-CH$_{1-3}$ Produced in WT and ΔXTFT *N. benthamiana* Plants. Glycan analysis of WT *N. benthamiana* produced E60scFv-CH$_{1-3}$ construct revealed a majority of Man8 and aglycosylated glycans. Man7, Man9, and GnGn type glycans were also observed. ΔXTFT *N. benthamiana* (denoted as GnGn) produced E60scFv-CH$_{1-3}$ showed aglycosylated, GnGn, and Man8 as the dominant glycosylation forms. This analysis demonstrates far less variation in glycosylation profiles of ΔXTFT *N. benthamiana* plant produced E60scFv-CH$_{1-3}$.

We also sought to identify the glycan composition of the E60scFv-CH$_{1-3}$ co-infiltrated with the CL. Glycan analysis revealed a reduction in the number of mannose residues present in both WT and GnGn produced E60scFv-CH$_{1-3}$. In addition, a predominance of GnGnXF glycans was observed in the WT plant produced E60scFv-CH$_{1-3}$ and an even greater predominance of the GnGn glycan profile in the ΔXTFT plant produced E60scFv-CH$_{1-3}$ was observed (Figure 34).
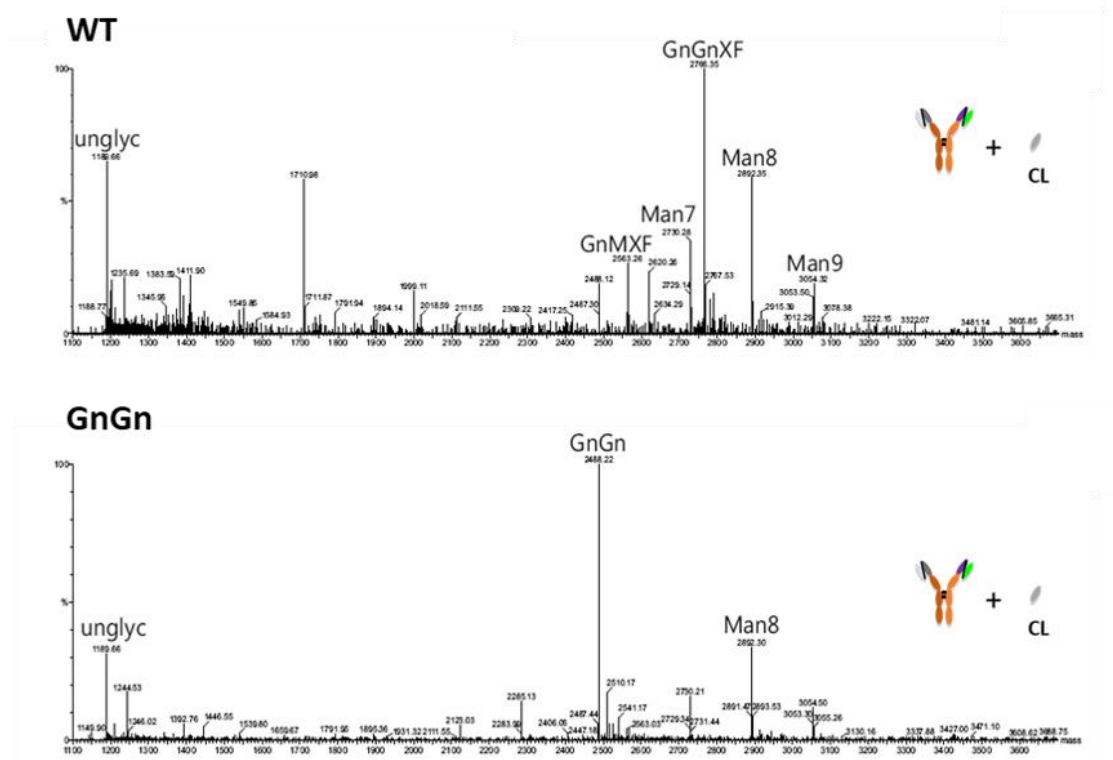
Figure 34. Glycan Analysis of E60scFv-CH$_{1-3}$ + CL Produced in WT and ΔXTFT *N. benthamiana* Plants. Co-expression of E60scFv-CH$_{1-3}$ and the CL in WT *N. benthamiana* plants showed a marked reduction in glycosylation profiles other than GnGnXF. Furthermore, co-expression of E60scFv-CH$_{1-3}$ and the CL in ΔXTFT *N. benthamiana* plants showed a significant reduction of all glycan profiles other than GnGn. Some aglycosylated and Man8 sample was detected, however, it appears that the addition of the CL significantly reduced the number of ManX glycan profiles. This observation suggests the possibility of an unfolded-protein stress response possibly occurring in the ER, resulting in the degradation of proteins and increased number of mannose residues in *N*-linked glycans.

The addition of the CL to our E60scFv-CH$_{1-3}$ design significantly reduced the degradation observed in the heavy chain of our E60scFv-CH$_{1-3}$. This suggests that the absence of the CL was affecting the proper folding of the E60scFv-CH$_{1-3}$, leading to an accumulation of the E60scFv-CH$_{1-3}$ in the ER and potentially leading to an ER stress response. More evidence of an ER response was revealed upon glycan analysis where both WT and ΔXTFT made E60scFv-CH$_{1-3}$theshowed the presence of increased mannose residues, indicating a retention of the E60scFv-CH$_{1-3}$ in the ER. Together, these results reinforce cell biology principles in the importance of proper protein folding and assembly of multisubunit protein molecules.

Yeast display of DENV D2 of the E protein

In addition to glycan analysis, we also investigated the ability of our E60scFv-CH$_{1-3}$ to bind to its target, domain 2 of the DENV E protein. To that end, a yeast display assay was used to test the binding of our E60scFv-CH$_{1-3}$. Yeast were induced to display D2 and were subsequently stained with various controls and the E60scFv-CH$_{1-3}$.(Figure 35) The results indicate binding of the parental E60 mAb to D2 of the E protein by the shifting of signal to the right whereas no binding was observed when the yeast cells were stained with an anti-Ebola IgG. Staining of the yeast cells with WT and ΔXTFT produced E60scFv-CH$_{1-3}$ showed binding as indicated by a shifting of the signal. These results indicate that, independent of the plant used to produce the E60scFv-CH$_{1-3}$, proper folding and assembly of the E60scFv-CH$_{1-3}$ likely occurred.
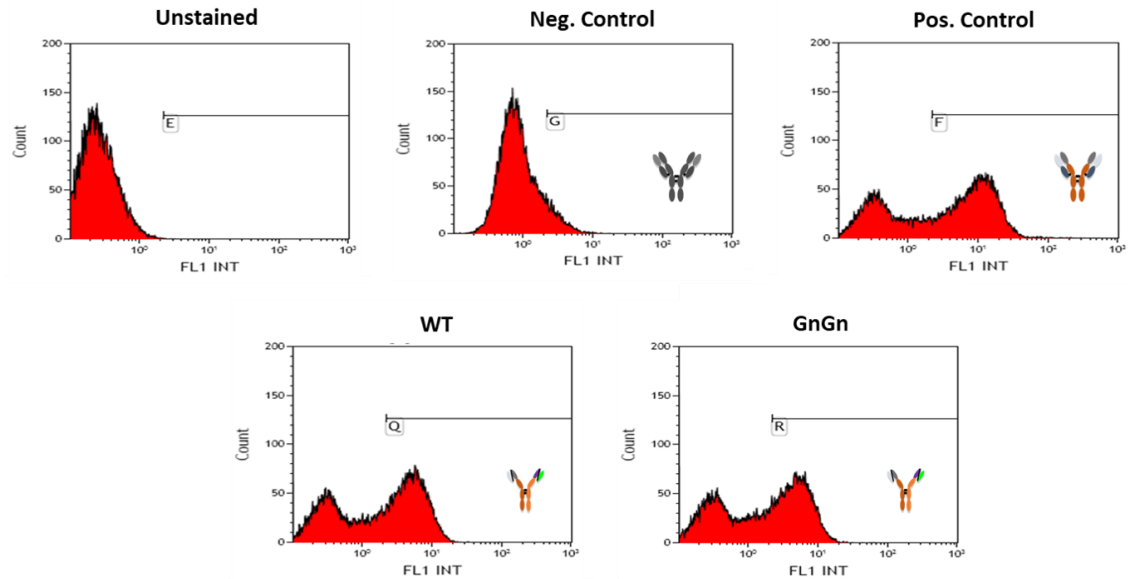
Figure 35. Binding of E60scFv-CH₁₋₃ to DENV-2 E Protein DI-II in a Yeast Display Assay. In order to assess the binding ability of the E60scFv-CH$_{1\text{-}3}$ to its target, an inducible yeast display assay was employed in which DI-II of the DENV-2 E protein is displayed. Yeast were induced to display DI-II of the DENV-2 E protein and stained with a negative control mAb (anti-Ebola 6D8), a positive control (pE60), and WT and ΔXTFT *N. benthamiana* produced E60scFv-CH$_{1\text{-}3}$. The unstained and 6D8 mAb stained assays showed no shift in fluorescence intensity thereby showing no binding to the displayed DI-II. Conversely, the pE60 mAb, WT and ΔXTFT *N. benthamiana* produced E60scFv-CH$_{1\text{-}3}$ showed a shift in fluorescence intensity, indicating the binding of the pE60 and E60scFv-CH$_{1\text{-}3}$ to DI-II of DENV-2 E. In addition to the shift in the peaks, a smaller peak can be seen on the left, which is owed to non-induced yeast cells. This data suggests that the plant produced E60scFv-CH$_{1\text{-}3}$ is properly assembled and folded, thereby having the proper structure to bind to its target.

Assembly of bsAb

Our original intent was to first convert a parental mAb into a E60scFv-CH$_{1\text{-}3}$ to reduce the number of possible bsAb combinations in the cell during expression and assembly. The KiH strategy described by Ridgway *et. al.* was planned to be employed. In this strategy, specific amino acid residues in the CH$_3$ domains of the heavy chains of the parental mAbs to be used to form the bsAb would be substituted to include amino acids with bulkier side chains on the "knob" and amino acids with less bulkier amino acid would be substituted in on the complementary strand (Ridgway et al., 1996)(Figure 36). This method was unsuccessfully attempted in our lab.
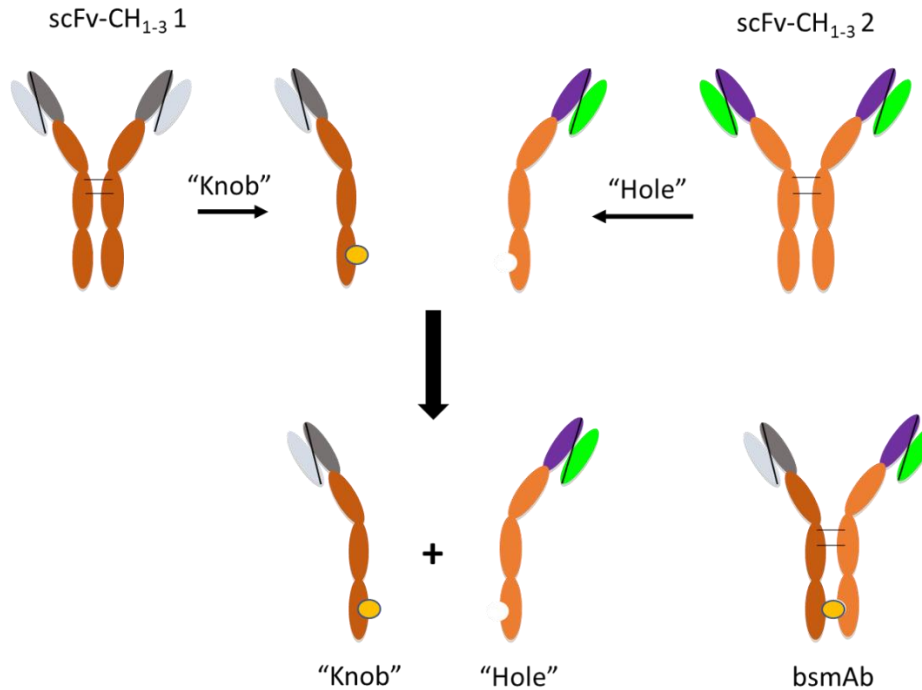
Figure 36. "Knobs-into-holes" bsAb Formation Strategy. The knobs-into-holes design relies on the substitution of amino acids with bulky side chains in key amino acids in the CH_3 region of the heavy chain. This would have the effect of introducing a bulging region or a "knob." The complementary strand of the second heavy chain to be used to form the bsAb would instead have amino acid substitution in which the side chains would be significantly less bulky thereby creating a "hole" in which the "knob" from the complementary strand would fit. Pairing of heavy chains with knobs and holes was described to be energetically favorable, thereby creating bsAbs.

Instead of the KiH approach, a bsAb with a structure based on the "Tetra pHu-E16" described by He et al. was pursued (J. He et al., 2014). This bsAb structure required the conversion of the variable regions of the parental mAbs into scFv. The scFv would then be fused to either the CH_{1-3} of a human IgG1 or the CL to produce a structure that is bi-valent for two separate epitopes (Figure 37). Assembly of mAbs involves the binding of the BiP chaperone to the heavy chain and is only displaced when a light chain is available for pairing with the heavy chain. Thus, the formation of light chain dimers is not a predictable possibility within the cell.

67
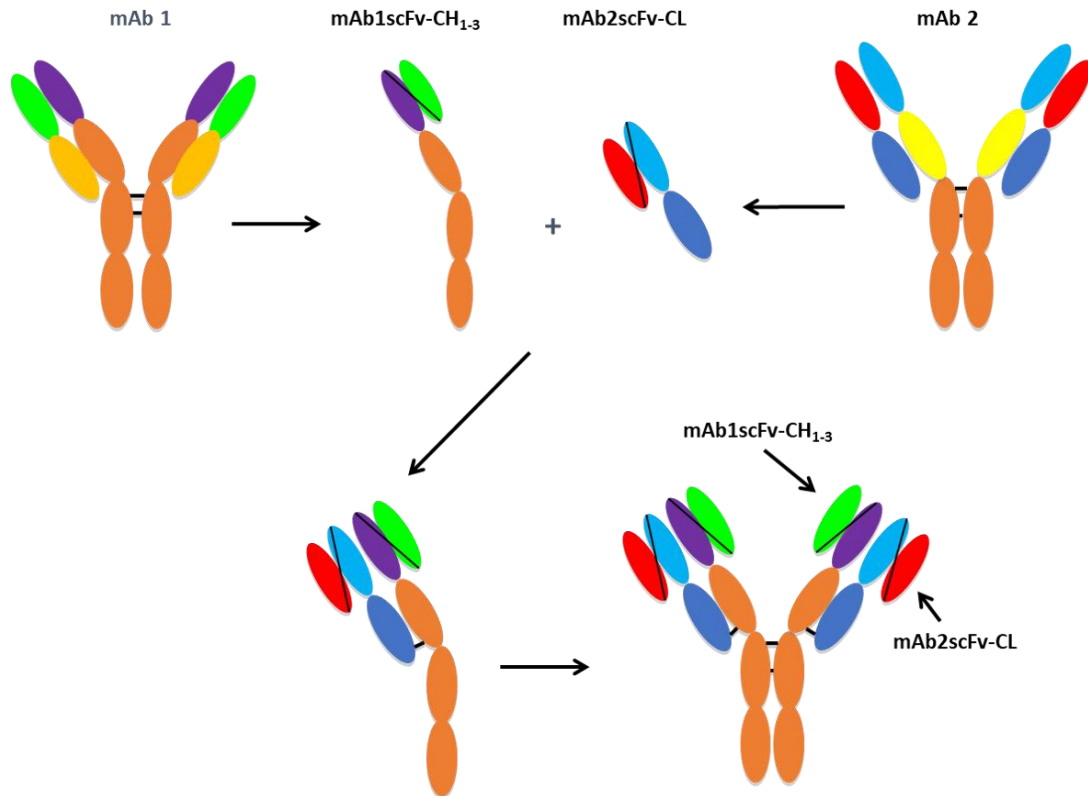
Figure 37. Design of Tetra bsAb. The design of the tetra bsAb relies on the conversion of parental mAbs to scFvs and subsequent fusion of CH_{1-3} or CL domains. This arrangement allows for the natural pairing of the CH_1 and CL domains, thereby aiding in proper folding and assembly of the molecule. Furthermore, an advantage of this design over the knobs-into-holes design is that the tetra bsAb molecule retains the avidity of the original parental molecules by retaining its bivalency. The tetra bsAb is in effect a tetravalent molecule. Based on principles of antibody assembly, the formation of heavy chain dimers within the cell is not anticipated.

The design of the tetra bsAb began by converting parental mAbs to scFv fused to either CH_{1-3} or CL. Parental mAbs against DENV, WNV, CHIKV, and ZIKV were constructed. The cloning strategy used in this research is highly amenable to rapid changes in variable regions of perspective tetra bsAbs. Thus, examples and data of different tetra bsAbs will be shown in this study, such as a Coomassie stained SDS-PAGE and WB of a tetra bsAb designed against the DENV and CHKV (Figure 38). The banding patterns of both the CH_{1-3} and CL fused scFv were present at expected locations, 67 kDa and 42 kDa respectively. Furthermore, the fully assembled tetra bsAb with an expected MW of approximately 217 kDa banded at a position higher than an assembled standard IgG of a 150 kDa MW, which was expected.

E60scFv-CH$_{1-3}$ + CHK152scFv-CL
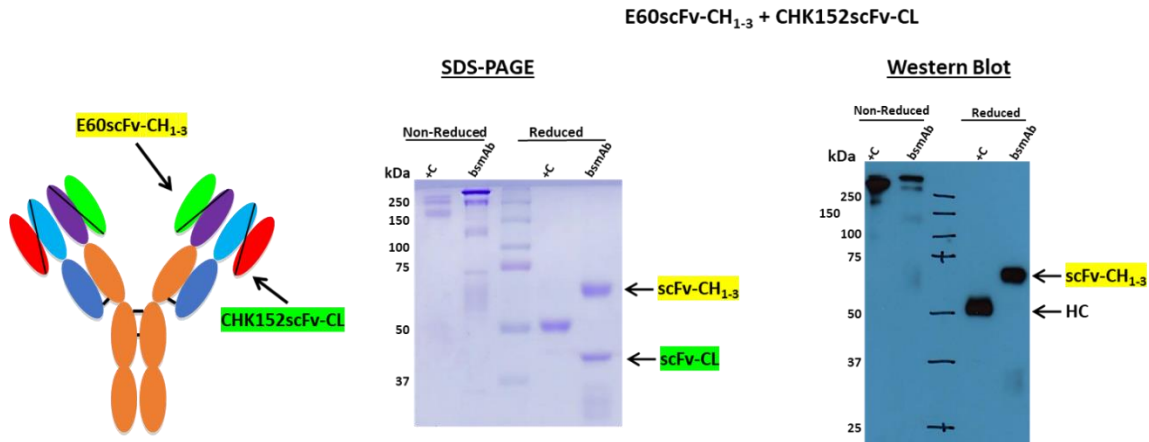
Figure 38. E60scFv-CH$_{1-3}$ + CHK152scFv-CL Tetra bsAb SDS-PAGE and Western Blot. SDS-PAGE and Western blot analysis of the E60scFv-CH$_{1-3}$ + CHK152scFv-CL tetra bsAb showed the expected banding position of the E60scFv-CH$_{1-3}$ component at approximately 67 kDa and the banding position of the CHK152scFv-CL component at the approximate position of 42 kDa. The fully assembled tetra bsAb was expected to band at approximately 217 kDa, which is a MW higher than that of a standard fully assembled IgG (150 kDa), which could be seen on non-reduced sample lanes in both SDS-PAGE and Western blot analysis. These data show the assembly of the tetra bsAb and reveal the ability of plants in producing complex molecules.

bsAb Functional Assays

bsAb Binds to Target in Inducible Yeast Display Assay

The cloning strategy employed to construct these bsAbs allows for rapid replacement of coding regions for the variable domains of the heavy and light chains from any mAb. Thus, various bsAbs were constructed to target co-circulating FVs and the CHKV alphavirus. One of those tetra bsAbs was the E60scFv-CH$_{1-3}$ + E16scFv+CL. This bsAb was assayed for binding to its target using a yeast display assay (Figure 39). The results of the assay indicate binding of the bsAb to both of its targets, the DENV E protein DI-II and the WNV E protein DIII.
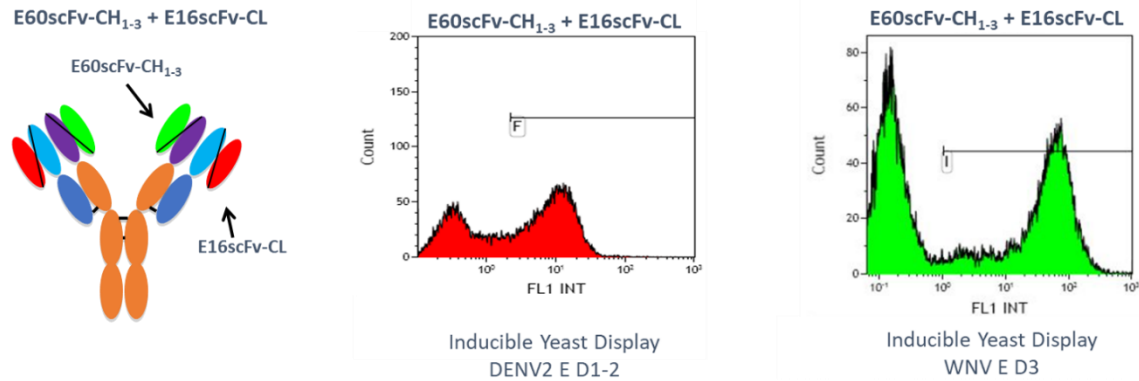
Figure 39. Inducible Yeast Display Assay and Binding of the Tetra bsAb E60scFv-CH$_{1-3}$ + E16scFv-CL to its Targets. Yeast were induced to display either the DI-II of the DENV-2 E protein or DIII of WNV E protein. The results indicate that the tetra bsAb was able to bind to both of its targets based on the observation of the shifting of fluorescence intensity in both of those assays. These results indicate that the bsAb was assembled correctly thereby conferring it the ability to bind to both of its intended targets.

bsAbs Neutralize DENV-2, ZIKV, and WNV RVP in Plaque Reduction Neutralization Test

The E60scFv-CH$_{1-3}$ + E16scFv+CL bsAb was then tested in the plaque reduction neutralization test (PRNT). This assay is designed to quantify the titer of a neutralizing antibody for a virus by using a sample containing an antibody, in this case a bsAb, and the virus of interest. The PRNT was first performed against the DENV-2, this time using the E16scFv-CL + E60scFv-CH$_{1-3}$ bsAb, a ΔXTFT made E60mAb, and a negative control (Figure 40). The results from this PRNT reveal EC$_{50}$s that are similar to each other with the ΔXTFT made E60mAb having identical EC$_{50}$s to that of the E60scFv-CH$_{1-3}$ + E16scFv-CL bsAb. The variant had a slightly higher EC$_{50}$ which may be due to the placement of the E60 component of the bsAb in the outer position of the bsAb, thereby making it a difficult to access its target epitope on the virus.
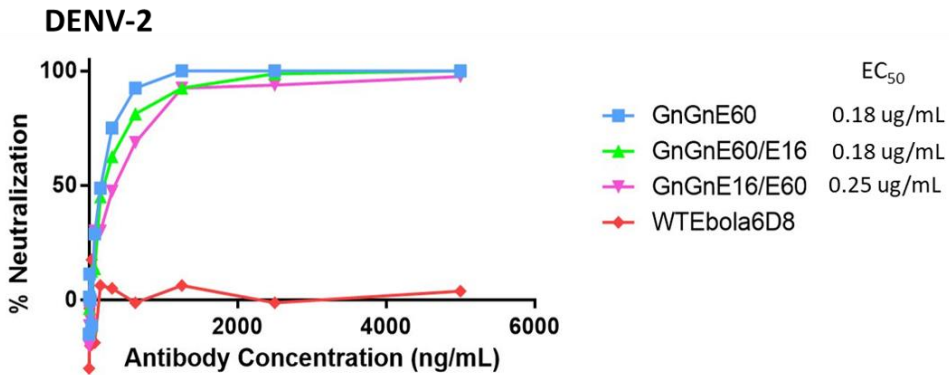
Figure 40. DENV-2 PRNT Assay Using the bsAb E60scFv-CH$_{1-3}$ + E16scFv-CL and its Variant. The PRNT assay against DENV-2 using the E60scFv-CH$_{1-3}$ + E16scFv-CL bsAb showed neutralization to DENV-2 similar to its plant made parental E60mAb. Interestingly, the related bsAb variant E16scFv-CL + E60scFv-CH$_{1-3}$, showed an EC$_{50}$ that was higher than both the other two molecules. This difference may be attributed to steric hinderance and possible lack of accessibility of the target epitope while the E60 variable regions are on the position of the CL.

The E16scFv-CL + E60scFv-CH$_{1-3}$ bsAb was then tested in a PRNT against the WNV. This PRNT test did not use the WNV, instead it used WNV reporter virus particles (RVPs). The WNV is a BSL 3 pathogen and thus was out of reach from our research facilities. WNV RVPs were specifically designed to measure antibody-mediated neutralization of WNV infection as a function of a reporter gene expression in permissive cell lines (Theodore C. Pierson et al., 2006). In this assay, the E16scFv-CL + E60scFv-CH$_{1-3}$ bsAb showed an EC$_{50}$ of 0.38 ug/mL whereas a mammalian cell made E16mAb had an EC$_{50}$ of 0.83 ug/mL (Figure 41A). In this instance the E16scFv-CL + E60scFv-CH$_{1-3}$ bsAb had an EC$_{50}$ that was slightly half that of the mammalian made E16, thereby showing an improved efficacy. The assay was repeated with the same bsAb and compared to a WT *N. benthamiana* made E16mAb (Figure 41B). Regarding the bsAb in this second assay, the results revealed an EC$_{50}$ of 0.24 ug/mL, which was similar EC$_{50}$ to the previous assay, however, the WT *N. benthamiana* made E16 mAb had an EC$_{50}$ of 1.59 ug/mL nearly 5 times greater than the bsAb.

71

WNV RVP

E16scFv-CH$_{1-3}$ + E60scFv-CL: EC$_{50}$ = 0.38 ng/mL
mE16: EC$_{50}$ = 0.83 ng/mL

WNV RVP

E16scFv-CH$_{1-3}$ + E60scFv-CL: EC$_{50}$ = 0.24 ng/mL
WT E16: EC$_{50}$ = 1.59 ng/mL
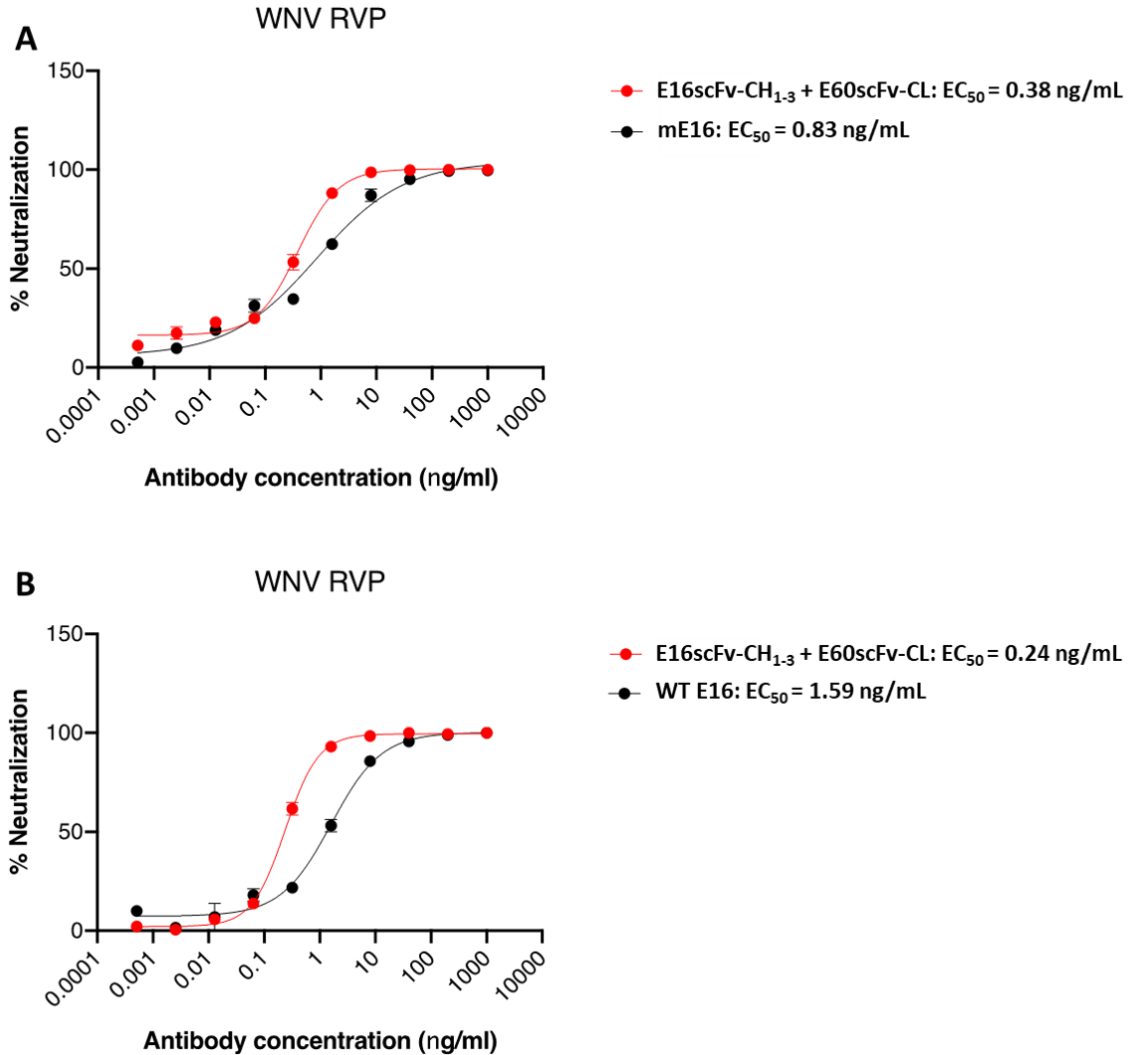
Figure 41. The E16scFv-CL + E60scFv-CH$_{1-3}$ bsAb Neutralized WNV RVPs. The PRNT was performed on WNV RVPs using the E16scFv-CL + E60scFv-CH$_{1-3}$ bsAb and mammalian cell made E16 mAb or WT *N. benthamiana* made E16 mAb. (A) The E16scFv-CL + E60scFv-CH$_{1-3}$ bsAb neutralized the WNV RVPs and yielded an EC$_{50}$ of 0.38 ng/mL, whereas the mammalian cell made E16 mAb yielded a nearly doubly higher EC$_{50}$ of 0.83 ng/mL. (B) Similarly, the E16scFv-CL + E60scFv-CH$_{1-3}$ bsAb neutralized the WNV RVP and showed an EC50 of 0.24 ng/mL, whereas the WT *N. benthamiana* made E16 mAb yielded a higher EC$_{50}$ of 1.59 ng/mL. In both PRNTs, the E16scFv-CL + E60scFv-CH$_{1-3}$ bsAb had a lower EC$_{50}$ when compared to mammalian cell or plant made E16 mAb EC$_{50}$s.

A PRNT assay was also done using WNV RVP to test the neutralization ability of the

E16scFv-CH$_{1-3}$ + ZV54scFv-CL bsAb. The E16scFv-CH$_{1-3}$ + ZV54scFv-CL bsAb was able to

neutralize the virus and had an EC$_{50}$ of 3.49 ug/uL whereas a mammalian cell made E16mAb had

an EC$_{50}$ of 3.12 ug/uL, which were quite comparable (Figure 42A). The assay was repeated using

the E16scFv-CH$_{1-3}$ + ZV54scFv-CL bsAb and a mammalian cell made ZV54 mAb. The results

revealed an EC$_{50}$ of 2.91, comparable to the previous assay using WNV RVPs, however, the

mZV54 had a much lower EC$_{50}$ of 0.34 ug/mL (Figure 42B). This result was surprising, since the

bsAb's EC$_{50}$ was nearly 9 times higher than the mZ54 mAb's EC$_{50}$.
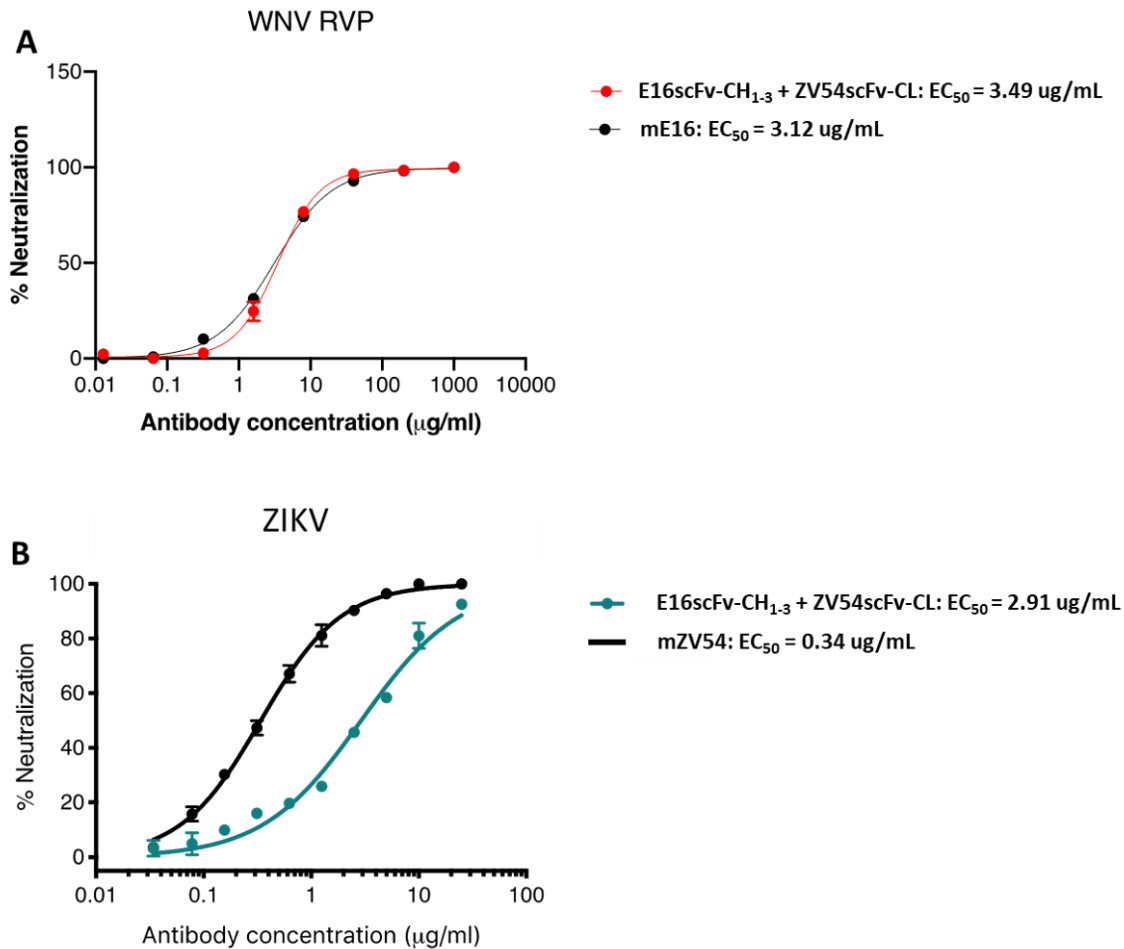
Figure 42. The E16scFv- CH$_{1-3}$ + ZV54scFv-CL bsAb Neutralizes both ZIKV and WNV RVPs.
(A) PRNT of WNV RVPs by the E16scFv-CH$_{1-3}$ + ZV54scFv-CL bsAb showed that the bsAb was able to neutralize the RVP and yielded an EC50 of 3.49 ug/mL, whereas the mammalian cell made E16 mAb also neutralized the RVP and yielded a similar EC50 of 3.12 ug/mL. (B) The same bsAb was used in a PRNT using the ZIKV where the bsAb neutralized the virus and yielded an EC50 of 2.91 ug/mL. A mammalian cell made ZV54 mAb also neutralized the virus, however, it yielded an EC50 of 0.34 ug/mL. These results show that the E16scFv-CH$_{1-3}$ + ZV54scFv-CL bsAb was able to neutralize both WNV RVPs and the ZIKV.

The bsAb Z54scFv-CH$_{1-3}$ + E60scFv-CL was also tested using the PRNT against the DENV-2 and the ZIKV. The ZIKV and the DENV-2 co-circulate and share the same *A. aegypti* mosquito vector, thus presenting the possibility of potential co-infections. The PRNT against the DENV-2 revealed quite similar EC$_{50}$s for both the Z54scFv-CH$_{1-3}$ + E60scFv-CL and mammalian cell made E60 mAb, 0.22 ug/mL and 0.36 ug/mL respectively (Figure 43A). The PRNT test against the ZIKV revealed slightly different results with the EC$_{50}$ of the Z54scFv-CH$_{1-3}$ + E60scFv-CL bsAb at 0.71 ug/mL and the mammalian cell made Z54 mAb at 0.38 ug/mL (Figure 43B). Overall, the results of the PRNT against both co-circulating DENV-2 and ZIKV viruses indicate that the bsAbs are comparable in their EC$_{50}$s to that of their parental mAbs, thereby offering an option for the treatment of these cocirculating viruses in a single recombinant-protein therapeutic molecule.
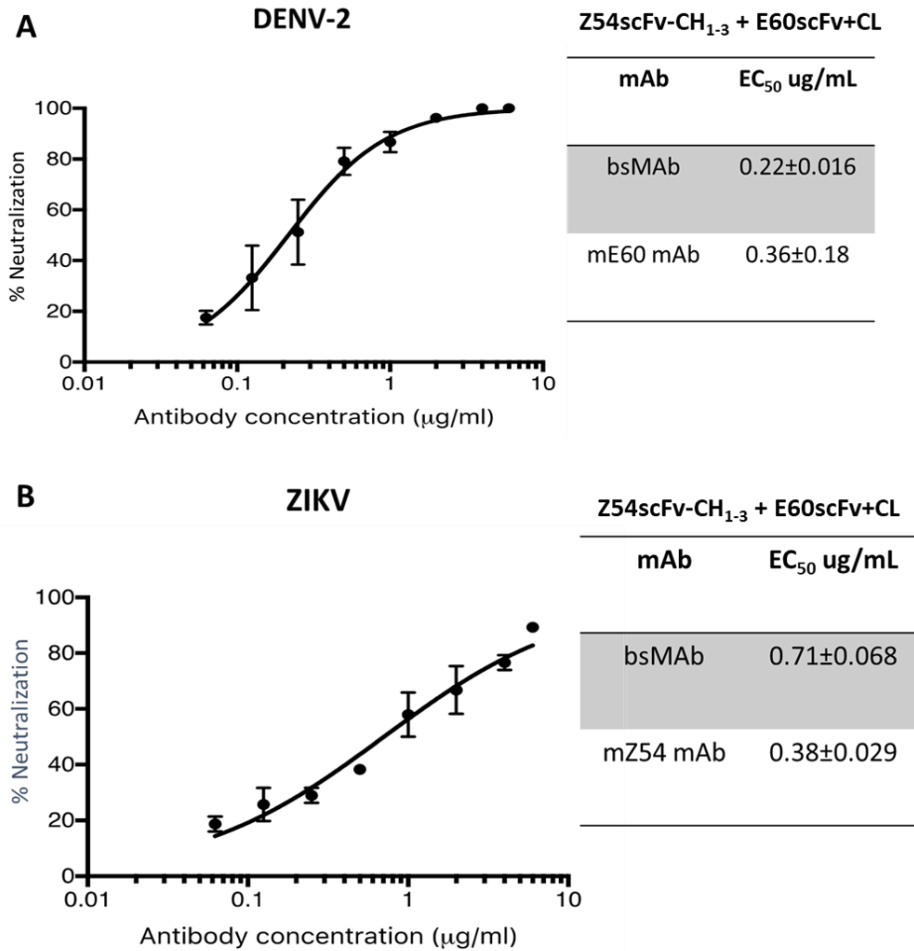
Figure 43. The Z54scFv-CH$_{1-3}$ + E60scFv-CL bsAb Neutralizes both DENV-2 and ZIKV. (A) The Z54scFv-CH$_{1-3}$ + E60scFv-CL bsAb was used in a PRNT to assess its ability to neutralize the DENV-2 virus. The results showed that the Z54scFv-CH$_{1-3}$ + E60scFv-CL neutralized the DENV-2 virus and yielded an EC$_{50}$ of 0.22 ug/mL whereas the mammalian cell made E60 mAb also neutralized the virus and yielded an EC$_{50}$ of 0.36 ug/mL. (B) The same Z54scFv-CH$_{1-3}$ + E60scFv-CL bsAb was subjected to a second PRNT where it yielded an EC$_{50}$ of 0.71 ug/mL whereas the mammalian cell made Z54 mAb yielded an EC$_{50}$ of 0.38 ug/mL. In both of these assays the Z54scFv-CH$_{1-3}$ + E60scFv-CL bsAb was able to neutralize the viruses and yielded EC$_{50}$s comparable to parental mAbs produced in mammalian cells, thereby demonstrating the potential efficacy of the bsAb in neutralizing the co-circulating viruses.

bsAb Prevents Antibody Dependent Enhancement of Infection

ADE is considered to be one of the main mechanisms of pathogenesis leading to DHF

and DSS. Research scientists attempting to produce a vaccine take into consideration the

possibility of ADE in their designs. Adding to the difficulty of that consideration, it has been

reported that ZIKV infections can exacerbate subsequent DENV infections to the extent of DHF

and DSS. Thus, a vaccine or therapeutic is needed that can treat those co-circulating viruses safely and efficiently. The Z54scFv-CH$_{1-3}$ + E60scFv-CL bsAb was subjected to an ADE assay in which DENV-2-bsAb or ZIKV-bsAb complexes were added to K562 cells bearing FcγR2a receptors, which have been implicated in mediating ADE. Treatment of K562 cells with mammalian cell produced E60-DENV-2 complexes showed a steady increase in K562 cell infection dependent on the amount of mAb added (Figure 44A). However, near 0.1 ug/mL of mE60 mAb, the % of infected K562 decreased until about 100 ug/uL where thereafter the % of K562 infected significantly decreased and neutralization of DENV-2 viruses was near complete. In contrast, the WT *N. benthamiana* produced Z54scFv-CH$_{1-3}$ + E60scFv-CL bsAb displayed very little infection of K562 cells, approximately below 4% of K562 infection across the range of bsAb concentration used. Although complete prevention of K562 cell infection with the DENV-2 did not occur when the DENV-2 virus was complexed with the Z54scFv-CH$_{1-3}$ + E60scFv-CL bsAb at concentrations lower than 10 ug/uL, a significant reduction in infection of K562 cells was observed when compared to the mammalian cell made E60-DENV-2 complex across the tested concentration range. Furthermore, near 0% infection of K562 cells was observed above 10 ug/uL of bsAb. A possible explanation for minimal K562 cell infection below 10 ug/mL could be due to the position of the DENV-2 binding component of the bsAb, which is on the light chain. The positioning of the E60 component on the light chain may introduce some difficulty in accessibility to its target epitope on the DENV-2 virus, thereby requiring higher concentrations of the bsAb to fully neutralize all DENV-2 virions and achieve 0% K562 infection.
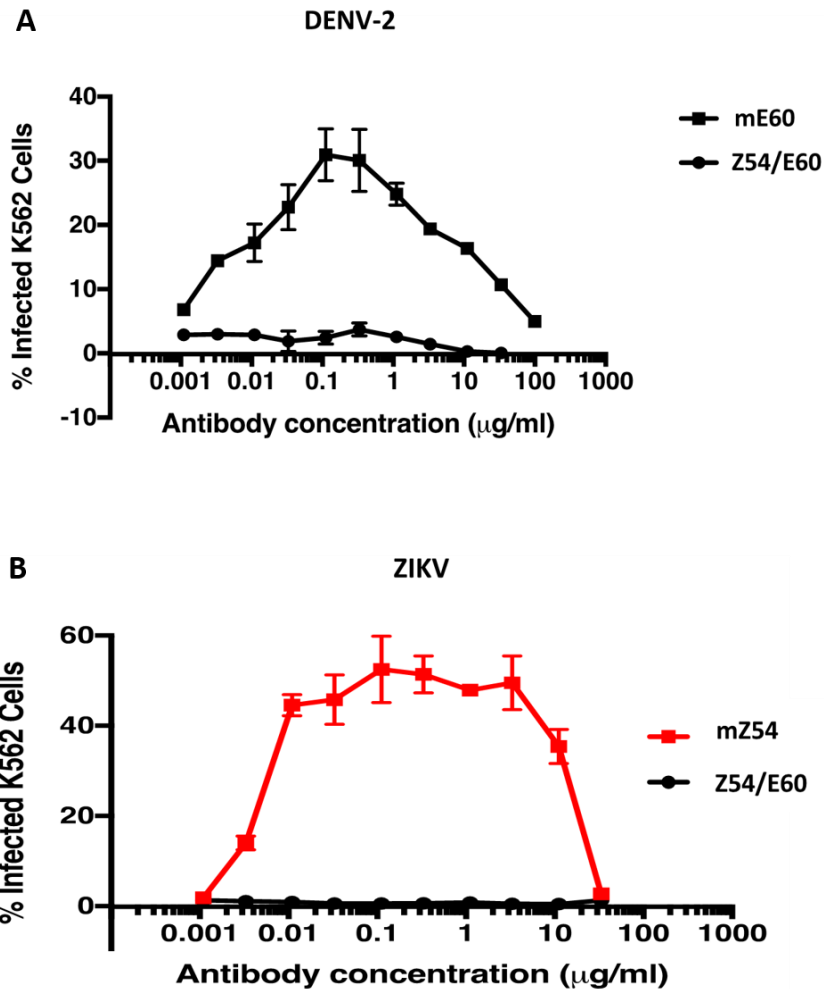
Figure 44. The Z54scFv-CH$_{1-3}$ + E60scFv-CL bsAb Significantly Reduced DENV-2 and ZIKV ADE *in vitro*. (A) The Z54scFv-CH$_{1-3}$ + E60scFv-CL bsAb was subjected to an ADE assay with the DENV-2 virus to assess the bsAbs ability to cause or prevent ADE. The data revealed that the Z54scFv-CH$_{1-3}$ + E60scFv-CL bsAb significantly reduced ADE whereas the mammalian cell made E60 mAb caused ADE in an mAb dose dependent manner. The remaining measurable DENV-2 infected K562 cells could be attributed to the position of the DENV-2 binding component of the bsAb, which is on the light chain in this particular bsAb. Thus, a greater dependency on the concentration of the bsAb to neutralize the virus is required, where at concentrations greater than 10 ug/mL the percentage of infected K562 cells is near 0. (B) A significant reduction in ADE was observed when K562 cells were treated with ZIKV-bsAb immune complexes. However, ADE was observed in an antibody concentration dependent manner when K562 cells were treated with mammalian made Z54 mAbs complexed with the ZIKV. This data shows the efficacy and safety of the plant-made bsAb in reducing ADE, which a major concern that has the potential to lead to severe forms of DENV disease.

Similarly, the addition of mammalian made Z54mAb-ZIKV complexes to K562 cells

caused an increase of infection in K562 cells by the ZIKV (Figure 44B). This too was dependent

on the concentration of mZ54 mAb added. Interestingly, a faux plateau was observed in the ZIKV

ADE assay that was not observed in the DENV-2 profile, indicating the possibility of slightly

different thresholds of ADE ability in these viruses. At a concentration of approximately 4 ug/uL of

mammalian cell made Z54 mAb, the percentage of K562 infected cells began to reduce until no

ADE was observed at approximately 30 ug/uL of mAb. In contrast the Z54scFv-CH$_{1-3}$ + E60scFv-

CL bsAb displayed virtually no ADE, where no significant increase in % of K562 cells infected by

the ZIKV was detected. These results reveal the efficacy of the Z54scFv-CH$_{1-3}$ + E60scFv-CL

bsAb in preventing ADE in both DENV-2 and the ZIKV, two viruses that cause significant disease

and co-circulate.

Discussion

The frequency of FV infections and the potential of their mosquito transmission vectors to

expand their range places an urgency on the development of vaccines and therapeutics to

combat them effectively. Dengvaxia, a vaccine developed by the Sanofi Pasteur pharmaceutical

company, attempted to protect us from DENV infection. This vaccine is a live attenuated

tetravalent formulation based on the highly successful Yellow Fever (YF) vaccine where coding

regions for the prME proteins of DENV serotypes 1-4 are expressed instead of the YF

counterparts. Despite the attempts for an urgently needed vaccine against DENV, the Dengvaxia

vaccine came with important limitations for its use. A particular study pointed out that in a noble

attempt to protect children, which are perhaps the most susceptible to DHF and DSS, in the

Philippines by administering the vaccine to millions of children, the vaccine actually caused illness

and was linked to the deaths of several children (Cohen, 2019). This was an alarming finding and

highlighted the difficulty in producing a vaccine against a virus that has 4 serotypes. As a result,

Sanofi has revised its indications for the vaccine and now advises against the use of the vaccine

in children who have not been previously exposed to any of the 4 DENV serotypes to prevent

possible severe dengue illness (e.g. DHF and DSS) in subsequent exposure to any DENV

serotype (Pasteur). In addition to a lack of a completely safe vaccine, there is also a lack of effective therapeutics to protect from DENV and ZIKV illnesses.

In addition to co-circulating, the DENV and ZIKV are antigenically similar with a reported amino acid similarity of approximately 55.6%, making the possibility of cross-reactive antibodies generated by either infection lead to ADE (Chang et al., 2017). A study conducted in mice by Fowler *et al* found that pup mice whom acquired anti-ZIKV mAbs had an increase in dengue disease severity, increased viral burden, and the acquired anti-ZIKV antibodies bound but did not neutralize DENV-2 when challenged by DENV-2 (Fowler et al., 2018). These studies and findings highlight the added concern of not just ADE caused by the exposure of heterologous DENV serotypes but also the possibility of ADE due to cross-reactive ZIKV and DENV antibodies.

In this study, our data indicated that the plant-made Z54scFv-CH$_{1-3}$ + E60scFv-CL bsAb both neutralized the DENV-2 and the ZIKV and virtually prevented ADE *in vitro* in both DENV-2 and ZIKV. ADE in DENV infections can occur in two ways: when subneutralizing antibodies bind to a virion and mediate the virion's entry into FcγR bearing cells and when neutralizing antibodies bind to a virion yet do not reach the threshold of antibodies needed to neutralize the virion (Dowd & Pierson, 2011). It is believed that the former is responsible for the ADE observed and leading to severe dengue infections. In those instances, mAbs formed from an initial infection of a particular DENV serotype bind to but do not neutralize subsequent heterologous DENV infections.

The virtual absence of ADE in our *in vitro* studies using the Z54scFv-CH$_{1-3}$ + E60scFv-CL bsAb is significant since ADE has been described as one of the main modes of pathogenesis in severe dengue disease, such as DHF and DSS. Furthermore, the virtual circumvention of ADE was entirely made possible by the type of glycan residues present at the Fc region of the Z54scFv-CH$_{1-3}$ + E60scFv-CL bsAb, which was dependent on the plant expression system. Glycan analysis of the E60scFv-CH$_{1-3}$ produced in WT and ΔXTFT *N. benthamiana* plants revealed a near homogenous *N*-linked glycans, which is a feature unmatched by CHO cells.

N-linked glycosylation in the Fc region of immunoglobulins is an important structural feature. The carbohydrate residues have a profound impact on the effector functions of the

immunoglobulin, such as recruitment of the C1q molecule in the complement classical pathway, ADCC, CDC, and half-life of the molecule (Jennewein & Alter, 2017). The glycoengineered *N. benthamiana* plants offer significant advantages in the production of immunoglobulins in their ability to form the core GnGn glycan structure that is common to most animals and humans. Furthermore, tailor made glycoproteins with specific glycans can be produced to sway towards a particular immune response, such as ADCC, CDC, or the targeting of particular FcγRs (Dent et al., 2016) .

bsAbs offer important advantages over standard mAb. Regardless of the particular design, of which many exist, a bsAb can bind to two different targets that may or may not be on the same antigen, molecule, or pathogen (Kontermann & Brinkmann, 2015). For example, a bsAb may bind to the same virus but target two different epitopes that may be important for binding or entry of the virion to the target cell, thereby blocking two important phases in the virus entry phases. Furthermore, in instances where a virus is neurotropic, such as the WNV, one of the arms of the bsAb could be used to bind to a highly expressed receptor on blood brain barrier brain capillary endothelial cells to gain access to the brain parenchyma and the other arm of the bsAb could be targeted towards the WNV for neutralization of the virus (Bourassa, Alata, Tremblay, Paris-Robidas, & Calon, 2019; Johnsen et al., 2017). Remarkably, targeting the infection life cycle of the EBOV, a group demonstrated the use of a bsAb in using a "Trojan Horse" strategy in which the EBOV was neutralized while already inside the cell in a late endosome (Wec et al., 2016). In both the WNV and the EBOV example, bsAb were used to gain access to and neutralize the viruses via the use of a secondary antigen binding site on the same molecule, a feat that separate parental molecules would not be able to achieve. In addition, bsAbs could be employed to bring two different cell types together, such T cells and cancerous cells (Frankel & Baeuerle, 2013). Derivatives of mAb seem to be limitless in their designs. A number of trispecific antibody (tsAbs) designs have been described and studies have shown promising results in potential protection against viruses such as HIV and solid tumors (Runcie, Budman, John, & Seetharamu, 2018; Xu et al., 2017).

This study demonstrated that plants were capable of producing complex proteins and glycosylate them with homogenous and mammalian like glycans. Glycan analysis revealed the importance of the CL in mAb assembly and it also revealed the superiority at which plants were able to homogenously glycosylate mAbs. Inducible yeast display assays verified that plant produced scFv-CH$_{1-3}$ and bsAbs recognized and bound to their targets. Furthermore, it was demonstrated that the Z54scFv-CH$_{1-3}$ + E60scFv-CL bsAb, which targets the co-circulating DENV-2 and ZIKV, neutralized and prevented ADE *in vitro*. This significant result makes this bsAb, which is safe and efficacious, a potential candidate for the treatment of the ZIKV and the DENV-2.

Future plans encompass *in vitro* efficacy studies of the Z54scFv-CH$_{1-3}$ + E60scFv-CL bsAb. Specifically, AG129 mice, mice deficient in interferon type I and type II receptors, would be challenged with the DENV and treated with the Z54scFv-CH$_{1-3}$ + E60scFv-CL bsAb, in pre and post DENV exposure scenarios. A129 mice, which lack interferon type I receptors, would be used in similar conditions when testing the Z54scFv-CH$_{1-3}$ + E60scFv-CL bsAb against ZIKV challenge.

CHAPTER 4

ATEZOLIZUMAB DERIVATIVES FOR DIAGNOSTICS IN CHECKPOINT IMMUNOTHERAPY

Introduction

Checkpoint immunotherapy has gained attention and has become key in the treatment of certain cancers. Anti-cancer therapy options have long included surgery, chemotherapy, and radiation therapy. However, much interest and research has led to the use of the immune system to attack cancer by the "training" of immune cells to recognize cancerous cells and by the administration of immune system molecules such as mAbs. To increase the possibility of a better outcome in a cancer treatment, some immunotherapies are coupled with traditional treatments such as chemotherapy and radiation.

The "training" of immune cells generally refers to the programing of T cells to recognize and effectively combat cancer. This involves leukapheresis of a patient's blood to collect their T cells, genetically modifying the T cells to encode a chimeric T cell receptor that is capable of identifying a cancer, and finally infusing the trained T cells back into the patient (Holstein & Lunning). This is referred to a CAR T cell therapy and has had great success in treating leukemia and lymphoma (Bagley & O'Rourke, 2019). However, attempts at translating the success of CAR T cell therapy to solid tumors has been modest at best (Khan, Khan, & Brentjens, 2019).

There are a variety of cancer immunotherapies for which the appropriate selection of a therapy largely depends on the type of cancer. Immunotherapies include the use of mAbs, anti-cancer vaccines, and checkpoint inhibitors. Each immunotherapy has advantages and disadvantage and must be chosen carefully.

The most common anti-cancer immunotherapy is the use of mAbs with over 2 dozen FDA approved mAbs (Bayer, 2019). mAbs contain the advantage of specificity towards a particular antigen and effector functions like ADCC and CDC via its Fc region (Kimiz-Gebologlu, Gulce-Iz, & Biray-Avci, 2018). Despite having characteristics of a magic bullet, anti-cancer mAbs are not

free of collateral biological damage. The side effects caused by some mAbs must be carefully monitored and can lead to potentially life-threatening situations.

Few anti-cancer vaccines are FDA approved and fall into two general categories: preventative and therapeutic (Christofi, 2019). The first FDA approved preventative anti-cancer vaccine was Gardasil and it protects against the Human Papilloma Virus, which causes cervical cancer and other HPV related cancers (Liu, 2014). Sipuleucel-T is a therapeutic anti-cancer vaccine designed to treat hormone-refractory prostate cancer. An increased availability of anti-cancer vaccines would be a tremendous health care advantage since it would prevent the development of cancer and associated burdens. However, efforts to produce safe and efficacious vaccines are hampered by the complexity of the immune system and immune-evasion tendencies of some cancers.

Immune checkpoint inhibition for anti-cancer therapies are frequently linked to mAbs. This strategy relies on the targeting of molecules involved in immune checkpoint inhibition, three of which are Cytotoxic T-lymphocyte-associated antigen 4 (CTLA-4), programmed death 1 (PD-1), and programmed death ligand 1 (PD-L1). It has become apparent that some cancer cells in tumor microenvironments have learned to escape immune surveillance by expressing immune checkpoint inhibitors, in effect enhancing their survival by suppressing anti-tumor activities of T cells (Christofi, 2019).

One of the major requirements of the immune system is to be able to discern between self and non-self. This is achieved by complex interactions between immune cells, mainly T cell and antigen presenting cells (APCs) such as dendritic cells in lymphoid tissues. A dysregulation in this process can lead to autoimmunity that can lead to disease. To prevent autoimmunity, immune checkpoint pathways are in place at various stages of an immune response (Kennedy, Bhatia, Thompson, & Grivas, 2019). CTLA-4 (present on T cells) and PD-1 (present on both T and B cells) are two key two receptors of immune checkpoint pathways (Hayashi & Nakagawa, 2019). The CTLA-4 receptor related immune checkpoint pathway operates at a very early stage of naïve T cell activation and stops T cells from proliferating that are potentially autoreactive,

83

whereas the PD-1 receptor related immune checkpoint operates after T cells have matured and are in circulation in the periphery (Buchbinder & Desai, 2016).

CTLA-4 and PD-1 have become targets in checkpoint immunotherapy for the treatment of some cancers. In 2011 the first anti CTLA-4 mAb was FDA approved and in 2014 two anti-PD-1 mAbs were approved, followed by the approval of 3 anti-PD-L1 mAbs in 2016 and 2017 (Kimiz-Gebologlu et al., 2018). The targeting of CTLA-4 for immune checkpoint therapy has a wider effect and thus carries a higher burden of toxicity as does the targeting of PD-1, however to a lesser extent. The targeting of PD-L1 has reduced potential toxicity by allowing the binding of the other PD-1 binding partner, PD-L2, thus not interfering with PD-1:PD-L2 interactions. The binding of PD-1 to PD-L1 significantly reduces T cell proliferation, cytokine production, and overall survival of T cell leading to the increased survival of tumor cells (Figure 45).
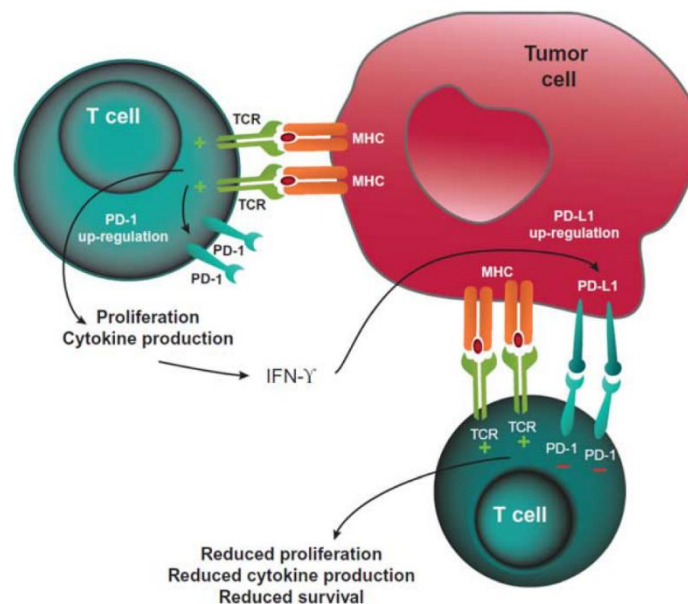
Figure 45. PD-1:PD-L1 Mediated Immune Evasion of Cancerous Cells. Some cancerous cells upregulate the expression of PD-L1 in attempts to increase their survival and avoid immune cell detection via the PD-1:PD-L1 immune checkpoint. In addition, the binding of PD-1 to PD-L1 causes T cells to not proliferate and enter a state of reduced survival and reduced cytokine production, further enhancing the survival and evasion of cancerous cells. The interruption of the PD-1:PD-L1 interaction by the use of mAbs based checkpoint immunotherapy has the effect of increased cancer cell killing by T cell and an increased inflammatory response. Figure credit: (Buchbinder & Desai, 2016)

The choice of cancer immunotherapy to be pursued depends on a couple of factors that include the type of cancer, patient's fitness for the immunotherapy, and the possibility of a positive response to the immunotherapy. Patients generally go through a screening process to determine candidacy to a given immunotherapy, which may include genetic screening and sampling of the cancerous mass. In the case of anti-PD-L1 immune checkpoint therapy, the level of PD-L1 expressed on cancerous cells is assessed. If a threshold of PD-L1 expression is met, the patient becomes a candidate for that therapy. To assists in diagnostic/screening, a molecule smaller than an mAb with similar affinity to PD-L1 would be greatly beneficial. A diabody, which is essentially two scFvs linked together, would be ideal. Diabodies are bivalent and have a smaller molecular structure than mAbs. Thus, diabodies would be an ideal molecule for diagnostics, imaging, and potential therapeutic applications since their smaller size of approximately 55 kDa confers them with faster pharmacokinetics that allows them to penetrate tissues deeper than an mAb would (Carmichael et al., 2003).

Data generated by Dr. Douglas Lake's research group (our collaborators) suggested that their CHO-cell made Atezolizumab-scFv (Atezolizumab is a chimeric anti-PD-L1 mAb) bound less effectively than the clinical grade Atezolizumab mAb and an Atezolizumab-scFv-Fc construct. Thus, the aim of this study was to design and develop an Atezolizumab-diabody that offers advantages of bivalency and small structure thereby conferring it with the ability to easily penetrate tissues. The diabody would be used for diagnostic purposes to aid medical professionals in their determination of the best treatment option for potential patients.

Material and Methods

Construction of PD-L1-Fc and Atezolizumab-derivatives expression vectors

The PD-L1-Fc construct was synthesized using GenBank Accession #Q9NZQ7 with added EcoRI, SacI, BsaI, Kozac, and plant signal peptide on the 5' end and a GGGGS linker and NheI site on the 3' end. The EcoRI and NheI sites were used to produce overhangs to ligate to human IgG hinge-CH_{2-3} IgG regions already in a pBluescript vector. The PD-L1-Fc coding

sequences were then digested cloned into the pBYR11eK2Md Gemini expression vector and transformed into *A. tumefaciens* strain EHA105. The Atezolizumab-scFv was cloned into the 3' MagnICON module pICH11599. The 3' MagnICON module pICH11599 was digested with EcoRI and BamHI. The coding sequences for the heavy chain and light chain variable regions of Atezolizumab were provided by Dr. Douglas Lake in a pcDNA3.1 plasmid. The coding sequences were copied using PCR with the addition of EcoRI, Kozac, and plant signal peptide on the 5' end and a 6X His-Tag sequence and BamHI site at the 5' end. The resulting construct was directly ligated into the 3' MagnICON module pICH11599 using the EcoRI and BamHI sites. The 3' module was then transformed into *A. tumefaciens* strain GV3101. The Atezolizumab-diabody was constructed by copying the VH and VL regions from the pcDNA3.1 via PCR with the following modifications: addition of an 8 amino acid linker -GGGSGGGG- between the variable heavy and light chains, the changing of the heavy variable region C-terminus amino acid sequence from TVSS to TVSLGGC to allow for the formation of a disulfide bond to stabilize the diabody. The final PCR product coding for the Atezolizumab diabody contained EcoRI, BsaI, and a plant signal peptide on the 5' end and a 6X His-Tag and SacI site on the 3' end. The Atezolizumab coding sequence was inserted to pBYR2eAK2Mc Gemini expression vector and transformed into *A. tumefaciens* EHA105.

Extraction and purification of PD-L1-Fc and Atezolizumab derivatives from *N. benthamiana* leaves.

        Five D.P.I., the PD-L1-Fc recombinant protein was harvested from *N. benthamiana* leaves using a two-step purification process. Initial clarification and final purification were done as described for the purification of bsAbs in the Material and Methods section of Chapter 3. The extraction and purification of the Atezolizumab derivatives was nearly identical to the procedure used for PD-L1-Fc, with the following exceptions: the homogenization buffer did not contain EDTA and immobilized metal affinity column chromatography (IMAC) was used instead of protein

A affinity chromatography, Atezolizumab-scFv was harvested 7 D.P.I and the Atezolizumab-diabody was harvested 5 D.P.I.

SDS-PAGE and Western blot Analysis

SDS-PAGE and Western blot analysis was performed as described in the Material and Methods section of Chapter 3.

Flowcytometry

RCJ-41T2 cells were harvested by trypsinization and diluted to $2X10^5$ cells per reaction tube. The cells were then treated with 5% FBS/PBS for 30 minutes at room temperature and subsequently stained with 10 ug/mL of Atezolizumab and derivatives thereof for 1 hour. The cells were then washed 2X with PBS and subsequently stained with Dylight 488 conjugated goat anti-human IgG at 1:25 for 1 hour (for Fc region bearing Atezolizumab and Atezolizumab derivatives) or stained with an anti-His Ab at 1:400 followed by staining with a FITC-conjugated goat anti-muse Ab at 1:40. All samples were then fixed with 4% formaldehyde/PBS for 15 minutes and analyzed by flow cytometry the following day.

Surface Plasmon Resonance

Affinity measurements for Atezolizumab, Atezolizumab-scFv, and the Atezolizumab-diabody were done by SPR as previously described by (H. Lai et al., 2014). Briefly, PD-L1 was immobilized on the sensor chip by an amine coupling kit as recommend by the manufacturer. Thereafter, Atezolizumab and Atezolizumab-variants were injected and allowed to flow over the chip. The equilibrium constant k_D was calculated as $k_D = k_{(d)}/k_{(a)}$.

Results

Purification of Atezolizumab derivatives and PD-L1 from leaves of *N. benthamiana.*

       N. benthamiana leaves expressing Atezolizumab derivatives were harvested 4 D.P.I.,
whereas PD-L1 expression leaves were harvested 7 D.P.I. The His-tagged recombinant protein
containing leaves and the PD-L1 recombinant protein containing leaves were then processed for
immobilized metal affinity chromatography (IMAC) and protein A affinity chromatography,
respectively. The recombinant proteins were analyzed by SDS-PAGE and gels subsequently
stained with Coomassie blue. The Atezolizumab-scFv with an approximate MW of 25 kDa was
relatively free of contaminating proteins as observed by this method (Figure 46A). Likewise, the
Atezolizumab His-tagged diabody appeared to be relatively free of contaminating proteins and the
expected MW under reducing conditions of 25 kDa (Figure 46C, lane 2) was observed. The
assembled diabody under non-reducing conditions was observed at the expected MW of 50 kDa
(Figure 46C, lane 1). The expected MW of PD-L1-Fc was 52 kDa, however, it was observed at
approximately 62.5 kDa under reducing conditions (Figure 46B, lane 1). This result was not
expected, however, further investigation revealed commercially available PD-L1-Fc with an
apparent MW of 70-75 kDa on SDS-PAGE (R& D SYSTEMS, Cat. # 156-B7). Under non-
reducing conditions, an expected MW of 102 kDa was not observed, instead, a band was
observed closer to the 150 kDa MW (Figure 46B, lane 2). The apparent discrepancy in expected
and observed MW of PD-L1-Fc may be due to extensive glycosylation of the recombinant PD-L1
protein. PD-L1 has 3 glycosylation sites in addition to the CH_2 glycosylation site of the Fc region,
which may influence its migration and reflect a higher MW in SDS-PAGE.
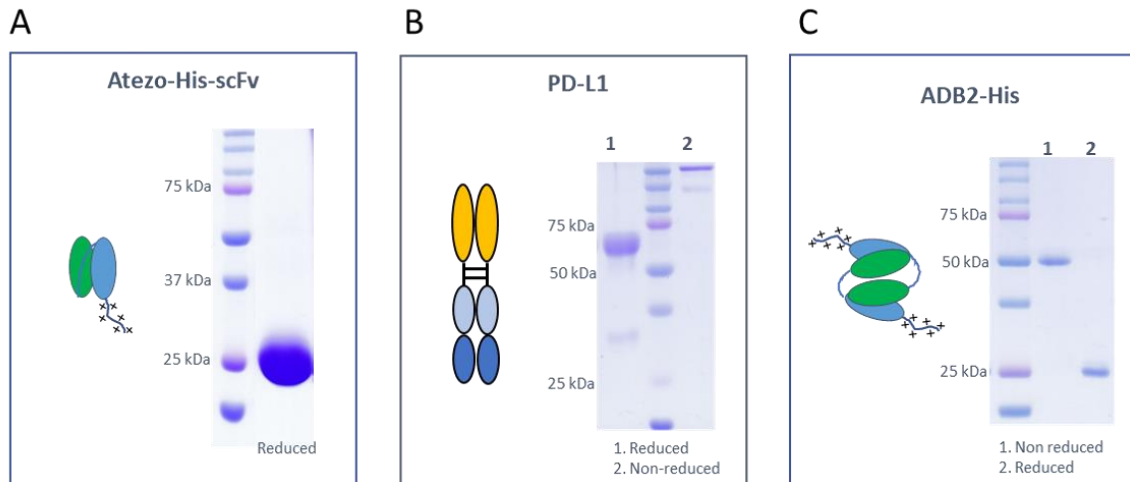
Figure 46. Assessment of Purity by Coomassie Stained SDS-PAGE of His-tagged Atezolizumab Derivatives and PD-L1-Fc. (A) The His-tagged Atezolizumab-scFv appeared to be relatively free of contaminating proteins upon purification by IMAC and it reflected its expected MW at 25 kDa. (B) The PD-L1-Fc protein was also relatively free of contaminating proteins. However, it appeared at a MW of 62.5 kDa although it was expected to be 52 kDa under reduced conditions (lane 1). PD-L1 contains 3 *N*-linked glycosylation sites in addition to the glycosylation site on the CH$_2$ domain of the IgG Fc region fused to the PD-L1. These glycosylation sites may be altering the migration pattern of PD-L1-Fc to appear higher in MW than expected. Under non-reducing conditions (lane 2), PD-L1-Fc also had a much higher MW than the expected 102 kDa. (C) The His-tagged Atezolizumab diabody also appeared to be relatively pure and free of contaminating proteins. Under reducing conditions, the His-tagged diabody appeared to have a MW of 25 kDa, as expected, and a MW of 50 kDa under non-reducing conditions, indicating proper assembly of the diabody. The two-step purification process appeared to be effective in removing contaminating proteins from the final preparations of the plant produced recombinant proteins.

Expression and assembly of PD-L1-Fc and Atezolizumab derivatives in *N. benthamiana*.

SDS-PAGE analysis of PD-L1-Fc and Atezolizumab derivatives showed MWs that corroborated with our expectations. To assert the identity of the expressed recombinant proteins, Western blots were performed on all three recombinant proteins. The Atezolizumab-scFv and Atezolizumab diabody were probed indirectly by first transferring the recombinant proteins of interest on to a PVDF membrane, followed by PD-L1-Fc and finally detecting with an anti-human gamma-chain HRP-conjugated mAb. Signal was observed for the Atezolizumab-scFv at the expected MW of 25 kDa, indicating a positive identification of Atezolizumab-scFv (Figure 47A). Similarly, a signal was observed for the Atezolizumab diabody at a MW of 25 kDa under reducing conditions (Figure 47C, lane 2) and a MW of 50 kDa under non-reducing conditions (Figure 47C,

lane 1), thereby indicating a positive identification of the Atezolizumab diabody. PD-L1-Fc was

detected directly using an HRP-conjugated anti-human gamma-chain. Signal was observed at

approximately 62 kDa, similar to the SDS-PAGE analysis MW, under reducing conditions (Figure

47, lane 2) indicating a positive identification of PD-L1-Fc. Under non-reducing conditions, a

strong signal band was observed at approximately 150 kDa thereby positively identifying PD-L1-

Fc and correct assembly thereof. A second band was observed under reducing conditions of PD-

L1-Fc at approximately 30 kDa, which may be due to degradation products of PD-L1-Fc. Such

bands are not uncommon and also seen in normal mAb samples.
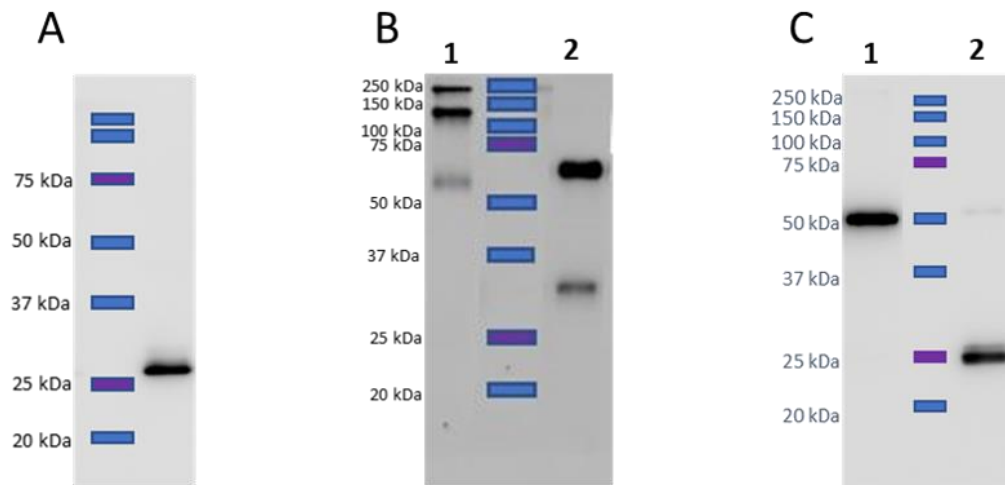
Figure 47. Western Blot Analysis of His-tagged Atezolizumab Derivatives and PD-L1-Fc. (A)
With a MW of approximately 25 kDa, Atezolizumab-scFv was positively identified and indicating
proper assembly and folding of the recombinant protein. (B) PD-L1-Fc was also identified at a
MW of approximately 62.5 kDa under reducing conditions, as observed in Coomassie stained
SDS-PAGE analysis (lane 2). A second band was also observed indicating possible degradation
products of PD-L1-Fc. (C) Under reducing conditions, the Atezolizumab diabody was detected at
approximately 25 kDa (lane 2) and at 50 kDa (lane1) under non-reducing conditions, indicating
proper folding and assembly of the diabody.

Binding specificity of Atezolizumab derivatives.

The binding specificities of Atezolizumab were assessed through flowcytometry using a

sarcomatoid Renal Cell Cancer (RCC) RCJ-41T2 cell line that expressed PD-L1 on its surface.

As a comparison for binding specificity, a clinical grade sample of Atezolizumab was used. In

addition to the plant made Atezolizumab-scFv and Atezolizumab-diabody, three more

Atezolizumab derivatives were tested. Of the additional three Atezolizumab derivatives, one of

the Atezolizumab-scFv-CH$_{1-2}$, was produced in *N. benthamiana* plants. The clinical grade

Atezolizumab mAb demonstrated a strong secondary fluorescence peak, indicating strong

binding of the mAb to PD-L1 on the surface of the RCJ-41T2 cells (Figure 48A). Secondary

fluorescent peaks were also observed when the RCJ-41T2 cells were treated with CHO-cell and

N. benthamiana plant made Atezolizumab-scFv-CH$_{1-2}$ recombinant proteins, indicating binding to

cell surface PD-L1 (Figure 48B,C). A CHO-cell made Atezolizumab-scFv was also tested,

however it did not reveal a very strong non-overlapping secondary fluorescent peak, indicating

potential weak binding of the *N. benthamiana* to PD-L1 on the cell surface (Figure 48D). Similarly,

an *N. benthamiana* made Atezolizumab-scFv did not display a strong non-overlapping secondary

fluorescent peak, also indicating the potential weak binding to the Atezolizumab-scFv to surface

PD-L1 (Figure 48E). The *N. benthamiana* made Atezolizumab-diabody did not display a very

strong non-overlapping secondary fluorescent peak and was arguably the weakest binding

Atezolizumab derivative of all (Figure 48F). The results shown here suggest that the CHO-cell

and plant made Atezolizumab derivatives lacking Fc regions do not bind well to PD-L1 displayed

on the surface of cells. This observation, however, may not be due entirely to the intrinsic binding

abilities of the Atezolizumab derivatives, but may be due to the detection method.
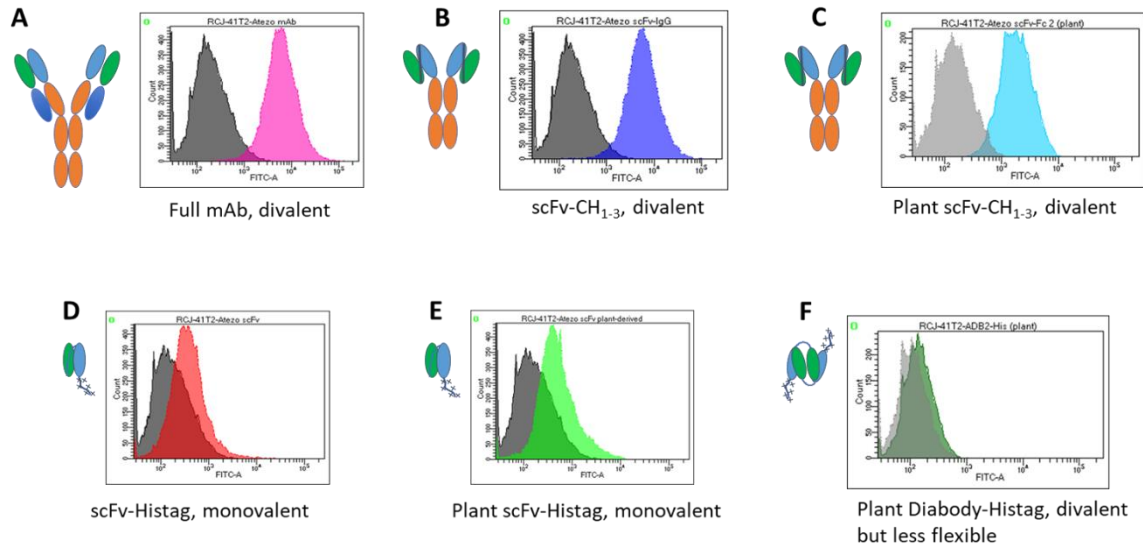
Figure 48. Binding of Atezolizumab and Atezolizumab Derivatives to PD-L1. RCJ-41T2 cells expressing PD-L1 were used in a flow cytometry assays to assess the binding of Atezolizumab derivatives made in CHO cell and *N. benthamiana*. (A) Clinical grade Atezolizumab mAb displayed a non-overlapping secondary fluorescent peak, indicating binding of the mAb to PD-L1 on the cellular surface. (B and C) CHO cell and *N. benthamiana* made Atezolizumab-CH_{2-3} displayed non-overlapping secondary fluorescent peaks, also indicating binding of the Atezolizumab derivatives to PD-L1. (D and E) CHO cell and *N. benthamiana* made Atezolizumab-scFvs did not display non-overlapping secondary fluorescent peaks, possibly indicating weak binding of the Atezolizumab derivatives to PD-L1. (F) The *N. benthamiana* made Atezolizumab-diabody displayed the weakest possible binding to PD-L1 of the Atezolizumab derivates with the most overlapping secondary fluorescent peak of the group. The apparent weak binding of the scFvs and diabody may be due to the method of detection and not the inherent binding abilities of the molecules.

Binding specificities and kinetics of Atezolizumab and Atezolizumab derivatives.

The binding specificities and kinetics of the Atezolizumab derivatives were assessed via SPR (Table 3). The recombinant PD-L1-Fc was coated on the chip surface and subsequently treated with the clinical grade Atezolizumab mAb or Atezolizumab derivatives. The k_D of clinical grade Atezolizumab mAb was determined to be 8.57×10^{-10} whereas the Atezolizumab derivative k_D values were 5.27×10^{-9} for the Atezolizumab-scFv and 2.08×10^{-9} for the Atezolizumab-diabody. The SPR results show a 10-fold different in binding affinities between the clinical Atezolizumab-mAb and Atezolizumab-derivatives.

	Mean k_D	S.D.	R square fit
Atezolizumab	8.57E-10	1.14E-10	0.999725
Atezolizumab-scFv	5.27E-09	2.94E-09	0.9978
Atezolizumab-Diabody	2.08E-09	5.32E-10	0.99905

Table 3. Binding Kinetics of Atezolizumab and *N. benthamiana* Produced Atezolizumab Derivatives via SPR. The binding kinetics of Atezolizumab and its plant produced derivatives were measure via SPR. The data show a kD value in the picomolar range for the clinical grade Atezolizumab mAb and kD values in the nanomolar range for both plant produced Atezolizumab-scFv and the Atezolizumab-diabody.

Discussion

Within the last decade cancer immunotherapy has made advances that has placed it as an additional treatment option to different cancer types. In particular, mAb based immunotherapy has made great advances with over 2 dozen FDA approved mAbs available to date. Immune checkpoint pathways controlled by CTLA-4 and PD-1 have been investigated for immunotherapy and has resulted in the development of multiple mAbs targeting those checkpoints, thereby aiding the immune system, specifically T cells, to identify and eliminate cancerous cells. In this study a diabody derived from the anti-PD-L1 mAb Atezolizumab, was investigated for its ability to bind to its PD-L1 target. SPR analysis demonstrated that the Atezolizumab-diabody bound to its intended target in the nanomolar range ($k_D = 2.08 \times 10^{-9}$) whereas the Atezolizumab mAb bound to the same intended target in the picomolar range ($k_D = 8.54 \times 10^{-10}$).

Strong binding to PD-L1 on the surface of RCJ-41T2 cells by clinical grade Atezolizumab and Atezolizumab-scFv-Fc but not by Atezolizumab-scFvs and the Atezolizumab-diabody was a peculiar result (Figure 43). Binding predictions would have all Atezolizumab derivatives demonstrate a secondary peak in fluorescence, thus the lack of a second peak seen in the Atezolizumab-scFvs and the diabody indicate a detection problem and not a binding problem inherent in the Atezolizumab derivatives.

The significantly smaller size of a diabody allows it to penetrate tissues where standard mAbs would not. This makes diabodies better candidates for diagnostics, imaging, and possible therapeutic use. Future research will encompass the use of a better detection mAb against the

Atezolizumab-scFv and Atezolizumab-diabody. Furthermore, functional cell-based assays whereby a reporter gene indicates binding or inhibition of binding of PD-1 to PD-L1 are planned for the future.

Plants have become a popular alternative in producing mAbs and other recombinant proteins such as enzymes. In addition to the diabody, an Atezolizumab-scFv and an Atezolizumab-scFv-Fc were produced in the *N. benthamiana* plant, demonstrating the ability of complex protein production, proper folding, and structure that is achievable in plants.

CHAPTER 5

SUMMARY AND OUTLOOK

FVs are responsible for a large percentage of arbovirus caused diseases. The diseases caused by the DENV and the ZIKV, for example, are largely self-limiting febrile illnesses. However, under some circumstances severe diseases and life altering consequences can result from infections with these viruses. Furthermore, the DENV and the YFV are endemic in some sectors of the tropical and subtropical regions of the world. After the 2015 outbreak of the ZIKV in South America, the ZIKV is expected to become endemic in some regions of South America, thereby increasing the possibility of co-infection with these viruses. Specific therapeutic treatments for illnesses caused by these pathogens do not exist, although recently an FDA approved vaccine for the DENV was made available this year in the United States, albeit its use is limited to just those who have previously been exposed to any DENV serotype for fear of vaccine induced ADE in those who have not been infected with any serotype of the DENV. There is no FDA approved vaccine for the ZIKV, however, several vaccines, including a DNA based vaccine, are currently under clinical evaluation (available, 2019) .

Thus, there is a need for safe and effective therapeutics for these co-circulating viruses. Here, data was presented in which a plant made anti-DENV pE60 mAb neutralized DENV-2 and did not cause ADE *in vitro*. Furthermore, the bsAb Z54scFv-CH$_{1-3}$ + E60scFv-CL neutralized both the DENV-2 and the ZIKV viruses, yielding EC$_{50}$s comparable to their individual parental mAbs.

Additionally, the Z54scFv-CH$_{1-3}$ + E60scFv-CL bsAb significantly reduced ADE in DENV-2 and ZIKV *in vitro* assays, whereas their mammalian cell made individual parental mAbs promoted ADE. The virtual elimination of ADE was attributed to the *N*-linked glycosylation profile conferred to the bsAb by the *N. benthamiana* tobacco plant. Specifically, we hypothesize that the *N*-linked glycan on the Fc region of the bsAb diminished its affinity to the FcγR2a found on K562 cells, thereby denying infection of the K562 via FcγR2a mediated endocytosis. Based on these data, we conclude that plant made E60 and the Z54scFv-CH$_{1-3}$ + E60scFv-CL bsAb are better the option for potential therapeutic use versus their mammalian cell made parental mAbs.

95

Further characterization and experiments of the bsAb would include mouse studies where mice (AG129 mice for the DENV-2 and A129 mice for the ZIKV) would be treated with the bsAb pre and post challenge with the DENV-2 or the ZIKV. This would allow us to evaluate the capacity of the bsAb to induce or circumvent ADE in an *in vivo* model.

Checkpoint immunotherapy has gained use in the treatment of certain cancers, such as small cell lung cancer (Atezolizumab), advanced urothelial bladder cancer (Pembrolizumab), and melanoma (Ipilimumab). Here, data was presented demonstrating the *N. benthamiana* capable of expressing, properly folding, and assembling Atezolizumab derivatives. Both the scFv and diabody Atezolizumab derivatives demonstrated binding to their PD-L1 targets *in vitro*. Their effective small sizes give them the potential to penetrate deep tissues, which is useful for imaging, diagnostics, and potential use for checkpoint immunotherapy.

Future research into the functionality of the Atezolizumab derivatives would involve a cell-based assay, such as the PD-1/PD-L1 Blockade Bioassay offered by Promega. Here, a PD-1 effector cell (T cell) contains a reporter gene that is activated upon inhibition of binding of its PD-1 receptor and a PD-L1 expressing cell. In this scenario, the Atezolizumab derivatives would be evaluated for their potential to inhibit that interaction. Further testing would also include the use of mouse models whereby the diabodies would be also evaluated for tumor reduction/elimination.

Plant glycoengineering has changed negatively held perceptions with plant produced therapeutic recombinant proteins. Concerns relating to plant specific carbohydrates, potential hypersensitivity, or adverse immune reactions to plant produced recombinant proteins have been alleviated with transgenic plants now capable of human like *N*-linked glycosylation.

REFERENCES

Aebi, M. (2013). N-linked protein glycosylation in the ER. *Biochimica et Biophysica Acta (BBA) - Molecular Cell Research, 1833*(11), 2430-2437. doi:https://doi.org/10.1016/j.bbamcr.2013.04.001

Apte-Sengupta, S., Sirohi, D., & Kuhn, R. J. (2014). Coupling of replication and assembly in flaviviruses. *Curr Opin Virol, 9*, 134-142. doi:10.1016/j.coviro.2014.09.020

Arntzen, C. (2015). Plant-made pharmaceuticals: from 'Edible Vaccines' to Ebola therapeutics. *Plant Biotechnol J, 13*(8), 1013-1016. doi:10.1111/pbi.12460

available, n. (2019). Phase 2 Zika Vaccine Trial Begins in U.S., Central and South America. *not available*.

Bagley, S. J., & O'Rourke, D. M. (2019). Clinical investigation of CAR T cells for solid tumors: lessons learned and future directions. *Pharmacology & Therapeutics*, 107419. doi:https://doi.org/10.1016/j.pharmthera.2019.107419

Balsitis, S. J., Williams, K. L., Lachica, R., Flores, D., Kyle, J. L., Mehlhop, E., . . . Harris, E. (2010). Lethal antibody enhancement of dengue disease in mice is prevented by Fc modification. *PLoS Pathog, 6*(2), e1000790. doi:10.1371/journal.ppat.1000790

Bayer, V. (2019). An Overview of Monoclonal Antibodies. *Seminars in Oncology Nursing*, 150927. doi:https://doi.org/10.1016/j.soncn.2019.08.006

Beltramello, M., Williams, K. L., Simmons, C. P., Macagno, A., Simonelli, L., Quyen, N. T. H., . . . Sallusto, F. (2010). The human immune response to Dengue virus is dominated by highly cross-reactive antibodies endowed with neutralizing and enhancing activity. *Cell Host & Microbe, 8*(3), 271-283. doi:10.1016/j.chom.2010.08.007

Beltrán-Silva, S. L., Chacón-Hernández, S. S., Moreno-Palacios, E., & Pereyra-Molina, J. Á. (2018). Clinical and differential diagnosis: Dengue, chikungunya and Zika. *Revista Médica del Hospital General de México, 81*(3), 146-153. doi:10.1016/j.hgmx.2016.09.011

Bendandi, M., Marillonnet, S., Kandzia, R., Thieme, F., Nickstadt, A., Herz, S., . . . Gleba, Y. (2010). Rapid, high-yield production in plants of individualized idiotype vaccines for non-Hodgkin's lymphoma. *Annals of Oncology, 21*(12), 2420-2427. doi:10.1093/annonc/mdq256

Bourassa, P., Alata, W., Tremblay, C., Paris-Robidas, S., & Calon, F. (2019). Transferrin Receptor-Mediated Uptake at the Blood–Brain Barrier Is Not Impaired by Alzheimer's Disease Neuropathology. *Molecular Pharmaceutics, 16*(2), 583-594. doi:10.1021/acs.molpharmaceut.8b00870

Brady, O. J., Osgood-Zimmerman, A., Kassebaum, N. J., Ray, S. E., de Araújo, V. E. M., da Nóbrega, A. A., . . . Marinho, F. (2019). The association between Zika virus infection and microcephaly in Brazil 2015–2017: An observational analysis of over 4 million births. *PLOS Medicine, 16*(3), e1002755. doi:10.1371/journal.pmed.1002755

Brand, C., Bisaillon, M., & Geiss, B. J. (2017). Organization of the Flavivirus RNA replicase complex. *Wiley Interdiscip Rev RNA, 8*(6). doi:10.1002/wrna.1437

Briant, L., Despres, P., Choumet, V., & Misse, D. (2014). Role of skin immune cells on the host susceptibility to mosquito-borne viruses. *Virology, 464-465*, 26-32. doi:10.1016/j.virol.2014.06.023

Buchbinder, E. I., & Desai, A. (2016). CTLA-4 and PD-1 Pathways: Similarities, Differences, and Implications of Their Inhibition. *Am J Clin Oncol, 39*(1), 98-106. doi:10.1097/COC.0000000000000239

Carmichael, J. A., Power, B. E., Garrett, T. P. J., Yazaki, P. J., Shively, J. E., Raubischek, A. A., . . . Hudson, P. J. (2003). The Crystal Structure of an Anti-CEA scFv Diabody Assembled from T84.66 scFvs in VL-to-VH Orientation: Implications for Diabody Flexibility. *Journal of Molecular Biology, 326*(2), 341-351. doi:https://doi.org/10.1016/S0022-2836(02)01428-6

Castilho, A., & Steinkellner, H. (2012). Glyco-engineering in plants to produce human-like N-glycan structures. *Biotechnol J, 7*(9), 1088-1098. doi:10.1002/biot.201200032

Chang, H.-H., Huber, R. G., Bond, P. J., Grad, Y. H., Camerini, D., Maurer-Stroh, S., & Lipsitch, M. (2017). Systematic analysis of protein identity between Zika virus and other arthropod-borne viruses. *Bulletin of the World Health Organization, 95*(7), 517-525I. doi:10.2471/BLT.16.182105

Chaturvedi, U. C., Agarwal, R., Elbishbishi, E. A., & Mustafa, A. S. (2000). Cytokine cascade in dengue hemorrhagic fever: implications for pathogenesis. *Pathogens and Disease, 28*(3), 183-188. doi:10.1111/j.1574-695X.2000.tb01474.x

Chen, Q. (2011). Expression and manufacture of pharmaceutical proteins in genetically engineered horticultural plants. *CRC Press*, 83-124.

Chen, Q. (2016). Glycoengineering of plants yields glycoproteins with polysialylation and other defined N-glycoforms. *Proc Natl Acad Sci U S A, 113*(34), 9404-9406. doi:10.1073/pnas.1610803113

Chen, Q., & Davis, K. R. (2016). The potential of plants as a system for the development and production of human biologics. *F1000Research, 5*, F1000 Faculty Rev-1912. doi:10.12688/f1000research.8010.1

Chen, Q., He, J., Phoolcharoen, W., & Mason, H. S. (2011). Geminiviral vectors based on bean yellow dwarf virus for production of vaccine antigens and monoclonal antibodies in plants. *Human Vaccines, 7*(3), 331-338. doi:10.4161/hv.7.3.14262

Chen, Q., & Lai, H. (2014). Plant-derived monoclonal antibodies as human biologics for infectious disease and cancer.

Chen, Q., & Lai, H. (2015). Gene Delivery into Plant Cells for Recombinant Protein Production. *BioMed Research International, 2015*, 10. doi:10.1155/2015/932161

Chen, Q., & Lai, H. (2015). The growing potential of plant-made monocolonal antibodies. *Drug Target Review, 2*, 41-11.

Chen, Q., Lai, H., Hurtado, J., Stahnke, J., Leuzinger, K., & Dent, M. (2013). Agroinfiltration as an Effective and Scalable Strategy of Gene Delivery for Production of Pharmaceutical Proteins. *Adv Tech Biol Med, 1*(1). doi:10.4172/atbm.1000103

Chen, Q., Santi, L., & Zhang, C. (2014). Plant-made biologics. *Biomed Res Int, 2014*, 418064. doi:10.1155/2014/418064

Chong, M. K., Chua, A. J. S., Tan, T. T. T., Tan, S. H., & Ng, M. L. (2014). Microscopy techniques in flavivirus research. *Micron, 59*, 33-43. doi:https://doi.org/10.1016/j.micron.2013.12.006

Christofi, T. B., S.; Falzone, L.; Libra, M.; Zaravinos, A. (2019). Current Perspectives in Cancer Immunotherapy. *Cancers, 11*.

Cohen, J. (2019). Controversy over dengue vaccine risk. *Science, 365*(6457), 961. doi:10.1126/science.365.6457.961

Couderc, T., & Lecuit, M. (2015). Chikungunya virus pathogenesis: From bedside to bench. *Antiviral Research, 121*, 120-131. doi:https://doi.org/10.1016/j.antiviral.2015.07.002

Cucunawangsih, & Lugito, N. P. H. (2017). Trends of Dengue Disease Epidemiology. *Virology (Auckl), 8*, 1178122X17695836. doi:10.1177/1178122X17695836

Dai, L., Song, J., Lu, X., Deng, Y.-Q., Musyoki, Abednego M., Cheng, H., . . . Gao, George F. (2016). Structures of the Zika Virus Envelope Protein and Its Complex with a Flavivirus Broadly Protective Antibody. *Cell Host & Microbe, 19*(5), 696-704. doi:https://doi.org/10.1016/j.chom.2016.04.013

Darbani B, F. S., Toorchi M, Zakerbostanabad S, Noeparvar S, C.Stewart CN Jr. (2008). DNA-Delivery Methods to Produce Transgenic Plants. *Biotechnology, 7*, 385-402. doi:10.3923/biotech.2008.385.402

Dejnirattisai, W., Wongwiwat, W., Supasa, S., Zhang, X., Dai, X., Rouvinski, A., . . . Screaton, G. R. (2015). A new class of highly potent, broadly neutralizing antibodies isolated from viremic patients infected with dengue virus. *Nature immunology, 16*(2), 170-177. doi:10.1038/ni.3058

Deng, Y.-Q., Dai, J.-X., Ji, G.-H., Jiang, T., Wang, H.-J., Yang, H.-o., . . . Qin, C.-F. (2011). A broadly flavivirus cross-neutralizing monoclonal antibody that recognizes a novel epitope within the fusion loop of E protein. *PLoS One, 6*(1), e16059-e16059. doi:10.1371/journal.pone.0016059

Dent, M., Hurtado, J., Paul, A. M., Sun, H., Lai, H., Yang, M., . . . Chen, Q. (2016). Plant-produced anti-dengue virus monoclonal antibodies exhibit reduced antibody-dependent enhancement of infection activity. *J Gen Virol, 97*(12), 3280-3290. doi:10.1099/jgv.0.000635

Dowd, K. A., & Pierson, T. C. (2011). Antibody-mediated neutralization of flaviviruses: a reductionist view. *Virology, 411*(2), 306-315. doi:10.1016/j.virol.2010.12.020

Duffy, M. R., Chen, T.-H., Hancock, W. T., Powers, A. M., Kool, J. L., Lanciotti, R. S., . . . Hayes, E. B. (2009). Zika Virus Outbreak on Yap Island, Federated States of Micronesia. *New England Journal of Medicine, 360*(24), 2536-2543. doi:10.1056/NEJMoa0805715

Ebi, K. L., & Nealon, J. (2016). Dengue in a changing climate. *Environmental Research, 151*, 115-123. doi:https://doi.org/10.1016/j.envres.2016.07.026

Edward, B. H., Nicholas, K., Roger, S. N., Susan, P. M., Daniel, R. O. L., & Grant, L. C. (2005). Epidemiology and Transmission Dynamics of West Nile Virus Disease. *Emerging Infectious Disease journal, 11*(8), 1167. doi:10.3201/eid1108.050289a

flickr. (2012). Culex pipiens.

Fowler, A. M., Tang, W. W., Young, M. P., Mamidi, A., Viramontes, K. M., McCauley, M. D., . . . Shresta, S. (2018). Maternally Acquired Zika Antibodies Enhance Dengue Disease Severity in Mice. *Cell Host Microbe, 24*(5), 743-750 e745. doi:10.1016/j.chom.2018.09.015

Frankel, S. R., & Baeuerle, P. A. (2013). Targeting T cells to tumor cells using bispecific antibodies. *Current Opinion in Chemical Biology, 17*(3), 385-392. doi:https://doi.org/10.1016/j.cbpa.2013.03.029

Gelvin, S. B. (2003). Agrobacterium-mediated plant transformation: the biology behind the "gene-jockeying" tool. *Microbiology and molecular biology reviews : MMBR, 67*(1), 16-37. doi:10.1128/mmbr.67.1.16-37.2003

Giritch, A., Marillonnet, S., Engler, C., van Eldik, G., Botterman, J., Klimyuk, V., & Gleba, Y. (2006). Rapid high-yield expression of full-size IgG antibodies in plants coinfected with noncompeting viral vectors. *Proc Natl Acad Sci U S A, 103*(40), 14701-14706. doi:10.1073/pnas.0606631103

Goodin, M. M., Zaitlin, D., Naidu, R. A., & Lommel, S. A. (2008). Nicotiana benthamiana: Its History and Future as a Model for Plant–Pathogen Interactions. *Molecular Plant-Microbe Interactions, 21*(8), 1015-1026. doi:10.1094/MPMI-21-8-1015

Grimsley N, H. B., Hohn T, Walden R. (1986). Agroinfection an alternative route for viral infection of plants by using the Ti plasmid. *Botany*.

Gubler, D. J. (1998). Dengue and dengue hemorrhagic fever. *Clinical microbiology reviews, 11*(3), 480-496.

Gunawardana, S. A., & Shaw, R. H. (2018). Cross-reactive dengue virus-derived monoclonal antibodies to Zika virus envelope protein: Panacea or Pandora's box? *BMC infectious diseases, 18*(1), 641-641. doi:10.1186/s12879-018-3572-0

Halstead, S. (2019). Recent advances in understanding dengue. *F1000Research, 8*, F1000 Faculty Rev-1279. doi:10.12688/f1000research.19197.1

Halstead, S. B. (2007). Dengue. *The Lancet, 370*(9599), 1644-1652. doi:https://doi.org/10.1016/S0140-6736(07)61687-0

Halstead, S. B. (2015). Pathogenesis of Dengue: Dawn of a New Era. *F1000Research, 4*, F1000 Faculty Rev-1353. doi:10.12688/f1000research.7024.1

Hasan, S., Saeed, S., Panigrahi, R., & Choudhary, P. (2019). Zika virus: A global public health menace: A comprehensive update. *Journal of International Society of Preventive and Community Dentistry, 9*(4), 316-327. doi:10.4103/jispcd.JISPCD_433_18

Hasan, S. S., Sevvana, M., Kuhn, R. J., & Rossmann, M. G. (2018). Structural biology of Zika virus and other flaviviruses. *Nat Struct Mol Biol, 25*(1), 13-20. doi:10.1038/s41594-017-0010-8

Hayashi, H., & Nakagawa, K. (2019). Combination therapy with PD-1 or PD-L1 inhibitors for cancer. *International Journal of Clinical Oncology*. doi:10.1007/s10147-019-01548-1

He, J., Lai, H., Brock, C., & Chen, Q. (2012). A Novel System for Rapid and Cost-Effective Production of Detection and Diagnostic Reagents of West Nile Virus in Plants. *Journal of Biomedicine and Biotechnology, 2012*, 10. doi:10.1155/2012/106783

He, J., Lai, H., Engle, M., Gorlatov, S., Gruber, C., Steinkellner, H., . . . Chen, Q. (2014). Generation and analysis of novel plant-derived antibody-based therapeutic molecules against West Nile virus. *PLoS One, 9*(3), e93541. doi:10.1371/journal.pone.0093541

Hiatt, A., Caffferkey, R., & Bowdish, K. (1989). Production of antibodies in transgenic plants. *Nature, 342*(6245), 76-78. doi:10.1038/342076a0

Hickman, H. D., & Pierson, T. C. (2016). Zika in the Brain: New Models Shed Light on Viral Infection. *Trends Mol Med, 22*(8), 639-641. doi:10.1016/j.molmed.2016.06.004

Holstein, S. A., & Lunning, M. A. CAR T-cell Therapy in Hematologic Malignances: A Voyage in Progress. *Clinical Pharmacology & Therapeutics, 0*(ja). doi:10.1002/cpt.1674

Houde, D., Peng, Y., Berkowitz, S. A., & Engen, J. R. (2010). Post-translational modifications differentially affect IgG1 conformation and receptor binding. *Molecular & cellular proteomics : MCP, 9*(8), 1716-1728. doi:10.1074/mcp.M900540-MCP200

Hwang, H.-H., Yu, M., & Lai, E.-M. (2017). Agrobacterium-Mediated Plant Transformation: Biology and Applications. *The Arabidopsis Book, 2017*(15).

Jefferis, R. (2005). Glycosylation of Recombinant Antibody Therapeutics. *Biotechnology Progress, 21*(1), 11-16. doi:10.1021/bp040016j

Jennewein, M. F., & Alter, G. (2017). The Immunoregulatory Roles of Antibody Glycosylation. *Trends Immunol, 38*(5), 358-372. doi:10.1016/j.it.2017.02.004

Johnsen, K. B., Burkhart, A., Melander, F., Kempen, P. J., Vejlebo, J. B., Siupka, P., . . . Moos, T. (2017). Targeting transferrin receptors at the blood-brain barrier improves the uptake of immunoliposomes and subsequent cargo transport into the brain parenchyma. *Scientific Reports, 7*(1), 10396. doi:10.1038/s41598-017-11220-1

Kennedy, L. C., Bhatia, S., Thompson, J. A., & Grivas, P. (2019). Preexisting Autoimmune Disease: Implications for Immune Checkpoint Inhibitor Therapy in Solid Tumors. *17*(6), 750. doi:10.6004/jnccn.2019.7310

Khan, J. F., Khan, A. S., & Brentjens, R. J. (2019). Chapter Eight - Application of CAR T cells for the treatment of solid tumors. In D. B. Teplow (Ed.), *Progress in Molecular Biology and Translational Science* (Vol. 164, pp. 293-327): Academic Press.

Kimiz-Gebologlu, I., Gulce-Iz, S., & Biray-Avci, C. (2018). Monoclonal antibodies in cancer immunotherapy. *Molecular Biology Reports, 45*(6), 2935-2940. doi:10.1007/s11033-018-4427-x

Kontermann, R. E., & Brinkmann, U. (2015). Bispecific antibodies. *Drug Discovery Today, 20*(7), 838-847. doi:https://doi.org/10.1016/j.drudis.2015.02.008

Kraemer, M. U. G., Reiner, R. C., Jr., Brady, O. J., Messina, J. P., Gilbert, M., Pigott, D. M., . . . Golding, N. (2019). Past and future spread of the arbovirus vectors Aedes aegypti and Aedes albopictus. *Nat Microbiol, 4*(5), 854-863. doi:10.1038/s41564-019-0376-y

Kuhn, R. J., Zhang, W., Rossmann, M. G., Pletnev, S. V., Corver, J., Lenches, E., . . . Strauss, J. H. (2002). Structure of dengue virus: implications for flavivirus organization, maturation, and fusion. *Cell, 108*(5), 717-725. doi:10.1016/s0092-8674(02)00660-8

Kyle, J. L., & Harris, E. (2008). Global Spread and Persistence of Dengue. *Annual Review of Microbiology, 62*(1), 71-92. doi:10.1146/annurev.micro.62.081307.163005

Lai, H., Engle, M., Fuchs, A., Keller, T., Johnson, S., Gorlatov, S., . . . Chen, Q. (2010). Monoclonal antibody produced in plants efficiently treats West Nile virus infection in mice. *Proc Natl Acad Sci U S A, 107*(6), 2419-2424. doi:10.1073/pnas.0914503107

Lai, H., He, J., Engle, M., Diamond, M. S., & Chen, Q. (2012). Robust production of virus-like particles and monoclonal antibodies with geminiviral replicon vectors in lettuce. *Plant Biotechnol J, 10*(1), 95-104. doi:10.1111/j.1467-7652.2011.00649.x

Lai, H., He, J., Hurtado, J., Stahnke, J., Fuchs, A., Mehlhop, E., . . . Chen, Q. (2014). Structural and functional characterization of an anti-West Nile virus monoclonal antibody and its single-chain variant produced in glycoengineered plants. *Plant Biotechnol J, 12*(8), 1098-1107. doi:10.1111/pbi.12217

Lai, Y. C., Chuang, Y. C., Liu, C. C., Ho, T. S., Lin, Y. S., Anderson, R., & Yeh, T. M. (2017). Antibodies Against Modified NS1 Wing Domain Peptide Protect Against Dengue Virus Infection. *Sci Rep, 7*(1), 6975. doi:10.1038/s41598-017-07308-3

Lee, Y. K. B., J.W.; Hellman, R.; and Hendershot, L.M. (1999). BiP and Ig LC Cooperate to Control the Folding of HC and Esure the Fidelity of Ig Assembly. *Mol Biol Cell, 10*.

Leonhard, S. E., Mandarakas, M. R., Gondim, F. A. A., Bateman, K., Ferreira, M. L. B., Cornblath, D. R., . . . Jacobs, B. C. (2019). Diagnosis and management of Guillain-Barre syndrome in ten steps. *Nat Rev Neurol*. doi:10.1038/s41582-019-0250-9

Li, K., Phoo, W. W., & Luo, D. (2014). Functional interplay among the flavivirus NS3 protease, helicase, and cofactors. *Virol Sin, 29*(2), 74-85. doi:10.1007/s12250-014-3438-6

Liu, J. K. H. (2014). Anti-cancer vaccines - a one-hit wonder? *The Yale journal of biology and medicine, 87*(4), 481-489.

Loos, A., & Steinkellner, H. (2014). Plant glyco-biotechnology on the way to synthetic biology. *Frontiers in plant science, 5*, 523-523. doi:10.3389/fpls.2014.00523

Malavige, G. N., Fernando, S., Fernando, D. J., & Seneviratne, S. L. (2004). Dengue viral infections. *Postgraduate Medical Journal, 80*(948), 588. doi:10.1136/pgmj.2004.019638

Malavige, G. N., Huang, L. C., Salimi, M., Gomes, L., Jayaratne, S. D., & Ogg, G. S. (2012). Cellular and cytokine correlates of severe dengue infection. *PLoS One, 7*(11), e50387. doi:10.1371/journal.pone.0050387

Mangione, J. N., Huy, N. T., Lan, N. T., Mbanefo, E. C., Ha, T. T., Bao, L. Q., . . . Hirayama, K. (2014). The association of cytokines with severe dengue in children. *Trop Med Health, 42*(4), 137-144. doi:10.2149/tmh.2014-09

Marillonnet, S., Giritch, A., Gils, M., Kandzia, R., Klimyuk, V., & Gleba, Y. (2004). In planta engineering of viral RNA replicons: Efficient assembly by recombination of DNA modules delivered by Agrobacterium. *Proc Natl Acad Sci U S A, 101*(18), 6852-6857. doi:10.1073/pnas.0400149101

Marillonnet, S., Giritch, A., Gils, M., Kandzia, R., Klimyuk, V., & Gleba, Y. (2004). In planta engineering of viral RNA replicons: efficient assembly by recombination of DNA modules delivered by Agrobacterium. *Proc Natl Acad Sci U S A, 101*(18), 6852-6857. doi:10.1073/pnas.0400149101

Martina, B. E., Koraka, P., & Osterhaus, A. D. (2009). Dengue virus pathogenesis: an integrated view. *Clinical microbiology reviews, 22*(4), 564-581. doi:10.1128/CMR.00035-09

Morens, D. M. (1994). Antibody-Dependent Enhancement of Infection and the Pathogenesis of Viral Disease. *Clinical Infectious Diseases, 19*(3), 500-512. doi:10.1093/clinids/19.3.500

Mukhopadhyay, S., Kuhn, R. J., & Rossmann, M. G. (2005). A structural perspective of the flavivirus life cycle. *Nat Rev Microbiol, 3*(1), 13-22. doi:10.1038/nrmicro1067

Murphy, B. R., & Whitehead, S. S. (2011). Immune Response to Dengue Virus and Prospects for a Vaccine. *Annual Review of Immunology, 29*(1), 587-619. doi:10.1146/annurev-immunol-031210-101315

Murray, C. L., Jones, C. T., & Rice, C. M. (2008). Architects of assembly: roles of Flaviviridae non-structural proteins in virion morphogenesis. *Nat Rev Microbiol, 6*(9), 699-708. doi:10.1038/nrmicro1928

Murray, N. E., Quam, M. B., & Wilder-Smith, A. (2013). Epidemiology of dengue: past, present and future prospects. *Clin Epidemiol, 5*, 299-309. doi:10.2147/CLEP.S34440

Ng, W. C., Soto-Acosta, R., Bradrick, S. S., Garcia-Blanco, M. A., & Ooi, E. E. (2017). The 5' and 3' Untranslated Regions of the Flaviviral Genome. *Viruses, 9*(6). doi:10.3390/v9060137

Nisonoff, A., Wissler, F. C., & Lipman, L. N. (1960). Properties of the Major Component of a Peptic Digest of Rabbit Antibody. *Science, 132*(3441), 1770-1771. doi:10.1126/science.132.3441.1770

Norkunas, K., Harding, R., Dale, J., & Dugdale, B. (2018). Improving agroinfiltration-based transient gene expression in Nicotiana benthamiana. *Plant methods, 14*, 71-71. doi:10.1186/s13007-018-0343-2

Oliphant, T., Engle, M., Nybakken, G. E., Doane, C., Johnson, S., Huang, L., . . . Diamond, M. S. (2005). Development of a humanized monoclonal antibody with therapeutic potential against West Nile virus. *Nature medicine, 11*(5), 522-530. doi:10.1038/nm1240

Oliphant, T., Nybakken, G. E., Engle, M., Xu, Q., Nelson, C. A., Sukupolvi-Petty, S., . . . Diamond, M. S. (2006). Antibody recognition and neutralization determinants on domains I and II of West Nile Virus envelope protein. *J Virol, 80*(24), 12149-12159. doi:10.1128/JVI.01732-06

Oliveira, E. R. A., Mohana-Borges, R., de Alencastro, R. B., & Horta, B. A. C. (2017). The flavivirus capsid protein: Structure, function and perspectives towards drug design. *Virus Res, 227*, 115-123. doi:10.1016/j.virusres.2016.10.005

Pasteur, S. DENGVAXIA package insert.

Pasteur, S. (2006). Aedes aegypti.

Patterson, J., Sammon, M., & Garg, M. (2016). Dengue, Zika and Chikungunya: Emerging Arboviruses in the New World. *The western journal of emergency medicine, 17*(6), 671-679. doi:10.5811/westjem.2016.9.30904

Perez, P., Hoffman, R. W., Shaw, S., Bluestone, J. A., & Segal, D. M. (1985). Specific targeting of cytotoxic T cells by anti-T3 linked to anti-target cell antibody. *Nature, 316*(6026), 354-356. doi:10.1038/316354a0

Peyret, H., & Lomonossoff, G. P. (2015). When plant virology met Agrobacterium: the rise of the deconstructed clones. *Plant Biotechnol J, 13*(8), 1121-1135. doi:10.1111/pbi.12412

Pierson, T. C., & Diamond, M. S. (2012). Degrees of maturity: the complex structure and biology of flaviviruses. *Curr Opin Virol, 2*(2), 168-175. doi:10.1016/j.coviro.2012.02.011

Pierson, T. C., Sánchez, M. D., Puffer, B. A., Ahmed, A. A., Geiss, B. J., Valentine, L. E., . . . Doms, R. W. (2006). A rapid and quantitative assay for measuring antibody-mediated neutralization of West Nile virus infection. *Virology, 346*(1), 53-65. doi:https://doi.org/10.1016/j.virol.2005.10.030

Pierson, T. C., Xu, Q., Nelson, S., Oliphant, T., Nybakken, G. E., Fremont, D. H., & Diamond, M. S. (2007). The stoichiometry of antibody-mediated neutralization and enhancement of West Nile virus infection. *Cell Host Microbe, 1*(2), 135-145. doi:10.1016/j.chom.2007.03.002

Prevention, C. f. D. C. a. (2019). Congenital Zika Syndrome & Other Birth Defects. *Center for Disease Control and Prevention*.

Rajapakse, S. (2011). Dengue shock. *Journal of emergencies, trauma, and shock, 4*(1), 120-127. doi:10.4103/0974-2700.76835

Rico-Hesse, R., Harrison, L. M., Salas, R. A., Tovar, D., Nisalak, A., Ramos, C., . . . Rosa, A. T. d. (1997). Origins of Dengue Type 2 Viruses Associated with Increased Pathogenicity in the Americas. *Virology, 230*(2), 244-251. doi:https://doi.org/10.1006/viro.1997.8504

Ridgway, J. B., Presta, L. G., & Carter, P. (1996). 'Knobs-into-holes' engineering of antibody CH3 domains for heavy chain heterodimerization. *Protein Eng, 9*(7), 617-621.

Rivera, A. L., Gómez-Lim, M., Fernández, F., & Loske, A. M. (2012). Physical methods for genetic plant transformation. *Physics of Life Reviews, 9*(3), 308-345. doi:https://doi.org/10.1016/j.plrev.2012.06.002

Rodenhuis-Zybert, I. A., Moesker, B., da Silva Voorham, J. M., van der Ende-Metselaar, H., Diamond, M. S., Wilschut, J., & Smit, J. M. (2011). A fusion-loop antibody enhances the infectious properties of immature flavivirus particles. *J Virol, 85*(22), 11800-11808. doi:10.1128/JVI.05237-11

Rosa, B. R., Cunha, A. J. L. A. d., & Medronho, R. d. A. (2019). Efficacy, immunogenicity and safety of a recombinant tetravalent dengue vaccine (CYD-TDV) in children aged 2–17 years: systematic review and meta-analysis. *BMJ Open, 9*(3), e019368. doi:10.1136/bmjopen-2017-019368

Rothman, A. L. (2004). Dengue: defining protective versus pathologic immunity. *The Journal of clinical investigation, 113*(7), 946-951. doi:10.1172/JCI21512

Runcie, K., Budman, D. R., John, V., & Seetharamu, N. (2018). Bi-specific and tri-specific antibodies- the next big thing in solid tumor therapeutics. *Molecular Medicine, 24*(1), 50. doi:10.1186/s10020-018-0051-4

Schahs, M., Strasser, R., Stadlmann, J., Kunert, R., Rademacher, T., & Steinkellner, H. (2007). Production of a monoclonal antibody in plants with a humanized N-glycosylation pattern. *Plant Biotechnol J, 5*(5), 657-663. doi:10.1111/j.1467-7652.2007.00273.x

Shaaltiel, Y., & Tekoah, Y. (2016). Plant specific N-glycans do not have proven adverse effects in humans. *Nat Biotechnol, 34*(7), 706-708. doi:10.1038/nbt.3556

Shaily, S., & Upadhya, A. (2019). Zika virus: Molecular responses and tissue tropism in the mammalian host. *Reviews in Medical Virology, 29*(4), e2050. doi:10.1002/rmv.2050

Sheludko, Y. V., Sindarovska, Y. R., Gerasymenko, I. M., Bannikova, M. A., & Kuchuk, N. V. (2007). Comparison of several Nicotiana species as hosts for high-scale Agrobacterium-mediated transient expression. *Biotechnology and Bioengineering, 96*(3), 608-614. doi:10.1002/bit.21075

Simmonds, P., Becher, P., Bukh, J., Gould, E. A., Meyers, G., Monath, T., . . . Ictv Report, C. (2017). ICTV Virus Taxonomy Profile: Flaviviridae. *J Gen Virol, 98*(1), 2-3. doi:10.1099/jgv.0.000672

Smit, J. M., Moesker, B., Rodenhuis-Zybert, I., & Wilschut, J. (2011). Flavivirus cell entry and membrane fusion. *Viruses, 3*(2), 160-171. doi:10.3390/v3020160

Srikiatkhachorn, A. (2009). Plasma leakage in dengue haemorrhagic fever. *Thrombosis and haemostasis, 102*(6), 1042-1049. doi:10.1160/TH09-03-0208

Stadlmann, J., Pabst, M., Kolarich, D., Kunert, R., & Altmann, F. (2008). Analysis of immunoglobulin glycosylation by LC-ESI-MS of glycopeptides and oligosaccharides. *PROTEOMICS, 8*(14), 2858-2871. doi:10.1002/pmic.200700968

Staerz, U. D., Kanagawa, O., & Bevan, M. J. (1985). Hybrid antibodies can target sites for attack by T cells. *Nature, 314*(6012), 628-631. doi:10.1038/314628a0

Strasser, R., Altmann, F., Mach, L., Glössl, J., & Steinkellner, H. (2004). Generation of Arabidopsis thaliana plants with complex N-glycans lacking β1,2-linked xylose and core α1,3-linked fucose. *FEBS Letters, 561*(1-3), 132-136. doi:10.1016/s0014-5793(04)00150-4

Strasser, R., Altmann, F., & Steinkellner, H. (2014). Controlled glycosylation of plant-produced recombinant proteins. *Current Opinion in Biotechnology, 30*, 95-100. doi:https://doi.org/10.1016/j.copbio.2014.06.008

Strasser, R., Stadlmann, J., Schahs, M., Stiegler, G., Quendler, H., Mach, L., . . . Steinkellner, H. (2008). Generation of glyco-engineered Nicotiana benthamiana for the production of monoclonal antibodies with a homogeneous human-like N-glycan structure. *Plant Biotechnol J, 6*(4), 392-402. doi:10.1111/j.1467-7652.2008.00330.x

Thomas, S. J., & Yoon, I.-K. (2019). A review of Dengvaxia®: development to deployment. *Human Vaccines & Immunotherapeutics*, 1-20. doi:10.1080/21645515.2019.1658503

Tian, Y., Grifoni, A., Sette, A., & Weiskopf, D. (2019). Human T Cell Response to Dengue Virus Infection. *Front Immunol, 10*, 2125. doi:10.3389/fimmu.2019.02125

Trabolsi, A., Arumov, A., & Schatz, J. H. (2019). T Cell–Activating Bispecific Antibodies in Cancer Therapy. *The Journal of Immunology, 203*(3), 585-592. doi:10.4049/jimmunol.1900496

Tsafrir S Mor, Y.-S. M., Kenneth E. Palmer, Hugh S Mason. (2002). Geminivirus Vectors for High Level Expression of Foreign Proteins in Plant Cells. doi:10.1002/bit.10483

Tuse, , D., Tu, T., & McDonald, K. A. (2014). Manufacturing Economics of Plant-Made Biologics: Case Studies in Therapeutic and Industrial Enzymes. *BioMed Research International, 2014*, 16. doi:10.1155/2014/256135

Tzfira, T., & Citovsky, V. (2002). Partners-in-infection: host proteins involved in the transformation of plant cells by Agrobacterium. *Trends in Cell Biology, 12*(3), 121-129. doi:https://doi.org/10.1016/S0962-8924(01)02229-2

Tzfira, T. L., B; Citovsky, V. (2018). Nuclear Import of Agrobacterium T-DNA. *NCBI Bookshelf*.

van Gils, M. J., & Sanders, R. W. (2017). Opposites attract in bispecific antibody engineering. *J Biol Chem, 292*(35), 14718-14719. doi:10.1074/jbc.H117.793497

Wec, A. Z., Nyakatura, E. K., Herbert, A. S., Howell, K. A., Holtsberg, F. W., Bakken, R. R., . . . Chandran, K. (2016). A "Trojan horse" bispecific-antibody strategy for broad protection against ebolaviruses. *Science (New York, N.Y.), 354*(6310), 350-354. doi:10.1126/science.aag3267

Whitehead, S. S., Blaney, J. E., Durbin, A. P., & Murphy, B. R. (2007). Prospects for a dengue virus vaccine. *Nat Rev Microbiol, 5*(7), 518-528. doi:10.1038/nrmicro1690

Wilder-Smith, A., & Gubler, D. J. (2008). Geographic Expansion of Dengue: The Impact of International Travel. *Medical Clinics of North America, 92*(6), 1377-1390. doi:https://doi.org/10.1016/j.mcna.2008.07.002

Xu, L., Pegu, A., Rao, E., Doria-Rose, N., Beninga, J., McKee, K., . . . Nabel, G. J. (2017). Trispecific broadly neutralizing HIV antibodies mediate potent SHIV protection in macaques. *Science (New York, N.Y.), 358*(6359), 85-90. doi:10.1126/science.aan8630

Yacoub, S., & Farrar, J. (2014). Dengue. 162-170.e162. doi:10.1016/b978-0-7020-5101-2.00016-9

Yao, J., Weng, Y., Dickey, A., & Wang, K. Y. (2015). Plants as Factories for Human Pharmaceuticals: Applications and Challenges. *International journal of molecular sciences, 16*(12), 28549-28565. doi:10.3390/ijms161226122

Zeitlin, L., Pettitt, J., Scully, C., Bohorova, N., Kim, D., Pauly, M., . . . Olinger, G. G. (2011). Enhanced potency of a fucose-free monoclonal antibody being developed as an Ebola virus immunoprotectant. *Proceedings of the National Academy of Sciences, 108*(51), 20690. doi:10.1073/pnas.1108360108

Zhang, X., Sheng, J., Plevka, P., Kuhn, R. J., Diamond, M. S., & Rossmann, M. G. (2013). Dengue structure differs at the temperatures of its human and mosquito hosts. *Proc Natl Acad Sci U S A, 110*(17), 6795-6799. doi:10.1073/pnas.1304300110

Zhang, Y., Li, D., Jin, X., & Huang, Z. (2014). Fighting Ebola with ZMapp: spotlight on plant-made antibody. *Science China Life Sciences, 57*(10), 987-988. doi:10.1007/s11427-014-4746-7

APPENDIX A

CURRICULUM VITAE

Adrian Esqueda
Ph.D. Candidate, Molecular and Cellular Biology
The Biodesign Institute, Center for Immunotherapy, Vaccines, and Virotherapy
School of Life Sciences
Arizona State University
A330AA, 1001 S. McAllister St, Tempe AZ 85287
Cell: (626) 217- 4469
Email: aesqueda@asu.edu

EDUCATION

Arizona State University, Tempe AZ
Ph.D. Candidate, Molecular and Cellular Biology Program
August 2011 – present (anticipated graduation December 2019)

California State University, Los Angeles
Biology Master's Program Graduate Student 2009-2011

California State University, Los Angeles
B.S. Microbiology, March 2008
Honors Thesis: Cloning of Bacterial Essential Genes and Purification of Encoded
Products of *Acinetobacter baumannii*

RESEARCH EXPERIENCE

2014-present   Arizona State University
Plant Produced Bispecific mAbs for the Treatment of Flaviviruses including Dengue and
Zika Viruses

2012-2013   Arizona State University
Effects of *in vitro* virus-like particle (VLP) production of Coronavirus MHV A59 utilizing
the wild type, truncated, and chimeric viral envelope (E) protein.

2009–2011   University of Southern California
Screening of small molecule inhibitors of Apurinic/Apyrimidinic Endonuclease 1 (APE-1).

2007-2008   California State University, Los Angeles (CSULA)
Cloning of *A. baumannii* essential genes into *E. coli* host and purification of protein gene
products.

2000-2002   Los Angeles City College/Jet Propulsion Laboratory
Assembly of CCD camera for NASA's Deep Impact Mission and re-assembly and
characterization of operating software for the VIRIS infrared telescope.

HONORS AND AWARDS

2017   Best Poster. "Plant Produced Bispecific Monoclonal Antibodies for the Treatment of Flaviviruses." A Esqueda, J Hurtado, H Lai, and Q Chen. MCB/Micro Retreat, School of Life Sciences, Arizona State University

2017   Poster of Distinction. "Plant Produced Bispecific Monoclonal Antibodies for the Treatment of Flaviviruses." A Esqueda, J Hurtado, H Lai, and Q Chen. American Society for Microbiology Arizona/S. Nevada Branch. 56th Annual Meeting. University of Arizona, Tucson Arizona

2017   Arizona State University, School of Life Sciences, Tempe AZ. Summer 2017 Funding Award

2016   Ehrlich Award for Immunology Application, poster winner. "Plant-derived Monoclonal Antibodies as Efficacious and Safe Therapeutics to Treat Dengue Virus Infection." A Esqueda, J Hurtado, M Dent, H Lai, QS Chen. Fusion 2016, Biodesign Institute, Arizona State University

2014   American Society for Microbiology. 2014-2017 ASM Robert D. Watkins Graduate Research Fellowship Honorable Mention.

2014   American Society for Virology Travel Grant Award. 33rd Annual Meeting of the American Society for Virology, held at Colorado State University, Fort Collins, CO

2013   American Society for Virology Travel Grant Award. 32nd Annual Meeting of the American Society for Virology, held at Penn State University, University Park, PA

2013-2014   Initiative for Maximizing Student Development (IMSD) Graduate Traineeship at ASU for one calendar year

2012-2013   Initiative for Maximizing Student Development (IMSD) Graduate Traineeship at ASU for one calendar year

2011-2012   Doctoral Enrichment Fellowship, Arizona State University

2009   MBRS-RISE M.S. to Ph.D. Fellow, California State University, Los Angeles

2008   Biomedical Post-Baccalaureate Research Education Program (BIOMED-PREP)

2006   MARC-U*Star Fellow, California State University, Los Angeles

2006   Dean's list at California State University, Los Angeles

2002   Consortium for Undergraduate Research Experience (CURE) Fellow, Table Mountain Observatory

TEACHING EXPERIENCE

Graduate Teaching Assistant
2012-2018   MIC206 Introduction to Microbiology Laboratory Techniques, School of Life Sciences, Arizona State University, Tempe AZ

2017-2018   Fall of 2017 and 2018: BIO353 Cell Biology, School of Life Sciences, Arizona State University, Tempe AZ

Undergraduate Student Mentoring
2011- present   Supervision, mentoring, and training of undergraduate students in microbiology and molecular biology techniques.

PRESENTATIONS

2019 Electronic Poster Presentation. American Society of Plant Biologists. "Plant Produced Bispecific Monoclonal Antibody Neutralizes Dengue-2 and Zika Viruses and Forgoes Antibody Dependent Enhancement of Infection." A Esqueda and Q Chen. August 3-7, 2019. San Jose, CA

2019 Oral Rapid-Fire Presentation and Poster Presentation. Fusion 2019 The Biodesign Institute Scientific Retreat. "Bispecific Monoclonal Antibody-based Therapeutics against Dengue and Zika Viruses." A Esqueda, H Sun, H Lai, and Q Chen. March 22nd, 2019. Phoenix, AZ

2018 Oral Presentation at the 37th Annual Meeting of the American Society for Virology. "Plant Produced Bispecific Monoclonal Antibody Neutralizes Flaviviruses and Reduces Antibody Dependent Enhancement." A Esqueda, H Sun, H Lai, and Q Chen. July 14th-18th at the University of Maryland. College Park, MD

2018 Poster Presentation. Arizona Wellbeing Commons. "Neutralization and Reduction of Antibody Dependent Enhancement of Infection of Dengue and Zika Viruses by a Plant-Produced Bispecific Antibody." A Esqueda, H Sun, H Lai, Q Chen. April 30th, 2018. Scottsdale, AZ

2017 Oral Presentation at the Society for the Advancement of Chicanos and Native Americans. "Plant Produced Bispecific Monoclonal Antibodies for the Treatment of Flaviviruses." A Esqueda, H Lai, QS Chen. October 19-21, 2017. Salt Lake City, UT

2017   Poster Presentation. Molecular and Cellular Biology and Microbiology Graduate Programs Retreat, School of Life Sciences. "Plant Produced Bispecific Monoclonal Antibodies for the Treatment of Flaviviruses." A Esqueda, J Hurtado, H Lai, and Q Chen., Arizona State University. Tempe AZ

2017 Oral Presentation Molecular and Cellular Biology Colloquium, School of Life Sciences. "Plant Produced Bispecific MAbs for the Treatment of Flaviviruses." Fall 2017. The Biodesign Institute, Arizona State University. Tempe AZ

2017 Poster Presentation. Fusion 2017 The Biodesign Institute Scientific Retreat. "Plant Produced Bispecific Monoclonal Antibodies for the Treatment of Flaviviruses." A Esqueda, J Hurtado, QS Chen. April 7, 2017. Carefree, AZ

2017 Poster Presentation at the 56th Annual Meeting of the AZ/Southern NV Chapter of the American Society for Microbiology. "Plant Produced Bispecific MAbs for the Treatment of Flaviviruses" A Esqueda, J Hurtado, H Lai, QS Chen. April 1, 2017. The University of Arizona, Tucson AZ

2016 Oral Presentation Molecular and Cellular Biology Colloquium, School of Life Sciences. "Plant Produced Bispecific MAbs for the Treatment of Flaviviruses." Fall 2016. The Biodesign Institute, Arizona State University. Tempe AZ

2016 Poster Presentation at the 55th Annual Meeting of the AZ/Southern NV Chapter of the American Society for Microbiology. "Plant-derived monoclonal antibodies as efficacious and safe therapeutics to treat dengue virus infection." A Esqueda, J Hurtado, M Dent, H Lai, QS Chen. April 16, 2016. Arizona State University. Tempe AZ

2016 Poster Presentation at Fusion 2016 Biodesign Institute Scientific Retreat. "Plant-derived monoclonal antibodies as efficacious and safe therapeutics to treat dengue virus infection." A Esqueda, J Hurtado, M Dent, H Lai, QS Chen. April 1, 2016. Carefree AZ

2014 Oral Presentation at the 33rd Annual Meeting of the American Society for Virology. "Characterization of Coronavirus Small Envelope Protein (E) Ion Channel Activity and its Role in Virus Assembly." A. Esqueda, J. Carrillo, S. M. Daskalova, M. Goryll, B. G. Hogue. June 21st – 25th 2017. Colorado State University. Fort Collins CO

2013 Oral and Poster Presentation at the 32nd Annual Meeting of the American Society for Virology.
Oral Presentation: "Significance of Coronavirus Envelope (E) Protein Ion Channel Activity in Virus Assembly." A. Esqueda, J. Carrillo, S. Daskalova, B. Hogue. July 20th – 24th 2013. Penn State. University Park PA
Poster Presentation: "Key Amino Acid Residues of Coronavirus Envelope (E) Protein are Important for Ion Chanel Activity." J. Carrillo, A. Esqueda, S. Daskalova, B. Hogue. July 20th – 24th 2013. Penn State. University Park PA

2013 Poster Presentation at More Graduate Education @ Mountain States Alliance. "A Single Point Mutation in the Coronavirus Envelope Protein Transmembrane Domain Reduces VLP Formation and Abrogates Cation Channel Activity." A Esqueda, J Carrillo, S Daskalova, M Goryll, and B Hogue. March 2013. Arizona State University. Tempe AZ

2008 Poster presentation at the 108th American Society for Microbiology General Meeting. "Vector construction and Essential Gene Cloning Using a Ligation Independent Cloning Strategy." LJ Real, OH Rogers, DH Gilling, CK Lam, A Esqueda, Q Huang, and H. Xu. June 1st – 5th 2008. Boston MA

2008 Poster Presentation at the CSULA 16th Annual Student Symposium. "Cloning of Bacterial Essential Genes and Purification of Encoded Products of *Escherichia coli* and

Acinetobacter baumannii." A. Esqueda and HH Xu. California State University Los Angeles. Los Angeles CA

2008 Poster presentation at the 20th Annual CSU Biotechnology Symposium. "Cloning of *Acinetobacter baumannii* Essential Genes and Purification of Encoded Protein Products." A Esqueda, Q Huang, C Lam, S Tan, DH Gilling, and HH. Xu. January 11th – 13th 2008. Oakland CA

2007 Poster Presentation at the Southern California Conference for Undergraduate Research. "Cloning of Bacterial Essential Genes and Purification of Encoded Products of *Escherichia coli* and *Acinetobacter baumannii.*" A Esqueda and HH Xu. Los Angeles CA

PROFESSIONAL SOCIETY MEMBERSHIPS

2016 - Present   Society for the Advancement of Chicanos and Native Americans
2013 – Present   American Society for Virology
2008 – 2016   American Society for Microbiology

PUBLICATIONS

1) M. Dent, J. Hurtado, A.M. Paul, H. Sun, H. Lai, M. Yang, **A. Esqueda**, F. Bai, H. Steinkellner, and Q. Chen. "Plant–produced anti-dengue virus monoclonal antibodies exhibit reduced antibody-dependent enhancement of infection activity." Journal of General Virology, **2016**, 3280-3290.
2) **A. Esqueda**, M.Z. Mohammed, S. Madhusudan, N Neamati. "Purification and specific assays for measuring APE-1 endonuclease activity." Methods in Molecular Biology, 2012. 928; 161-47.
3) K. Ramkumar, V. N. Yarovenko, A. S. Nikitina, I. V. Zavarzin, M. M. Krayushkin, L. V. Kovalenki, **A. Esqueda**, S. Odde, and N. Neamati. "Design, Synthesis and Structure-activity Studies of Rhodanine Derivatives as HIV-1 Integrase Inhibitors." *Molecules,* **2010**, 15, 3958-3992.
4) **A. Esqueda** , Z.M. Mohammed, S. Madhusudan, N. Neamati, and Y. Zheng (ed.). *Rational Drug Design*, Methods in Molecular Biology, vol. 928, DOI 10.1007/978-1-62703-008-3_13, © Springer Science+Business Media New York **2012**
5) F. Aiello, Y. Shabaik, **A. Esqueda**, T.W. Sanchez, F. Grande, A. Garofalo, and N. Neamati. Design and Synthesis of 3-Carbamoylbenzoic Acid Derivatives as Inhibitors of Human Apurinic/Apyrimidinic Endonuclease 1 (APE1). *ChemMedChem* **2012**, 7, 1–16